University of Alberta

The Role of Clay in Salt Hydrolysis during Bitumen Upgrading

by

Yissella Londono

A thesis submitted to the Faculty of Graduate Studies and Research in partial fulfillment of the requirements for the degree of Master of Science
in

Chemical Engineering

Department of Chemical and Materials Engineering

Edmonton, Alberta
Spring, 2007

Your file Votre référence
ISBN: 978-0-494-29990-6
Our file Notre référence
ISBN: 978-0-494-29990-6

University of Alberta

Library Release Form

Name of Author: Yissella Londono

Title of Thesis: The Role of Clay in Salt Hydrolysis during Bitumen Upgrading

Degree: Master of Science

Year this Degree Granted: 2007

Signature

March 29/07

University of Alberta

Faculty of Graduate Studies and Research

The undersigned certify that they have read, and recommend to the Faculty of Graduate Studies and Research for acceptance, a thesis entitled **The Role of Clay in Salt Hydrolysis during Bitumen Hydrolysis** submitted by **Yissella Londono** in partial fulfillment of the requirements for the degree of **Master of Science in Chemical Engineering**.

Dr. Murray Gray

Dr. Subir Bhattacherjee

Dr. William McCaffrey

March 26, 2007

Date

ABSTRACT

When water-in-oil emulsions from the extraction of oils sands enter the upgrading process, the water is evaporated leaving the chloride salts of sodium, calcium and magnesium. Subsequent reactions with steam can lead to release of hydrochloric acid, causing serious corrosion problems. This hydrolysis process may be influenced by the clay minerals suspended in the bitumen.

The interactions between clays and chloride salts were investigated through experiments on a model emulsion of a mixture of pure chloride salts, kaolinite and water in an oil phase. A constant flow of steam was bubbled through this mixture at 150-350°C to induce chlorides to hydrolyze. Ion chromatography of the overhead condensate detected an increase in chloride evolution when salts were exposed to steam in the presence of clays. The main mechanism for the increase in hydrolysis was likely the increase in the surface area of the chloride salts, due to their distribution on the surface of the clay particles. Additives to control the release of chloride from the solution were effective in the presence of clays.

ACNOWLEDGEMENT

I am deeply grateful to Dr. Murray R. Gray for being a mentor of strong ethical value and human excellence beyond his high academic credentials, and for guiding me as a graduate student to higher paths of knowledge and professional opportunities.

Thanks for the funding provided by Champion Technologies and the valuable collaboration of Mrs. Tuyet Le and Dr. Randy Mikula along the project. I also want to express my gratitude to Mrs. Leanne Swekla and the entire faculty, administrative and technical staff at the University of Alberta for sharing with me the legacy of community and diversity of the institution.

Finally my recognition to my original family and God for being my spiritual foundation and for empowering me to be a better person every day; and to my chosen family: the elite of wonderful friends from all over the world for showing me that friendship overcomes any difference of language and culture.

TABLE OF CONTENTS

	Page
CHAPTER 1. INTRODUCTION	**1**
1.1. Background	1
1.2. Research Hypotheses	6
CHAPTER 2. LITERATURE REVIEW	**7**
2.1. Challenges Associated With Desalting Heavy Oils	7
2.1.1. Solubility of Water in the Crude Oil	7
2.1.2. Limited Differential Density	9
2.1.3. Effects of Solids Contaminants	10
2.2. Solids and Chlorides in Bitumen	11
2.2.1. Fine Solids in Athabasca Bitumen	12
2.2.2. Characterization of Clays in Athabasca Bitumen	17
2.2.3. Chlorides in Bitumen	22
2.3. Hydrolysis of Chlorides	22
2.3.1.1. Hydrolysis Reactions at Refining Temperatures	24
2.3.1.2. High Temperature Fusion-Type Reactions	26
2.3.1.2.1. Molten Salts + SiO_2 in the Presence of Steam	27
2.3.1.2.2. Molten Salts + Metakaolin in the Presence of Steam	29
2.4. Structure of Clay and Interactions with Salts	31
2.4.1. Chemical Structure of Kaolinite	34
2.4.2. Physical Structure of Kaolinite	37
2.4.3. Interactions of Kaolinite with Water	40

2.4.3.1. Thermal Analysis of Kaolinite 41

2.5. Cation Exchange Capacity of Clay Minerals 44

2.5.1. Tetrahedral Substitutions 45

2.5.2. Substitutions in the Interlayer Sheet 45

2.6. Surface Area 45

2.6.1. Factors Affecting Surface Area 45

2.6.2. Surface area from size distributions 47

2.6.3. Surface Properties of Clay Minerals 47

2.7. Dependence of Exchange Capacity of Kaolinite on Variations in Surface Area 49

2.8. Inhibition of Hydrolysis of Salts 52

CHAPTER 3. MATERIALS AND METHODS 54

3.1. Reagents 54

3.2. Sample Preparation and Steam Simulated Distillation 57

3.3. Recovery of solids from the oil system feed 59

3.4. Ion saturation of clays 60

3.5. Analytical Methods and Instrumentation 58

3.5.1. Solids Analysis 60

3.5.1.1. Scanning Electron Microscopy 60

3.5.1.2. Particle Size Distribution 61

3.5.1.3. X-ray Photoelectron Spectroscopy (XPS) 61

3.5.2. Determination of Chloride Concentrations via Ion Chromatography 62

3.5.2.1. Ion Chromatography Principle 62

3.5.2.2. Ion Chromatography Analysis Method 63

3.5.2.3. Analysis of Hydrolysis Condensate Samples 65

CHAPTER 4. RESULTS AND DISCUSSION 67

4.1. Effect of Clays on Hydrolysis of Salts 68

4.1.1. Statistical Significance of the Effect of Clay in Hydrolysis of Salts 69

4.1.2. Study of the Correlation between Surface Area, Morphology of Salts and Chloride Evolution 70

4.1.3. Cation Content of Condensate Samples 75

4.1.4. Quantitative Analysis of Solids after Reaction 76

4.2. Experiments with Pure Salts 80

4.2.1. Additivity of Pure Salts in Kaolinite 84

4.2.2. Role of Cation-Saturation of Clay in Hydrolysis of Salts 87

4.2.3. Characterization of Ion Exchanged Clays 89

4.3. Inhibition of the Hydrolysis of Salts and Clay 92

CHAPTER 5. CONCLUSIONS AND RECOMMENDATIONS 97

5.1. Conclusions 97

5.2. Recommendations 99

REFERENCES 100

APPENDICES 106

I. Dixon's Test for Outliers Detection 107

II. Additivity of Clay, Acid and Inhibitor 108

II.a. Differential Recovery of Chloride 108

II.b. Cumulative Chloride Evolution 109

II.c. Comparison of Inhibitors 109

III. Data for Different salt/clay ratios 110

III.a. Differential Recovery of Chloride 110

III.b. Cumulative Chloride Evolution 111

IV. Chloride Input 109

IV.a. Baseline Conditions: 0.05 grs mixed salts

(70%NaCl + 20 % CaCl2 2(H2O)+ 10% MgCl2 6(H2O)) 112

IV.b. Baseline Conditions: 0.05 grs Pure salts (100% NaCl) 112

IV.c. Baseline Conditions: Pure salts 0.05 grs (100% CaCl2 2(H2O)) 112

LIST OF TABLES

Table	Page
2.1. Vanadium, viscosity and salt content for some heavy crudes	11
2.2. Analysis of Athabasca oil sands	13
2.3. Effect of solids removal on metal analysis from bitumen	15
2.4. Metals and chlorine content of Athabasca bitumen	16
2.5. Relative concentrations, mol/mol calcium, of alkali and alkaline earth metals and chlorine in bitumen	17
2.6. XPS surface analysis for total clay sized fractions (<3 mm) and ultra-fine fractions (<0.3 mm)	21
2.7. Thermodynamic calculations of hydrolysis of chlorides	26
2.8. Thermodynamic properties for the hydrolysis of NaCl in presence of steam	28
2.9. Classification of phyllosilicates related with clays	33
2.10. Calculation of the unit cell mass of kaolinite	35
2.11. Chemical oxides composition of source clay KGa1-b	36
2.12. Dependence of water release with temperature and type of clays	41
2.13. N_2 BET surface areas of various clay minerals	49
2.14. Effect of surface area on exchange capacity of kaolinite	50
3.1. Kaolinite low defect physical and chemical data	55
3.2. Silica physical and chemical properties	56
3.3. ICS-2000 ion chromatography system specifications	66

4.1. t-Test: two-sample assuming equal variances for the hydrolysis at 150-350 °C of a mixture of salts emulsified in oil as aqueous solution in paraflex and dried at 150 °C 69

4.2. Extent of cumulative hydrolysis and particle size analysis by light scattering (hydrolysis at 150-350 °c of a mixture of salts of Na Cl + $CaCl_2$.2(H2O) +$MgCl_2$ 6(H2O)) emulsified in oil as aqueous solution in Paraflex and dried at 150 °C) 71

4.3. Cation concentration in overhead condensate after hydrolysis of an emulsion of mixed salts + kaolinite in pure oil. 76

4.4. EDX analysis in solids vs. temperature of hydrolysis of an emulsion of mixed salts + kaolinite in pure oil 78

4.5. Surface Area of solids after reaction measured with the Brunauer, Emmett and Teller Method (BET) 90

4.6. XPS Analysis of clay + mixed salts solids after hydrolysis 91

4.7. Percentage of inhibition as a function of temperature of hydrolysis for an emulsion of kaolinite + mixed salts 94

LIST OF FIGURES

Figure	Page
1.1. Corrosion in the crude-column overhead condenser	2
1.2. Electrostatic desalting operation	4
2.1. Solubility of water in 17° API blended bitumen	9
2.2. Correlation between the fines and clay portion of the Athabasca oilsands	13
2.3. Composition of the clay fraction in Athabasca oilsands	19
2.4. Yields of hydrochloric acid for the hydrolysis of NaCl	30
2.5. Electro micrograph of Kaolinite	39
2.6. Thermogravimetric curve of a KGa-1 kaolinite sample	43
2.7. Differential thermal analysis curve of a KGa-1 kaolinite sample	44
2.8. Base-exchange capacity vs. surface area for controlled particle size fractions of pure kaolin	51
3.1. Particle size distribution of silica	57
3.2. Schematic diagram of glass distillation apparatus	59
3.3. Ion analysis process	63
4.1. Effect of clay on hydrolysis of emulsified chloride salts (70 wt% Na Cl + 20 wt% $CaCl_2.2(H2O)$ + 10 wt% $MgCl_2$ 6(H2O)) on a (10:1 clay to salt weight ratio).	68
4.2. SEM micrographs of solids after hydrolysis of an emulsion of salts in oil: a) mixed salts only, b) kaolinite + mixed salts c) mixed salts and silica	73
4.3. Particle size distribution	74

4.4. Energy dispersive X-Ray analysis of solids after hydrolysis. Upper panel, salts crystals only. Lower panel, kaolinite aggregates with salt crystals 79

4.5. Evolution of chloride from $CaCl_2.2(H2O)$ emulsified as a function of the presence of clay (10:1 clay to salt weight ratio).Upper panel: $CaCl_2.2(H2O)$; Lower panel: $CaCl_2.2(H2O)$ with kaolinite 81

4.6. SEM micrographs of solids after hydrolysis of kaolinite + NaCl 82

4.7. Size Distribution of solids after hydrolysis NaCl 83

4.8. Incremental recovery of chloride on the hydrolysis of Na and Ca mixtures with kaolinite (on a 50:50 chloride input weight ratio). Predicted results from the means of two experiments with pure salts and kaolinite 85

4.9. Effect of cation-saturation of clay on the hydrolysis of emulsified chloride salts on a (10:1 clay to salt weight ratio) 88

4.10. Inhibition of chloride evolution at 1:1 weight ratio inhibitor vs. mixed salts 93

4.11. Incremental release of chloride for the hydrolysis of kaolinite + mixed salts + inhibitor emulsified in oil. 95

4.12. Particle size distribution mixed salts + clay with and without inhibitor 96

NOMENCLATURE

v=Downward velocity of the water droplet relative to the oil, m/sec,

d=Diameter of the water droplet, μm,

$\Delta\rho_{ow}$=Differential density between the oil and water, and

μ_o=Dynamic viscosity of the oil, cp.

CHAPTER 1

INTRODUCTION

1.1. Background

Crude oils often contain inorganic salts such as sodium chloride, magnesium chloride and calcium chloride, as well as clays, in suspension or dissolved in entrained water (i.e. brine). Salt corrosion is caused by the hydrolysis of these metal chlorides to hydrogen chloride (HCl) when crude oil is heated in the presence of steam. The subsequent formation of hydrochloric acid may be accelerated for the interaction between the salts and clay.

High chlorides in the feed to the atmospheric distillation unit heater can generate large quantities of hydrochloric acid (HCl). Fig 1.1 illustrates how chlorides in crude oil form areas of hydrogen chloride release in the top section of the crude column, which can cause severe corrosion of the overhead line (White and Barletta, 2002). Ye (2000) observed how hydrogen chloride may also combine with ammonia to form ammonium chloride (NH_4Cl), which increases not only the likelihood of column tray fouling but also the pressure downstream of the column; thus preventing the overhead-tower stream and diesel from being drawn out. All of these problems can reduce crude runs and reduce unit reliability.

Desalting of crude oil upstream of the crude distillation unit is a key process operation for the removal of undesirable components from crude oil before it reaches any of the major unit operations. This technique consists of washing the crude oil with fresh water to remove soluble salts. A typical desalter includes a stage for mixing fresh water with an oil stream and another means of separating the water and oil. In chemical desalting, water and chemical surfactant (demulsifiers) are added to the crude, heated so that the salts and other impurities dissolve into the water or attach to the water, and then held in a tank where they settle out.

Figure 1.1. Corrosion in the crude-column overhead condenser

(White. and Barletta, 2002)

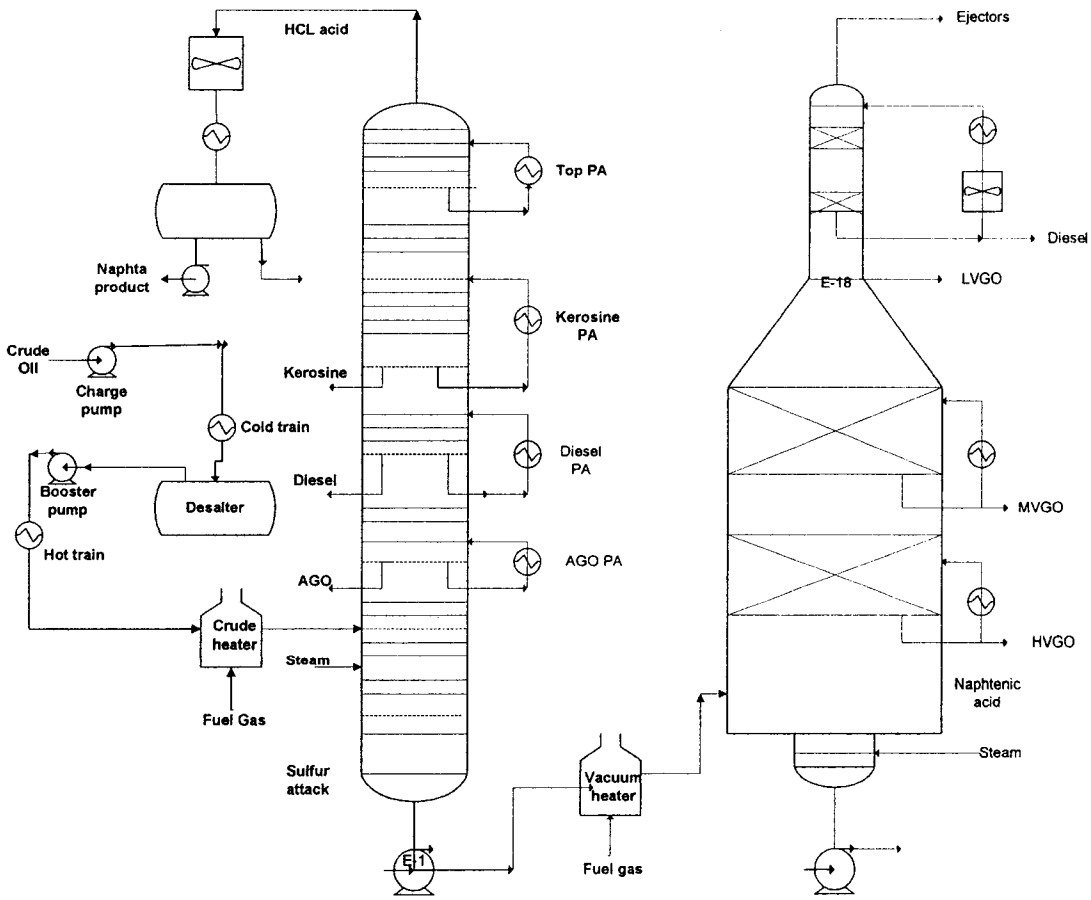

The two most typical methods of crude-oil desalting, chemical and electrostatic separation use hot water as the extraction agent. Electrical desalting adds the application of high-voltage electrostatic fields between an arrangement of two horizontal bar grids and the water. The oil flows across both of these fields as it transits the desalter. The AC fields enhance the oil-water separation by retaining the suspended water globules, which increases their local concentration and rate of coalescence. The water layer is then grounded through the bottom of the vessel (Figure 1.2). Both methods of desalting are continuous. Waste water and contaminants are discharged from the bottom of the settling tank to the wastewater treatment facility. The desalted crude is continuously drawn from the top of the settling tanks and sent to the crude distillation unit.

While desalting is an effective process for conventional crudes, for heavier crudes single-stage desalting removes only 90-95% of salt, leaving salt contents of 1.36-2.72 Kg/158.98 m^3 (3-6 lb/1000 bbl) to cause downstream corrosion. The poor desalting of heavy oils is ascribed to their high viscosity, the presence of suspended solids and semi-soluble components, and the limited differential density for driving the sedimentation-based separation. Consequently a two-stage treatment is required to improve desalting efficiency and stabilize unit operations.

For example, BP refineries uses multiple stage desalting as best practice to treat crudes with 14-16 ° API with around 85-90 % salt removal for a single stage desalter and 97-99% for a two stage desalter (Anonymous, 1997) . The high viscosity of heavy oil makes impossible the coalescing of the droplets, practically requiring an infinite residence time to separate the fluid. (Popp and Dinolescu,

1997; Choi, 2002). Consequently, the refining industry needs strategies to deal with the residual salt in heavy crudes after conventional desalting operations.

Mined oil sands bitumen has a high sediment and clay content that forms very stable emulsions that make desalting completely ineffective. The fine solids tend to be surface active and prevent the oil-water phases from separating efficiently (Kotlyar et al., 1999). Similarly, the observations from Levine and Sanford (1980,1985) as well as from Hall and Tollefson (1982) on clay-bitumen interactions, confirmed that bitumen recovery loss was influenced by its high concentration of clays and fine solids which contribute to the stabilization of emulsion droplets in bitumen. Once stabilized, the droplets do not coalesce; therefore, they build up and cause short circuiting of the desalter grids.

Figure 1.2. Electrostatic Desalting Operation (White and Barletta, 2002)

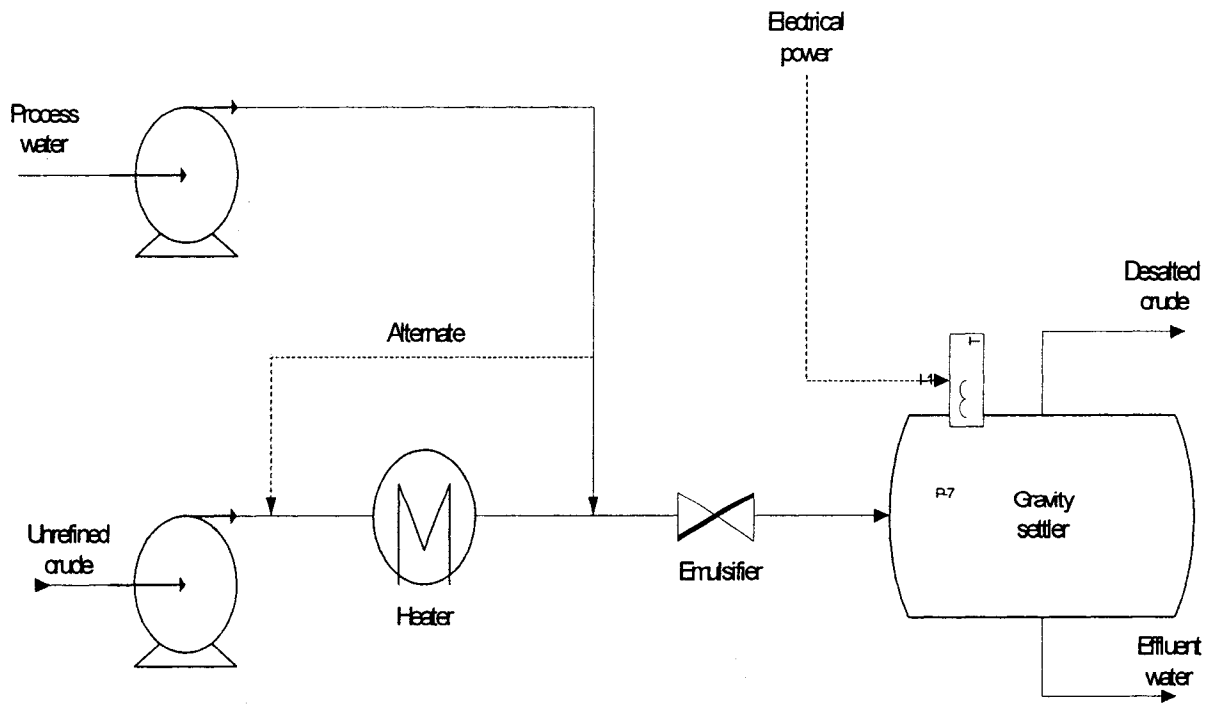

In the early years of the oil sands operations, the mined oil sands near the Athabasca River had a low salt content, due to washing of the formation over geological time periods. The salt content of the water used in the extraction operations was low, and the hydrolysis of the salts was not a significant contributor to corrosion and fouling. As the mining operations moved further from the river, the salt content in the ore increased. The recycling of the process water gave accumulation of the chloride salts, giving corrosion problems first at Syncrude in the early 1990's. Washing and centrifugation of the extracted bitumen gave only partial removal of the salts. Mining operations at Suncor and CNRL anticipate elevated salt concentrations in the years ahead. In fact, the concentrations of Cl ion in the pond water of Suncor operations have increased from 20-60 ppm in 1984 to 91 ppm in 2000 and the average concentrations on the west bank of the Athabasca river peaks at about 350 ppm (Beardow, 2000).

The combination of the worldwide trend to use of heavy oil and the growth of mining of oil sands in Alberta has increased the need to deal with the hydrolysis of chloride salts in upgrading. Although chemical demulsification has benefits in partial removal of emulsified water, upgraders and refiners need to understand the behavior of the inevitable residual salts in their feed streams, and the interactions of those salts with fine solids and other components of the crude oil or bitumen.

1.2. Research Hypotheses

Given the need of the industry to deal more effectively with the residual salts emulsified in heavy oils and bitumens, and the common presence of fine solids in these streams, this research is focused on elucidating the role of clays in modifying the behaviour of chloride salts at process conditions. Based on the available background information, the following research hypotheses lay the basis of this work:

a) Clays will increase the extent of hydrolysis of a given salt mixture.
b) Ion exchange between the salts and the clays is a mechanism for increasing the extent of hydrolysis.
c) An increase in the surface area of the salt crystals will increase the extent of hydrolysis.

CHAPTER 2

LITERATURE REVIEW

2.1. Challenges Associated With Desalting Heavy Oils

The production of heavy oil is usually associated with the co-production of varying amounts of residual water, formation solids, and corrosion products. This residual water is normally the source of mineral salts appearing in the crude oil. The salts contained in the water are then left behind as either dry crystals in the oil or as crystals attached to drops of saturated solution. Heavy crude oils place severe strains upon conventional desalting practices, including solubility of water in crude oil, limited differential density and high levels of semi-soluble, suspended contaminants.

2.1.1. Solubility of Water in the Crude Oil

Warren and Armstrong (2001), observed that the solubility of water in crude oil increases with temperature (Figure 2.1). Their experimental work on heavy crude oils of the Orinoco Tar Belt suggested that this solubility approaches 0.4% by volume at 150°C. Further studies led Warren and Armstrong (2001) to conclude that although there is no carrying of salt from the water dissolved in the oil after the desalting process, salt crystals may precipitate from highly saline drops after dehydration. By acting as any other interface, the surface of these salt crystals acts tends to collect insoluble or semi-soluble contaminants that create a barrier between the crystal and the wash water.

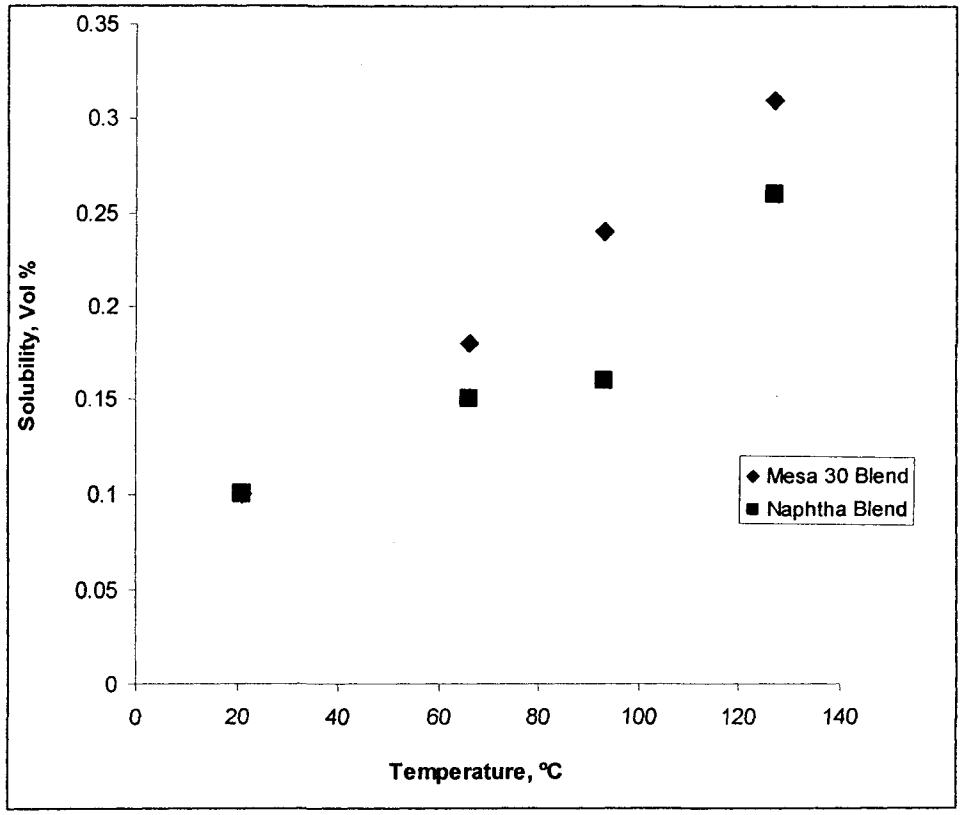

Figure 2.1. Solubility of water in 17° API blended bitumen (Warren and Armstrong, 2001).

The behavior of water in oil at elevated temperatures and the drying of crude oil is more of a concern for heavy oil producers, due to the practices of desalting under pressure to reduce the oil viscosity, and evaporation of water to meet pipeline specification. Typical common-carrier pipelines limit bottom sediment and water to 0.5 wt%, therefore, drying of heavy oils to meet this requirement can result in streams with dehydrated solids. As noted above, the surface properties of such solids can make subsequent desalting very difficult.

2.1.2. Limited Differential Density

The oil-water emulsion that enters the desalter is subjected to a coalescing force. Once the water drops coalesce and settle into one phase, separation of the oil and water phases within the desalter vessel is achieved through gravity differences according to the Stokes' Law (2.1). By inspection of equation 2.1 below, the rate of separation is directly related to the drop size of the dispersed phase as well as the differential density of the phases, and inversely proportional to the viscosity of the oil or continuous phase.

$$\upsilon = 1.78 \times 10^{-6} (\Delta p_{ow}) d^2 / \mu_0 \qquad (2.1)$$

The use of fresh wash water in field dehydration operations greatly reduces the available differential density due to its lower settling capacity when compared to the saline produced water. Moreover, the driving force for separation of the two phases is small due to similar densities between heavy oil and water .

High operating temperatures of desalting may also severely reduce the differential density between the oil and water that is necessary as a driving force for sedimentation. (Warren and Armstrong, 2001; Pruneda et al., 2005). Consequently, the low value of $\Delta\rho_{ow}$ and the high viscosity (μ_0) combine to give low settling velocities for driving the sedimentation-based separation.

2.1.3. Effects of Solids Contaminants

In addition to salt content (Table 2.1), heavy oils often tend to increase the entrainment of suspended solids due to its high density and viscosity. These solids are highly contaminant and may consist of formation fines, corrosion products, precipitated minerals and organic components. Through a variety of processing schemes for upgrading of heavy oil, Warren and Armstrong (2001) found these solids-based contaminants tend to accumulate at the drop surfaces, stabilizing the water dispersions that gradually degrade the performance the desalting vessels. Warren and Armstrong (2001), observed that these materials also accumulate at the phase boundary between the oil and water layers where they retard the sedimentation of water drops and produce a characteristic interface "rag" layer that adversely affects the sedimentation of water drops due to the presence of other suspended phase materials. If this diffuse interface layer can be maintained in a steady-state over an extended period of operation it won't compromise the performance of the desalter. However, as the interface film becomes thicker it needs to be resolved or removed by interface sludge jets or by mixing of the interface sludge into the "rag" layer and further removal of this mixture during mud washing.

Warren and Armstrong (2001) also remarked that scale accumulation of sediments in the bottom of the vessel involves interference with flow distribution within the vessel. As a result, the process will be unstable leading to an inefficient operation. The y suggested that removal of these sediments can be accomplished through a mud-wash or sand-jetting system.

Table 2.1. Vanadium, viscosity and salt content for some heavy crudes. (White and Barletta, 2002)

Crude type	Vanadium, ppmw	Viscosity at 538°C,cst	Salt content, Kg/454 Kg of crude
Maya	291	95	6
Cold Lake	124	75	20
Lloydminster (LLB)	100	70	42
Canadian blend	155	80	40

2.2. Solids and Chlorides In Bitumen

As mentioned in the introduction, after the conventional froth treatment of bitumen from mined oilsands, the treated bitumen still contains water. This water carries as dissolved salts such as Na, K, Ca and Mg chlorides and fine solids which are resistant to demulsification and centrifugation or gravity settling. The use of paraffinic solvents to precipitate a portion of the bitumen can flocculate and remove these components, as at the Albian Sands Muskeg River mine (Tipman et al., 2001). This approach reduces the yield of bitumen, therefore, a majority of oil sands operations must deal with salts and fine solids in the product stream from the extraction process.

2.2.1. Fine Solids In Athabasca Bitumen

The terminology that is adopted in the oil sands industry for "fines" is that portion that exhibits a particle size less than 44 microns (Gray and Masliyah, 1998). Clay minerals on the other hand, belong to the fines portion with a mean particle size less than 2 microns. The unconsolidated silica sand (SiO_2) in oil sands comprises particles ranging from less than 75 μm to more than 300 μm (Fong et al, 2004). Clay minerals only appear in the fine solids fraction which comprises 18% of the oil sands (Table 2.2).

Table 2.2. Analysis of Athabasca oil sands (Kotlyar et al., 1982)

Oil sand	Composition (%)			Fine Solids[2] (≤38 μm)
	Bitumen[1]	water	solids	(%)
Estuarine	9.9	4.9	85.2	17.9
Marine	9.7	4.4	85.9	16.6

[1]By difference
[2]Expressed as wt% of bitumen-free, dry oil sand solids

Sanford and Levine (1985) observed that there is a fair correlation between the fines and clay portion of Athabasca bitumen (Figure 2.2).

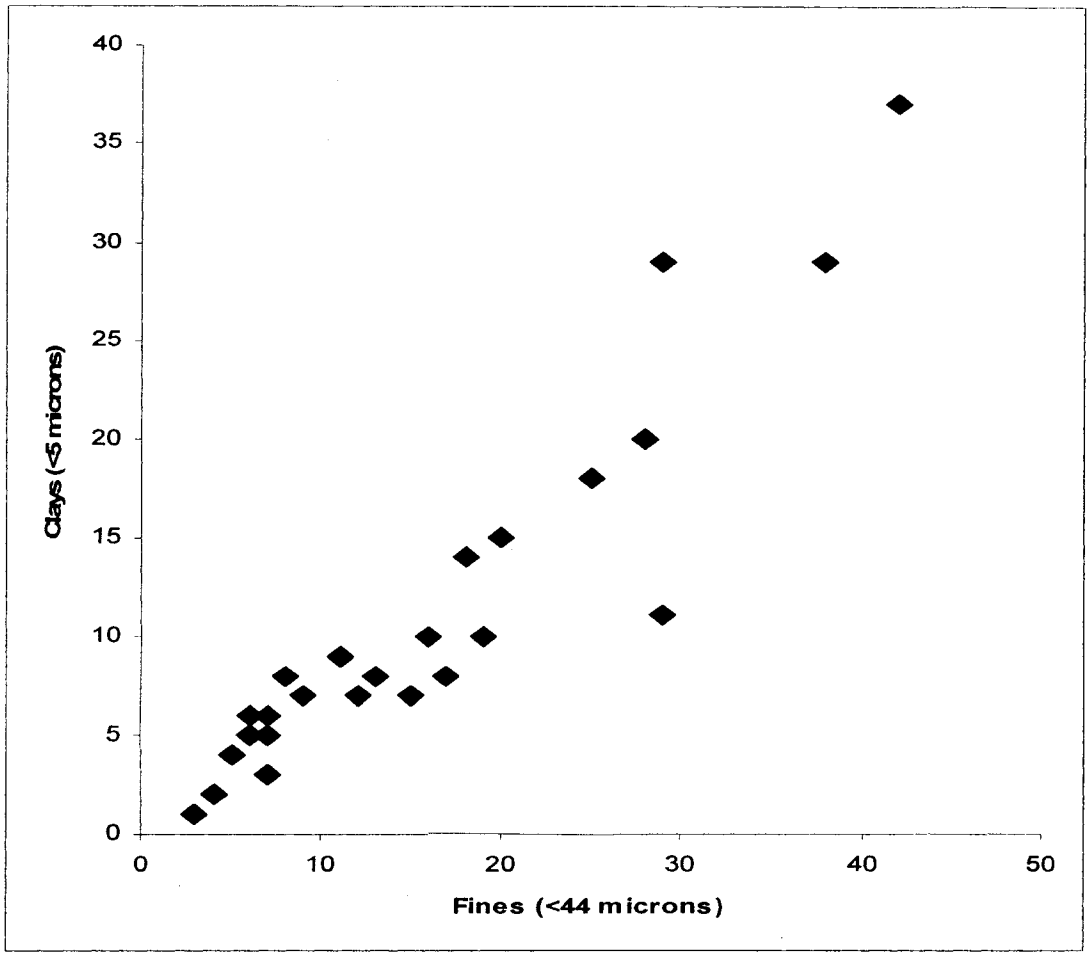

Figure 2.2.Correlation between the fines and clay portion of the Athabasca oil sands. (Sanford and Levine, 1985)

Kotlyar et al. (1982,1999) developed a better understanding of the nature of the solids component of bitumen and their role in bitumen quality and processing. They analyzed the fines content in both estuarine and marine oil sands, and the bitumen metals content from a representative sample of Athabasca bitumen. They used toluene in a batch extraction unit to remove with the bitumen samples from the ores, following by low speed centrifugation. This procedure allowed the separation of the bitumen into a continuous phase soluble in toluene where the fine solids and inorganic particles were dispersed and a so-called "rag layer" where asphaltene precipitated with the organic particles. As they observed, the amount of inorganic Ca and Mg remained high in the "clean bitumen portion" as well as the amount of Fe, Ti and Al that is a defining characteristic for the fines and the clay portions respectively.

Sparks et al.(2003)observed the fine solids as water bi-wettable aluminosilicates coated with water and organic material that might have implications during the hydrolysis reaction if further interactions between the salts and the asphaltenes covering the solids would occur. The highly active surface of the fine solids allows them to form a rigid barrier between water droplets and the continuous phase of bitumen. As a consequence, these clay-water entities are dispersed into the bitumen, forming a stable colloidal system that is extremely difficult to separate, as confirmed by the work of Fong et al. (2004), who found that bitumen losses due to the presence of clay particles, at various concentrations, were highly significant.

Table 2.3 indicates the metal analysis of bitumen before and after removal of solids. It can be seen that removing of fine solids decreases the concentration of Ca by 98%, which may have implications in the interactions between the fine solids and with the dissolved inorganic salts entrained in the water droplets as will be discussed in the results of this work.

Table 2.3. Effect of solids removal on metal analysis from bitumen

(Kotlyar et al., 1999)

	Concentration (w/w % of sample)						
Source	Fe	Mn	Ca	Ti	V	Ni	Al
Original bitumen	0.4	0.012	0.14	0.14	0.082	<0.02	0.64
BS-free bitumen	0.01	0.002	<0.02	<0.005	0.088	<0.02	<0.05

The data of Table 2.4 illustrate the metals and chlorine content from a dried sample from a coker feed of Athabasca Bitumen subjected to elemental analysis. Sub-samples were ashed and the residue dissolved in acid prior to analysis for metals by inductively coupled plasma spectroscopy. (Cookson, 2000).

Table 2.4. Metals and Chlorine Content of Athabasca Bitumen (Cookson, 2000)

	n	Wt%	MW	gmol/100kg	mol/mol Ca	mol/mol Al
Solids	6	0.38				
		PPM, wt/wt				
Chlorine	4	25.2	35.45	0.071	0.382	
Aluminum	8	477	26.98	1.77		**1.0**
Calcium	8	75	40.078	0.186	**1.0**	0.105
Iron	8	258	55.845	0.462		0.261
Potassium	8	51	39.0983	0.131	0.705	0.0743
Magnesium	8	34	24.305	0.140	0.752	0.0792
Sodium	8	42	23.0	0.182	0.976	0.103
Nickel	8	90				
Silicon	8	702	28.0855	2.50		1.413
Vanadium	8	238				

The nickel and vanadium are present in oil-soluble organic form whereas the remaining elements are primarily present as inorganic salts and clay complexes.

The data from the analysis of metals and chlorine from the feed and the coke (Tables 2.4 and 2.5) are consistent in that the relative molar concentrations of Mg, Na and K to Ca are all within a factor of two. In contrast, the analytical data for leachable ion contents of the pond water from the same depositional environment where the bitumen sample was extracted (Table 2.5) suggests that chlorides will be associated mainly with Na, but the bitumen and coke both show much more Ca and Mg. This could lead to a large difference in the reactivity of the chlorides, depending on which cation is associated with the chlorine.

Table 2.5. Relative concentrations, mol/mol calcium, of alkali and alkaline earth metals and chlorine in bitumen (calculated from data of Chung et al., 2000)

Element	Feed Bitumen (mol/mol calcium)	Coke, from analysis of ash	Pond water
Calcium (Ca)	1.0	1.0	1.0
Magnesium (Mg)	0.75	0.56	0.78
Sodium (Na)	0.97	0.64	56
Potassium (K)	0.70	0.56	0.46
Chlorine (Cl)	0.38	na	33

The presence of the same relative amount of Ca in the feed bitumen as well as in the pond water is an important fact that highlights the high exchangeability of this cation, which agree also with the work of Baptista et al (1989) and may have implications in the interactions between clay and inorganic salts in bitumen when undergoing hydrolysis in the presence of steam.

2.2.2. Characterization of Clays in Athabasca Bitumen

The high concentrations of silicon and aluminum from Tables 2.3 and 2.4 provided evidence of the presence of clay mineral in the bitumen. Clay minerals only appear in the fines fraction of oil sands (paticle size <44 μm). Clay minerals predominantly belong to the solids portion less than 2 microns (Gray and Masliyah, 1998).

Many authors define clays as a "natural, earthy, fine-grained material, largely composed of hydrous aluminum and magnesium silicates, which develops plastic

properties when mixed with a limited amount of water" (Gillot, 1987). Chemical analysis of clays shows that the composition is frequently silica, alumina and water, with considerable quantities of iron, alkalis and alkaline earths (Grim 1953).

Several studies have been conducted over the last 25 years to elucidate the clay mineralogy of the Athabasca oil sands solids. In one of the earlier studies, Bayliss and Levinson (1976) analyzed 13 core samples from ranges 7 to 16 west of the fourth meridian. They found that the clay fraction is predominantly kaolinite and illite with the occasional presence (up to 6%) of chlorite, up to 1% montmorillonite and up to 10% mixed-layer clays in some locations. The kaolinite-to-illite ratio ranged from 1 to 2. In a later analysis of fine tailings from the extraction process, Kessick (1979) identified only kaolinite and illite in the clay fraction. Ignasiak et al. (1983) identified the main clay minerals to be kaolinite and illite–smectite mixed layers with less than 10% expandibility. In addition, they observed well-crystallized, ordered kaolinite in the solids that remained following bitumen extraction from oilsands. Poorly ordered kaolinite was observed to be associated with precipitated asphaltenes and the presence of dehydrated halloysite was also suggested. In another study, Ignasiak et al. (1985) found kaolinite and illite to be the predominant minerals, with minor quantities of chlorite, but no smectite or mixed-layer clay minerals.

Kotlyar et al. (1984, 1985) also reported the presence of kaolinite and illite, but no smectite or mixed-layer minerals. Other studies by Kotlyar et al. (1987,1990) showed up to 90 wt.% amorphous minerals (the rest being kaolinite and illite) in the clay fraction of an oil-free oil sands solid. The amorphous minerals were attributed to Fe and Al oxides with tightly bound organics. In a study of 10 different oil sands core

samples, Smith and Ng (1993) reported from 4 to 12 wt.% swelling clay minerals in the clay fraction. The primary clay minerals were kaolinite and illite. Other studies have indicated the presence of montmorillonite in smaller amounts (Li et. al., 2004; Sparks et. al. 2003; Tu et al., 2004). A more recent analysis of the clay fraction in Athabasca Oilsands is given in the figure 2.3 below.

Figure 2.3. Composition of the clay fraction in Athabasca oilsands (Cuddy, 2004).

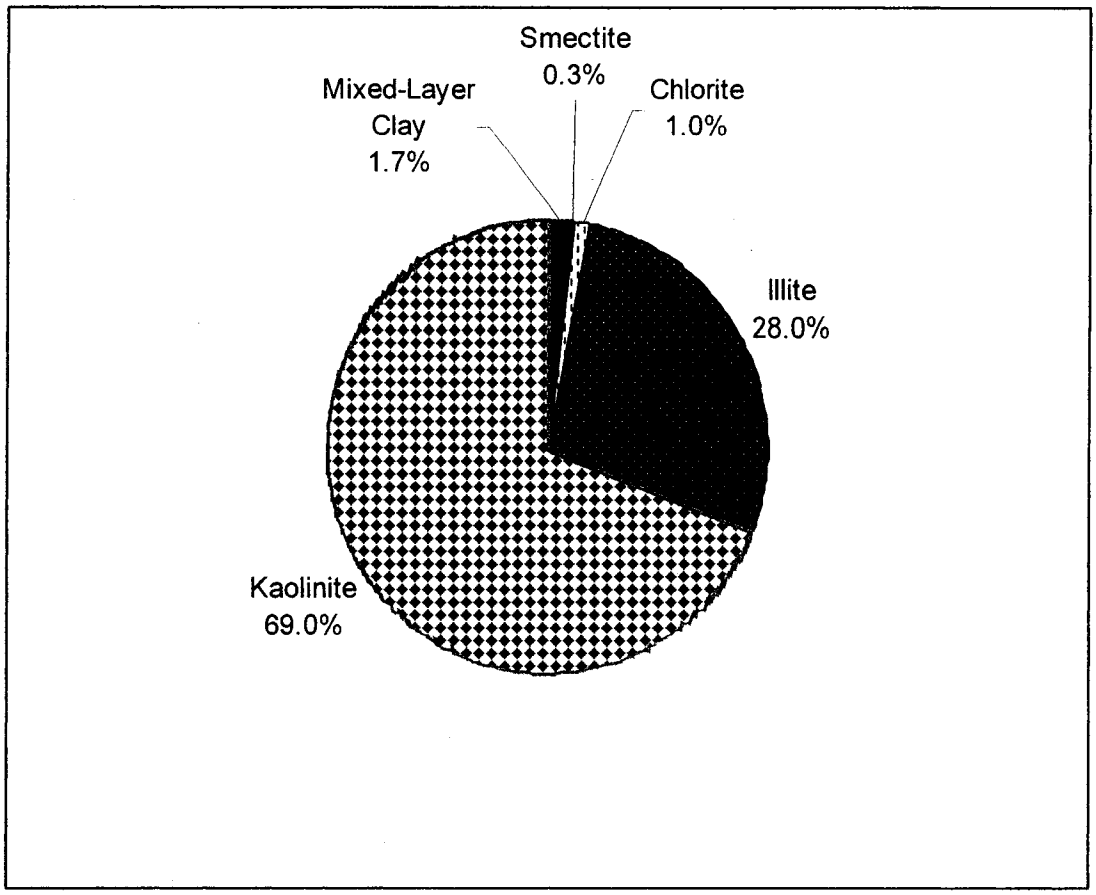

Tu et al. (2004) studied ores with poor processing characteristics by separating the solids fractions into fines (<44 μm), clay material (< 3 μm) and its ultrafine subfraction (<0.3 μm). The reported high surface area of Athabasca oil sands clay fraction and its ultrafine sub-fraction (Omotoso and Mikula, 2003) may contribute significantly to increase the overall surface area of the salt crystals also suspended into the continuous phase of the water- in- oil emulsion.

XPS elemental analysis of the total clay fractions shows that the major elements detected in the outer surface layers are carbon, oxygen, silicon and aluminum. The occurrence of sodium in the samples as show in Table 2.6 strongly suggests that kaolinite in oil sands is present as the sodium form (Tu et al., 2004). Furthermore, the presence of silica in both clay and ultrafines might account for the high surface area exhibited by these fractions. As some studies reported a linear relationship between surface area and cation exchange capacity of Kaolinite (Grim, 1939; Speil, 1940; Harman and Fraulini,1940; Johnson and Lawrence, 1942; Worrall et al., 1958). The surface area might play a major role on the interactions between clays and chlorides during the upgrading of bitumen.

Table 2.6. XPS surface analysis for ultra-fine fractions (<0.3 μm) and total clay (<3 μm) from Athabasca oil sands (Tu et al. 2004).

Elemental Composition (atomic %)										
Fraction		**C**	**O**	**Si**	**Al**	**Na**	**K**	**Mg**	**Ca**	**Fe**
Ultra-Fines	Silica	4.7	60.3	33.7	1.9	0.3	0.2	0.1	b.d.l	b.d.l
Total Clay	Na-Kaolinite	10.7	61.3	13.9	13.2	0.7	b.d.l	0.3	b.d.l	b.d.l
	Kaolinite	6.2	69.6	11.5	10.9	b.d.l	b.d.l	b.d.l	b.d.l	b.d.l
	Smectite	3.2	68.8	16.0	7.0	1.3	b.d.l	0.5	0.8	1.1
	Illite	11.6	62.6	13.2	8.5	b.d.l	2.3	b.d.l	0.3	1.5
	Silica	8.5	62.6	23.4	1.1	b.d.l	b.d.l	b.d.l	b.d.l	b.d.l

b.d.l below detection limit

There is considerable disagreement in the literature on the significance of swelling clays in the oil sands deposits, particularly montmorillonite. These disagreements may stem from difference in the analytical methods, the separation methods, and the origins of the original samples. Every study, however, identifies kaolinite as the dominant clay mineral. Consequently, an understanding of kaolinite-salt interactions during hydrolysis is urgently needed.

2.2.3. Chlorides In Bitumen

The connate water in the oil sand matrix contains various amounts of salts including sodium and chloride concentrations ranging from 10-1000 mg/kg of oil sands as well as calcium and magnesium ions whose which concentrations varying up to about 40 mg (Gray and Masliyah, 1998; Parkash and Surinder, 2003) .Chlorides are also found in the pond water; therefore in the emulsified process water. Studies on chemistry modeling of tailings pond ion concentrations made by Wallwork (2004), predict an increase in the concentrations of chloride of circa 40 mg/l per year. Moreover, froth from the naphtha-based processes (Suncor, Syncrude, CNRL), contains nearly 7.3% of emulsified water that is diluted with naphtha to promote its coalescence (Romanova et al., 2004).

As already mentioned in the Introduction, desalting of heavy oils uses two stages: upstream dehydrator and downstream desalter. The crude oil is heated upstream of the dehydrator to lower its viscosity, which increases the falling speed of water droplets through crude. The heated crude at 138°C-150°C enters the dehydrator where the coalesced water droplets will fall by gravity and collect in the bottom of the dehydrator. The dehydrated crude rises to the top and exits the dehydrator through the outlet header towards the second stage of desalting for further water-washing. (Choi, 2002). After dehydration of the oil, the remaining oil-wetted salts will associate with the suspended clays, thus promoting the stabilization of water-in-oil emulsions and sludge formation. Salt content of crude oil is usually measured in pounds of chlorides, expressed as equivalent sodium chloride, per thousand barrels of clean (water-free)

crude or 10 lbs salt/ 1000 bbl crude -expressed as NaCl- (Nelson W.L.,1958; Surinder, 2003).

From the studies made by Choi (2005), as well as process practices it can be concluded that chlorides of sodium, calcium and magnesium are found in bitumen and heavy oil in several forms; namely a) dispersed droplets of both connate and injection water-soluble salts; b) salt crystals resulting from dehydration of water from crude oil; and c) salt crystals associated with fine solids, again resulting from dehydration of oil.

2.3. Hydrolysis of Chlorides

When the chloride salts from bitumen are subjected to dry steam during upgrading operations, they can undergo hydrolysis reactions. Upon hydrolysis, a portion of the chloride from the salt particles gets converted into hydrochloric acid, which will condense in the overhead system of the distillation column where it will corrode the overhead condensers. Although the hydrolysis reaction also produces a stoichiometric equivalent quantity of reacted calcium and magnesium salts, the volatility of hydrogen chloride results in its separation from these basic compounds with the result that zones of condensation are bathed with hydrochloric acid thus contaminating a variety of downstream processes.

When reacted with amines, hydrochloric acid can give amine hydrochlorides (Sagues et al.,1982). Reactor effluent streams from hydrotreating, which releases ammonia, are subject to ammonium chloride salt fouling and corrosion at temperatures up to ~149°C.

2.3.1.1. Hydrolysis Reactions at Refining Temperatures

A portion of the chloride salts contained in the crude oil are hydrolysable at temperatures from 120 ^{0}C up to 340°C when they are subjected to dry steam. One of the earliest studies is evidenced by Roberts et al. (1939) who implemented methods for extraction of salts from oil and for analysis of the aqueous extract. From the results obtained on 4 crudes by 6 extraction methods, they observed that the reactivities of the pure salts are in the sequence Mg>Ca>>Na. Similarly, Samuelson (1954), studied the relationship between salt content of crude petroleum and evolution of hydrogen chloride on distillation; four typical crude oils were desalted to varying degrees, and raw and desalted samples then distilled in laboratory under simulated refinery conditions to determine amounts of hydrogen chloride evolved, hypothesized on the following reactions:

$$MgCl_2 + 2H_2O = Mg(OH)_2 + 2HCl \quad (2.2)$$

$$CaCl_2 + 2H_2O = Ca(OH)_2 + 2HCl \quad (2.3)$$

$$NaCl + H_2O = NaOH + HCl \quad (2.4)$$

Despite the general acceptance of the former equations, the experimental work of Eaton (2000) suggests that metal hydroxychlorides are alternate products from the hydrolysis of the divalent magnesium and calcium salts. Their experimental work on pure chloride salts implied that only magnesium and calcium salts should react with steam at temperatures to 350 °C, and confirmed that the proper overall reactions for MgCl2.6(H2O) and potentially for CaCl2.2H20 at temperatures to 350 °C are:

$$MgCl_2 \cdot 6(H_2O)\ (s) = Mg(OH)Cl\ (s) + HCl(g) + 5H_2O(g) \qquad (2.5)$$

$$CaCl_2 \cdot 2(H_2O)(s) = CaOHCl(s) + HCl(g) + H_2O(g) \qquad (2.6)$$

Both reactions pathways above are supported by thermodynamic calculations made at the University of Alberta, showing that the hydrolysis of both anhydrous $MgCl_2$ and $MgCl_2 \cdot 6(H_2O)$ were favorable at the experimental conditions, whereas thermochemical data for calcium hydroxychloride implied that the equivalent hydrolysis reaction of anhydrous $CaCl_2$ to form Ca(OH)Cl was not favorable over the same range of temperature at atmospheric pressure as shown in Table 2.7, only the hydrated form of the Calcium salt was favorable. Finally, the conversion of sodium chloride was thermodynamically unfavorable at 150-350 °C with steam at 1 atmosphere pressure. The formation of the MgClOH was confirmed by Gray et al. (2006), by X-ray diffraction analysis of the salts remaining in the crude after the hydrolysis reaction. The XRD patterns were mostly assigned to the magnesium hydroxychloride (MgOHCl) form of magnesium.

Table 2.7. Thermodynamic calculations of hydrolysis of chlorides (Factsage version 5.3). (Gray et al, 2000. University of Alberta)

Salt to Hydrolyze	T(°C)	ΔG_R (kJ/mol)
$MgCl_2$	150 °C	-21.35
	350 °C	-35.00
$CaCl_2$	150 °C	52.6
	350 °C	52.9

The information provided above suggests that only calcium and magnesium chlorides are a problem in upgrading processes.

2.3.1.2. High Temperature Fusion-Type Reactions

Briner and Roth (1948) studied the thermodynamics of the release of hydrochloric acid for a system consisting in molten alkali salts + fine solids in the presence of steam at high temperatures up to 800 °C. The importance of their study lies in the fact that the conditions of thermodynamic equilibrium determine the rate and yield of the hydrolysis, mainly the temperature as well as the presence of additives like kaolin. However, it can be noted that the driving forces for reactions at 600-800 °C may be completely different than those driving the hydrolysis of salts at 150-350 °C which is the temperature range of interest in this work.

2.3.1.2.1. Molten Salts + SiO_2 in the Presence of Steam

Briner and Roth (1948) calculated the effect produced by the addition of SiO_2 over the hydrolysis of NaCl, represented by the Equation 2.8.

$$2\,NaCl + H_2O \longrightarrow 2\,HCl + Na_2O \qquad (2.7)$$

$$2\,NaCl + H_2O + SiO_2 \longrightarrow 2\,HCl + 2\,Na_2.SiO_3 \qquad (2.8)$$

The equilibrium constant given by the equation 2.9 below:

$$K_p = \frac{P^2_{HCl}}{P_{H2O}} \qquad (2.9)$$

is linked to the free energy ΔG, as illustrated by the equation 2.10:

$$\Delta G = -RT \ln K_p \qquad (2.10)$$

ΔG is also related to the enthalpy and entropy of the reaction through the fundamental equation of thermodynamics:

$$\Delta G = \Delta H - T\Delta S \qquad (2.11)$$

From the equilibrium constant and a given water vapor pressure, we can use thermodynamic data to calculate the equilibrium pressure for the ($P_{HCl} = \sqrt{(K_p . P_{H2O})}$) which affects the yield of production for hydrochloric acid. Table 2.8 illustrates the

variation of P_{HCl} as a function of temperature at a P_{H20} = 101.33 Kilopascals after applying the method of Lewis for the hydrolysis of NaCl with SiO_2.

Table 2.8. Thermodynamic properties for the hydrolysis of nacl in presence of steam (Briner and Roth, 1948)

T (°C)	ΔG cal	K_p	P_{HCl} Kpa
25	40800	$1.26.10^{-30}$	$1.13.10^{-13}$
400	30300	$1.26.10^{-10}$	$1.13.10^{-3}$
800	19860	$9.22.10^{-5}$	770.07

The data of table 2.8 show that an increase in temperature favours the equilibrium towards the hydrolysis and consequently the formation of hydrochloric acid. The relevance to this work lies in that this trend is also valid for processing conditions between 150 °C and 350 °C as will be illustrated in the following chapter. From the value of free energy for the Na_2O deduced by Kelley et al. (1939), Briner and Roth (1948) calculated the formation energy for SiO_2 and Na_2SiO_3 and also the corresponding entropies which from equations 2.8,2.9 and 2.10 can be used to determine the equilibrium pressure towards the release of hydrochloric acid.

2.3.1.2.2. Molten Salts + Metakaolin in the Presence of Steam

The equilibrium of hydrolysis with the addition of metakaolin will be represented by the equation 2.12 below:

$$2NaCl+2SiO_2.Al_2O_3+H_2O_2 \longrightarrow 2HCl+Na_2O+SiO_2 \longrightarrow 2HCl+2SiO_2Al_2O_3.Na_2O_3 \quad (2.12)$$

Studies from Klever and Kordes (1930) were useful for calculating the heat of formation for metakaolin with the following thermo chemical equation:

$$SiO_2 + Al_2O_3 = 2\ SiO_2.Al_2O_3 \quad (2.13)$$

ΔH= 15.8 Kcal, reaction strongly endothermic.

Thus, the increase in the heat of reaction over the hydrolysis of a metallic chloride with the addition of the combination Al_2O_3 + SiO_2 will be equal to 15.8 Kcal/kg as illustrated by equation 2.14:

$$2MCl_2+2SiO_2+Al_2O_3 + H_2O \leftrightarrow 2HCl +2\ SiO_2.Al_2O_3.M_2O \quad (2.14)$$

In the same way, based upon the equality of entropies of two reactions, the free energy will increase the amount of 15.8 Kcal/Kg, thus leading to a significant increase of the equilibrium constant for the hydrolysis, and at the same time a notable increase over the yields of production of hydrochloric acid.

The yields of hydrochloric acid from the experiments of Briner and Roth (1948) for the hydrolysis of NaCl in presence of kaolin are summarized in Figure 2.4. It illustrates that the release of hydrochloric acid depends strongly from both temperature and the presence of clay. Briner and Roth (1948) ascribed this behavior to the energetic gain from the formation of a silico-aluminate when combining metakaolin and the alkaline oxide derived from the NaCl.

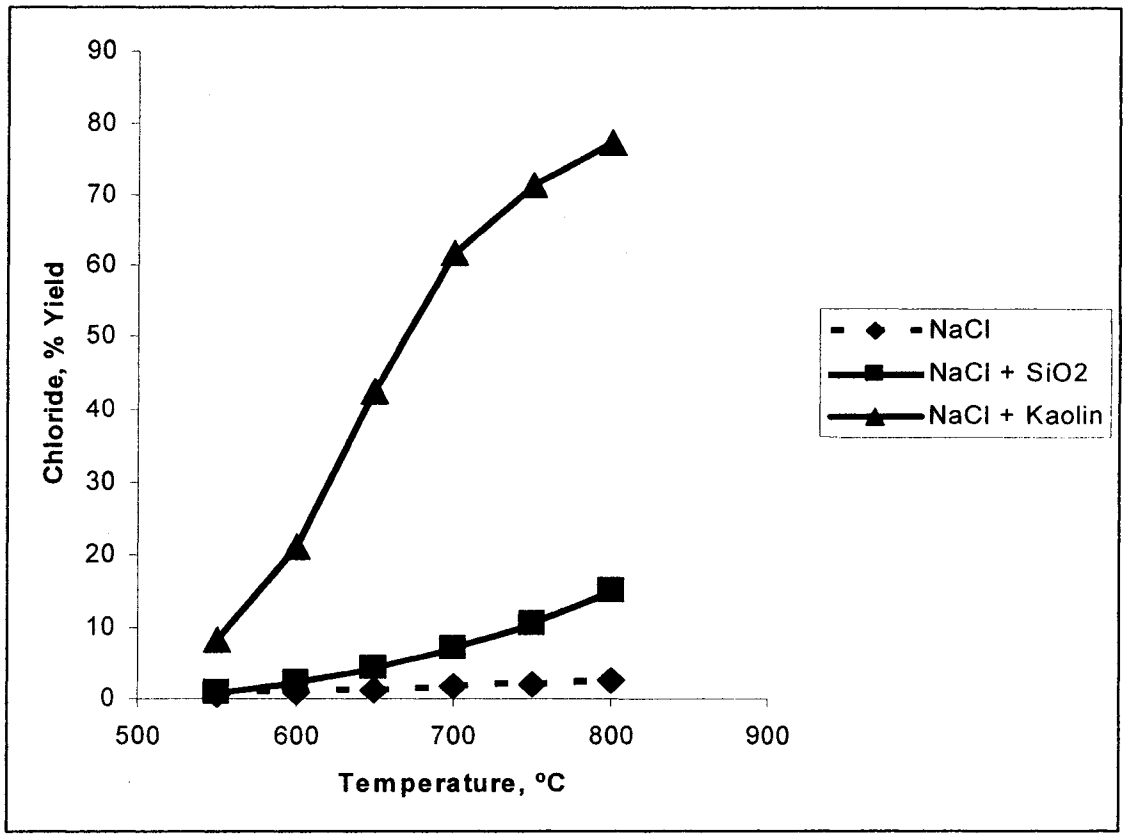

Figure 2.4. Yields of hydrochloric acid for the hydrolysis of NaCl. (Briner E. and Roth P., 1948)

The favorable effect of kaolin in the hydrolysis of salts is calculated by Briner and Roth (1948) and explained as a variation in the free energy and the reaction entropy of the system. Figure 2.4 above illustrates the yield of chloride for the three reactions above at 700 °C when the salts are still in solid state. The addition of kaolin increases the yield of hydrochloric acid by a factor of 9 when compared to the hydrolysis of NaCl only. The energetic gain and consequently the increase over the yield of hydrochloric acid is proportional to the increase of the heat of reaction. For example, at 550 °C, the addition of kaolin increased the extent of release of chlorine from sodium chloride from 0.52% to 8.2%. Consequently, the fine solids which are mainly clays may play an important role in hydrolysis of the chlorides.

2.4. Structure of Clay and Interactions with Salts

As seen in the previous sections, bitumen separated from the oil sands contains clay particles associated with the dissolved salts entrained in the water droplets. These clay-water entities may increase the extent of hydrolysis of the salts that are dispersed into the deasphalted phase of bitumen, as it will be showed by the experiments done with kaolinite and chloride salts. The following elements are essential for the calculation of structural formulae of most clay minerals and silicates: Si, Al, Fe^{3+}, Fe^{2+}, Mg, Ti, Mn (in special cases), P, Ca, Na, K and H_2O evolved below 105 °C (H_2O^-) and between 105 °C-1000 °C (H_2O^+). (Jackson, 1979; Lim and Jackson, 1982; Laird et al., 1989; Amonette and Zelazny, 1994).

Clay minerals belong to the phyllosilicate group. Phyllosilicates are characterized by layers, whose elementary organizational levels are "sheets". Considering the

difference in ionic diameter, three types of coordination determine the elementary polyhedra that make up the various sheets of the crystal structure:

-4 fold coordination (SiO_4^{4-} or AlO_4^{5-} tetrahedron).

- 6 fold coordination (octahedron whose centre is occupied by a Al^{3+} , Fe^{3+} , Fe^{2+} , Mg^{2+}) -12 fold coordination cation for the most part (dodecahedron whose centre is occupied by a cation with a wide diameter: K^+ , Na^+ , Ca^{2+} and the vertices are formed by O^{2-} anions of two opposite tetrahedral sheets).

The sheet's framework is formed by cation-anion bonds (bonds intermediate and covalent bonds) whose length will be used as a reference in the calculation of the cell dimensions. Ionic diameters will be used for the determination of cation coordination. Bonds of the silicate crystal framework are typically intermediate between ionic and covalent. Consequently, each bond is polar and characterized by an electric dipole moment. This is of great importance for the electric charge distribution at the outer surfaces of each layer in a phyllosilicate structure. (Sainz-Diaz et al. 2001).

Its important to study the structure of the tetrahedral "sheets" in order to classify and define the most important clays relevant to this work:

- The Tetrahedral Sheets: SiO_4^{4-} or AlO_4^{5-} tetrahedral are linked together by sharing three of four vertices (three basal oxygens, the fourth being the apical oxygen). This means that one O^{2-} anion bonds with a Si^{4+}- Si^{4+} or a Si^{4+}- Al^{3+} cation pair. These bonds form a two dimensional lattice (tetrahedral sheet) defining hexagonal cavities.

- The Octahedral Sheets: Octahedra are laid on a triangular face. They are linked together by sharing their six vertices. This means that each anion is bonded to three cations in the trioctahedral type. The edge of the octahedron corresponds to the ionic diameter of the O^{2-} or OH^- anions.

Layers result from the association of several ionic sheets, according to a limited number of combinations. The different patterns exhibited by the tetrahedral and octahedral sheets and the manner in which the layers are stacked rule the differentiation of clays. The classification of clays according to the layer pattern is described in Table 2.9.

Table 2.9. Classification of phyllosilicates related with clays. (Meunier,2005)

Layer type	Group	Sub-group	Species
1:1	Serpentin-kaolin	Serpentines	Chrysolite, antigorite, lizardite, amesite, berthierine
		Kaolins	Kaolinite,dickite,nacrite
2:1	Talc-pyrophyllite	Talcs Pyrophyllites	Talc, willemseite Pyrophyllite
	Smectite	Saponites	Saponite, hectorite, stevensite
		Montomorillonites	Montomorillonite, beidellite, nontronite
	Mica	Trioctahedral micas	Trioctahedral mica
		Dioctahedral micas	Muscovite, paragonite, illite, phengite, celadonite, glauconite

Among the previous classification of clays, the properties of Kaolinite will be emphasized in the next section due to its reported abundance in bitumen solids as well as its relevance for this experimental work.

2.4.1. Chemical Structure of Kaolinite

Kaolinite is a 1:1 layer mineral, in which one tetrahedral SiO_4 layer shares corners with an octahedral sheet of, e.g., $AlO_2(OH)_4$. The thickness of this two-sheet unit is about 7Å and a product of advance weathering processes. One layer of the mineral consists of an alumina octahedral sheet and a silica tetrahedral sheet that share a common plane of oxygen atoms and repeating layers of the mineral are hydrogen bonded together . As a consequence of this structure, the silica/oxygen and alumina/hydroxyl sheets are exposed and interact with different components (Grim, 1968).

In the unit cell of a kaolinite, four sites of the dioctahedral sheet are occupied by Al^{3+} cations and two are vacant (Table 2.10). The negative charge of the oxygen anion framework is balanced by the positive charge of the tetrahedral and octahedral cations. The distance between two neighbouring 1:1 layers corresponds to the thickness of the combined tetrahedral sheet + octahedral sheet (theoretically:2.11 + 2.15= 4.21 Å) to which is added the thickness of the interlayer spacing. The interlayer spacing of kaolinite is 7.15 Å. and increases with the substitution rate of Mg^{2+} for Fe^{2+}.

Table 2.10. Calculation of the unit cell mass of kaolinite. (Meunier, 2005)

Element	Mass	Stoich. Coef	Kaolinite
Si	28.09	4	112.36
Al	26.98	4	107.92
Mg	24.30		
O	16	18	28.8
H	1	8	8
Total			516.28

Some oilsand clays mainly the kaolinite and illite types, contain appreciable quantities of iron oxide, with calcium and magnesium species, either adsorbed as coatings or acting as cementing agents between the clays. In the wet state this iron oxides form hydrated gels which can link rigid clay particles and consequently trap oil and water.(Table 2.11).

Table 2.11. Chemical oxides composition of source clay KGa1-b (Meunier,2005)

Source Clay: KGa-1	% Oxide
SiO2	43.36
Al2O3	38.58
Fe2O3	0.35
TiO2	1.67
MgO	0.04
CaO	0.04
Na2O	0.05
K2O	0.00
P2O5	0.37
Ignition loss 110–550_C	13.60
Ignition loss 550–1000_C	1.45
Total	99.51

Minerals composed of 1:1 layers such as kaolinite, exhibit two types of outer surfaces: a siloxane surface and a surface formed by (OH)- groups. The layers are electrically neutral, thus preventing the adsorption of ions or molecules in the interlayer spaces. The small dimension of clay minerals increases greatly the contribution of edge to the overall surface. These sites are electrically charged, therefore, neutrality is obtained only by adsorption of ions from surrounding solutions. This condition is the basis for the clays cation exchange which will be explained with further details in the following sections.

2.4.2. Physical Structure of Kaolinite

As a consequence of its well-packed structure, kaolinite particles are not easily broken down and the kaolinite layers are not easily separated. Hence, most sorption activity occurs along the edges and surfaces of the structure. Kaolinite can form a barrier that is not easily degraded and naturally occurring sediments and deposits containing an abundance of kaolinite interspersed with other minerals are effective in controlling the migration of dissolved species (Devidal et al., 1996). Clay impurities will affect the degree of disorder and the particle size of the clay (Balan et al., 2001).

Kaolinite is non-expanding and as a result of its high molecular stability, isomorphous substitution is limited or nonexistent (Mitchell, 1993). Kaolinite is the least reactive clay (Suraj et al., 1998). However, its high pH dependency enhances or inhibits the adsorption of metals according to the pH of the environment (Mitchell, 1993), and this metal adsorption is usually accompanied by the release of hydrogen (H+) ions from the edge sites of the mineral. Adsorption may also take place on the flat exposed planes of the silica and the alumina sheets (Spark et al., 1995).

Kaolinite particles differ in a few quantitatively measurable properties from other clay particles. Most clay and other mineral particles, when suspended in water, obey the classical laws of colloidal suspensions in that they tend to form more stable suspensions at low ionic strengths than at high ionic strengths (Verwey and Overbeek, 1948). Aqueous suspensions of kaolinite, however, display the exact opposite

behavior; they are most stable in the presence of salt (NaCl), while they flocculate in distilled water (Schofield and Samson,1954).

Kaolinite crystals very often exhibit the shape of hexagonal prisms. These prisms are flattened and have defects due to substitution of Al3+ for Fe3+. They grow thicker until they take the shape of "books" several tens of microns thick and progressively transform into a rhombohedral morphology. Experimental works on kaolinite (Fialips et al. 2000) show that crystal morphology depends on supersaturation and Ph conditions.

Kaolinite is a material of naturally fine particle size. Individual kaolinite particles are often finer than two microns. Kaolinite is a flake shaped mineral with high aspect ratio (ratio of mean diameter to thickness) of approximately ten. Often the kaolinite plates are stacked together by cohesive forces.

The kaolinite crystals are often bonded together randomly by weak bonds, or by iron oxides or organic matter. The so-called coarse flakes are in effect stacks of fine particles which because of their greater mass are perceived as coarse particles. The shape and size of aggregates vary significantly and stacking occurs either by aggregation or coalescence as shown in the electron micrograph of figure 2.5.

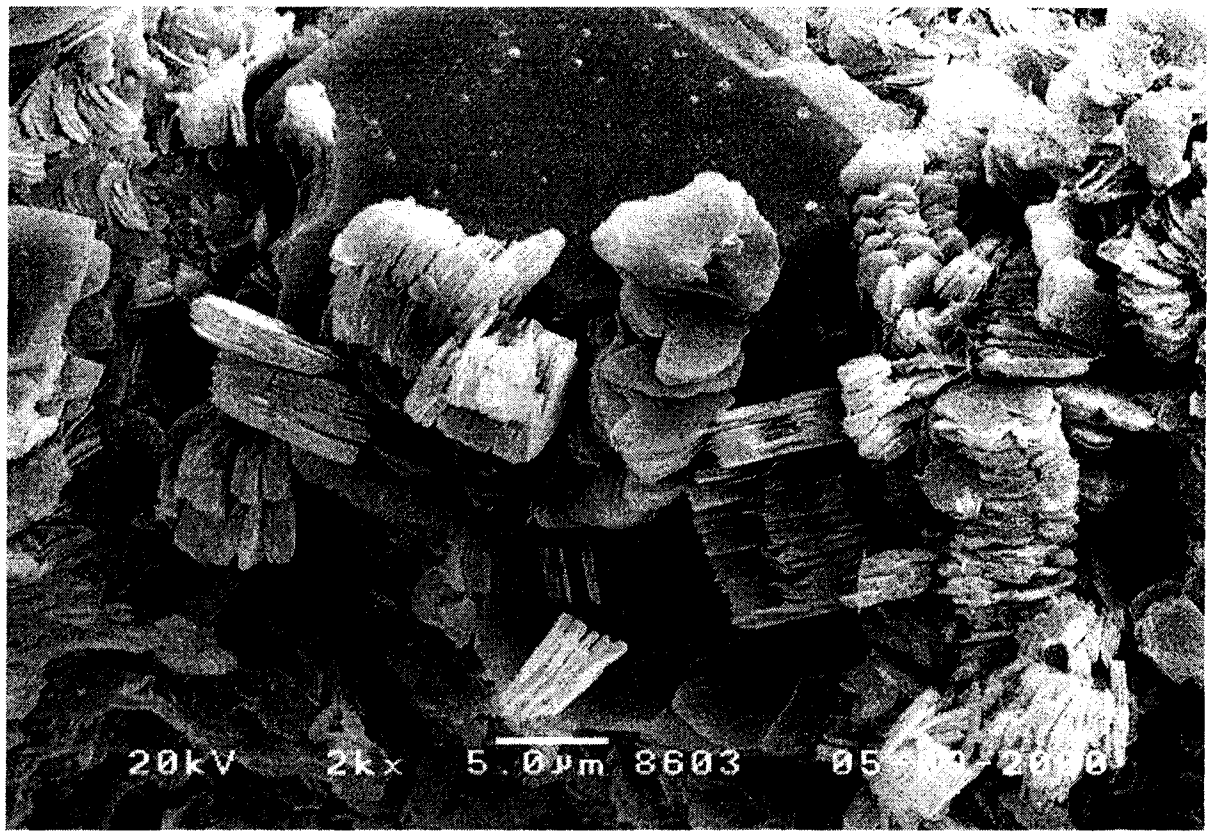

Figure 2.5. Electro micrograph of kaolinite.

http://webmineral.com/data/Kaolinite.html (COPYRIGHT OMNI LABORATORIES Reproduced with permission of the copyright owner. October 6, 2006)

Oscarson et al.(1989) studied the effect of steam on selected properties of clays. Steaming the clay did not affect its cation exchange capacity, nor was there any detectable change in the mineralogical composition of the clay as indicated by X-ray diffraction analysis. Scanning electron microscopy showed that the aggregate size and the particle morphology of the clay were altered. Steam significantly affects the specific volume (SV) of the clay even at temperatures as low as 110 °C.

A large variety of molecular species can be introduced between the 1:1 layers of kaolinite. In addition to the molecular species, certain inorganic salts also can be introduced between the 1:1 layers (sometimes called intercalates). Although kaolinite normally has a low compressibility due to its well-packed structure, the adsorption of the divalent metal cations may cause swelling of the kaolinite. The empty spaces that are developed between the molecules absorb the external pressure and the compression index increases (Mitchell, 1993; Grim, 1968; Chen et al., 2000).

2.4.3. Interactions of Kaolinite with Water

Water frequently forms an intercalate with kaolinite, in the form of the mineral halloysite which has the formula $Al_2Si_2O_5(OH)_2 \cdot 2H_2O$. The addition of the two molecules of water increases the thickness of the layer from 7 A to 10 A. Kaolinite itself can be hydrated by a relatively simple chemical treatment to produce both a dihydrate, similar to halloysite, and a monohydrate with a thickness of about 8.6 A.

Similarly, the concept of water adsorption also exhibits a different physical reality for each type of clays. Indeed, in neutral minerals such as kaolinite, only the external crystal surfaces exhibit an adsorption capacity. This is not the case of smectites like montmorillonite, which can adsorb water in their interlayer spaces. Due to the plasticity of clays, the lost of water can be reversible, but once the crystalline structure is modified at higher temperatures the process is irreversible (Table 2.12).

Table 2.12. Dependence of water release with temperature and type of clays (Meunier, 2005)

Clay	Temperature range (°C)
Kaolinite	500-600
Montmorillonite	500-750
Illite	350-600

2.4.3.1.Thermal Analysis of Kaolinite

The energetic state of water in clays is another chemical property of potential concern to this work. The water molecules impregnating clay materials can be released by evaporation. There are several different types of water and hydroxyl groups associated with a clay matrix that is liberated with increasing temperature. Thermogravimetric analysis (TGA) is often used to qualitatively determine the binding energies of these different types of water, which can then be used to help characterize a mineral.

In TGA, the mass of a sample is monitored vs. temperature while it is heated according to a program in a specific atmosphere (oxidizing, reducing, inert). At lowest temperatures, adsorbed water is lost from clay surfaces in defect sites or at broken bond sites.

Upon heating, kaolinite starts to lose water at approximately 400 °C, and the dehydration approaches completion at approximately 525 °C (Grim, 1968; Bergaya et al., 1996). The dehydration depends on the particle size and crystallinity.

Franco et al. (2004), studied the effects of temperature on the structure of Kaolinite. The results of their thermal analysis on untreated Kga-1 which is the same

clay used in this work, are illustrated in figure 2.5. The thermogravimetric (TG) curve shows that a continuous heating rate originates a slight mass loss below 140 °C, associated with the loss of the loosely bonded adsorbed water on the particle surface. Between 140 and 230 °C the TG curve shows that the mass remains constant. A slight mass loss between 230 and 440 °C is followed by a change in the slope of the TG curve, indicating a faster mass loss from 440 to 580 °C.

After this temperature the mass loss rate decreases and stops at 835 °C. These three stages of mass loss are associated with the dehydroxylation process. The different rates of mass loss, between 230 and 835°C, indicate that the dehydroxylation of KGa-1 occurs in several stages (Figures 2.6 and 2.7).

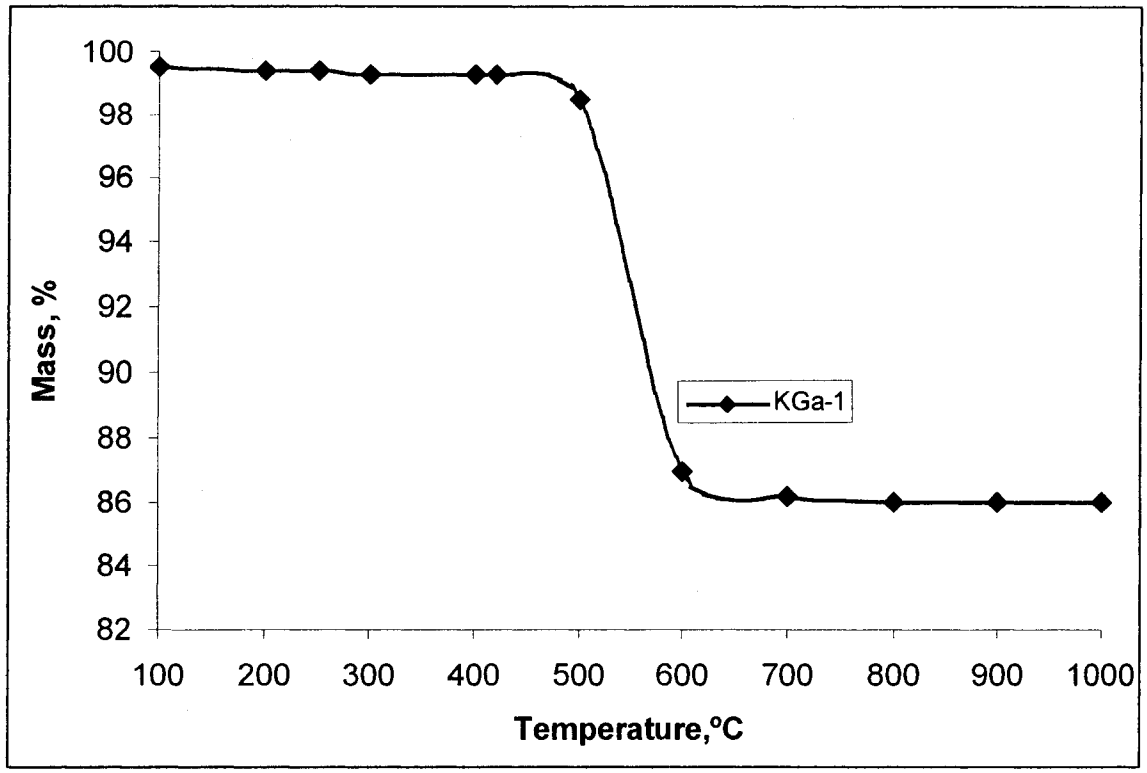

Figure 2.6. TG Curves of a KGa-1 Kaolinite Sample (40 mg). (Franco et al.,2004)

Similarly, the differential thermal analysis (DTA) curve of untreated KGa-1 (Fig. 5a) shows a weak endothermic effect centred at 100°C associated with the loss of adsorbed water, whereas the dehydroxylation process originates an endothermic effect (between 400 and 650°C) centered at 506°C. (Figure 2.8)

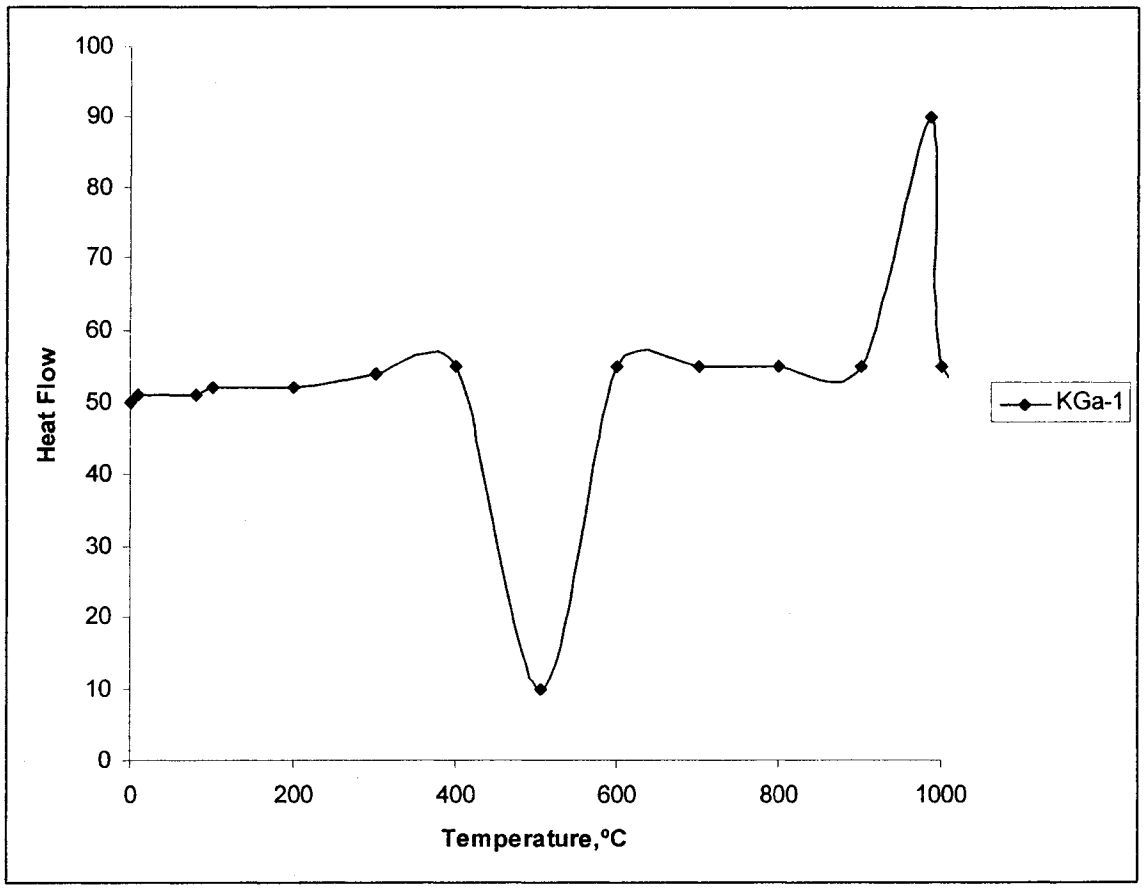

Figure 2.7. DTA curves of a Kaolinite KGa-1 sample (40 mg). (Franco et al.,2004)

2.5. Cation Exchange Capacity Of Clay Minerals

The cation exchange capacity (CEC) is one of the basic properties of clay minerals. It has two origins. One origin is substitution in the tetrahedral- and/or octahedral sheet of the clay mineral layer. Substitution of aluminium by magnesium or of silicon by aluminium leads to a negative net charge. This part of the CEC is considered to be constant since it is almost not sensitive to the pH of the system. The second origin is tetrahedral substitution caused by dissociation of aluminol groups on the edges. Since

the acidity of these groups is weak, the edge charges are pH dependent and the CEC depends on the pH. At pH 7 about 20% of the CEC of smectites is located at the edges (Lagaly, 1981).

2.5.1. Tetrahedral Substitution

As a consequence of its well-packed structure, kaolinite particles are not easily broken down and the kaolinite layers are not easily separated. Unlike smectites, kaolinite is non-expanding and as a result of its high molecular stability, isomorphous substitution is limited or nonexistent (Mitchell, 1993). Kaolinite is the least reactive clay (Suraj et al.,1998).

In low temperature natural minerals, the ionic substitution most frequently observed in the tetrahedral sheet is Si^{+4} replaced by Al^{3+}. The difference of valency between both ions produces a negative charge (positive charge deficiency) and changes the symmetry of the tetrahedral sheet (Meunier, 2005).

2.5.2. Substitutions in the Interlayer Sheet

Cation substitutions in the interlayer sheet usually occur when cations are fixed in the interlayer zone with the water molecules of their hydration sphere. Thus, those cations gain a property typical of smectites and vermiculites: Exchangeability with ions in solution (Sposito 1989; Mercury et al. 2001)

Several methods to determine the cec have been developed. In the early days of clay science determination of the cation exchange capacity was performed by saturating the clay with one cation, then washing out excess salt and finally replacing

the cation by several exchange/washing cycles with another cation (Mehlich, 1948). The collected solutions were employed for the determination of the amount of the replaced cation.

As already mentioned, the clay sheet consists of three sub-units: a octahedral center layer consisting of mainly aluminium (Al) cations; two tetrahedral layers consisting mainly of silica (Si) and oxygen (O) atoms. In the octahedral layer some of the Al^{3+} atoms are substituted by magnesium^{2+} atoms which give rise to a net negative charge on the layer. Similarly, some of the Si^{4+} may be substituted by Al^{3+} resulting in negative charge in the tetrahedral layers.

The exchange process involves replacing one exchangeable atom in the clay by one charged atom from the solution (Equation 2.15). The magnitude of such cation exchange is commonly measured in terms of milli equivalents of cations absorbed per 100 grams (meq/100g).

$$Na^+ - Clay + Ca^{2+} + Cl^- \longrightarrow Ca^{2+} - Clay + 2Na^+ + Cl^- \qquad (2.15)$$

Kaolinite exhibits a cation exchange capacity of 2-10 μeq m^2 and as for all the clay minerals the exchange capacity is controlled by the divalent (Ca and Mg) ions compared to the monovalent (Na and K) (Baptista et al.,1989).

Baptista et al.,(1989) studied the role of oil sand clay in oil sand processing through processing samples of oilsands with various bitumen contents in a series of batch tests. It was found that the percentage of exchanged cations released from the clays relative to the total cations existing in the clays is almost 100% for calcium,

about 62% for sodium, 15% for magnesium and only 7% for potassium. There is an inverse relationship between the cation exchange capacity of clays and the amount of oilsands froth obtained. The contribution to the exchange capacity of the total oil sand solids from each of its fractions is 59% from clays, 15% from silt and 26% from coarse material.

2.6. Surface Area

There is a convenient mathematical idealization which asserts that a cube of edge length, 1 cm possesses a surface area of 6^2 cm^2. However, perfect or ideal geometric forms are unattainable due to voids, steps, pores and other surface imperfections that will always create real surface area greater than the corresponding geometric area.

The specific surface of clay (So) corresponds to the sum of the surfaces of all the exchangeable sites accessible to a given ion or molecule. These sites stretch along basal faces and edges of crystals in proportions that vary according to the type of mineral and to the local Ph conditions. The maximum value of the specific surface of a phyllosilicate is equal to the sum of the sum of the surfaces of all the faces of each elementary layer.

2.6.1. Factors Affecting Surface Area

When a cube, real or imaginary, of 1m edge-length is subdivided into smaller cubes each 1 um in length there will be formed 1018 particles, each exposing an area of 6 x 10-12 m^2. This million fold increase in exposed area is typical of the large surface areas exhibited by fine powders when compared to undivided material. Whenever

matter is divided into smaller particles new surfaces must be produced with a corresponding increase in surface area.

The range of specific surface area can vary widely depending upon the particles' size and shape and also the porosity. The influence of pores can often overwhelm the size and external shape factors.

2.6.2. Surface area from size distributions

Although particulates can assume all regular geometric shapes and in most instances highly irregular shapes, most particle size measurements are based on the so called "equivalent spherical diameter". This is the diameter of a sphere which would behave in the same manner as the test particle being measured in the same instrument.

Optical devices, based upon particle attenuation of a light beam or measurement of light scattering angles, also give equivalent spherical diameters. At best, surface areas calculated from particle size will establish the lower limit by the implicit assumptions of sphericity or some other regular geometric shape, and by ignoring the highly irregular nature of real surfaces.

2.6.3. Surface Properties of Clay Minerals

Among the most important parameters of clays are their surface area (including textural porosity) and surface acidity. Clays have the ability to disperse different clay materials in aqueous suspensions into fundamental particles 1-10 nm thick with a high surface area (up to 800 m^2/g). Omotoso et al. (2002) found that the large surface

area kaolin and illite from the Athabasca oilsands is imparted by varying degrees of smectitic interstratifications.

The most common procedure for determining the surface area of a powder is to derive the amount of adsorbed inert gas (typically nitrogen), as seen on Table 2.13.

Table 2.13. N_2 BET surface areas of various clay minerals (Lowell et al,1984)

Clay	**S.A., m^2/g**
Kaolinite[b]	8.75
Na, Ca-montmorillonite[c]	31.0
Na, Ca-montmorillonite[d]	80.2
Na, Ca-montmorillonite[e]	93.9

[b] Kga-1, well crystallized
[c] SWy-1, Wyoming
[d] STx-1, Texas
[e] SAz-1,Arizona

2.7. Dependence of Exchange Capacity Of Kaolinite on Variations in Particle Size or Surface Area

Many authors (Grim, 1939; Speil, 1940; Harman and Fraulini, 1940; Johnson and Lawrence, 1942; Worrall et al., 1958) have studied the dependence of the exchange capacity of kaolinite on variations in particle size or surface area. In many cases it has

be demonstrated that there is a practically linear relation between the geometric area and exchange capacity.

Johnson and Lawrence (1942), determine the exchange capacity of six closely mono-disperse fractions of purified kaolinite with different particle sizes.The mean particle size of each fraction was calculated from Stokes' law and the corresponding specific surface area was determined from the viscosity relations on additions of NaOH to the electrodialyzed fractions. They found a linear relation between surface area and exchange capacity for all of the fractions studied, which covered the particle-size range of kaolinite rather completely (Table 2.14).

Table 2.14. Effect of surface area on exchange capacity of kaolinite (Johnson and Lawrence 1942)

Mean particle Size μm	Specific Surface Area M^2/g clay	Exchange Capacity Meq Mn^{2+}/100 gr clay
10	1.1	0.4
4.4	2.5	0.6
2.5	4.5	1.0
0.95	11.7	2.3
0.52	21.4	4.4
0.28	39.8	8.1

Ormsby and Shartsis (1960), also found that there is a close association between surface area and exchange capacity based on the high values obtained for the correlation coefficients from exchange and surface data from eight controlled particle size fractions of kaolinite. Their results of surface area measurements (by using the Brunauer, Emmett and Teller both in nitrogen and water adsorption isotherms) correlated well with range of surfaces areas from 10 to 0.05 μm. Specifically, they found a 99% of variation in exchange capacity due to a change in surface area of kaolinite. They conclude that the exchange behavior of pure kaolinite is a surface phenomenon instead of an isomorphous substitution phenomenon within the clay lattice (Figure 2.8).

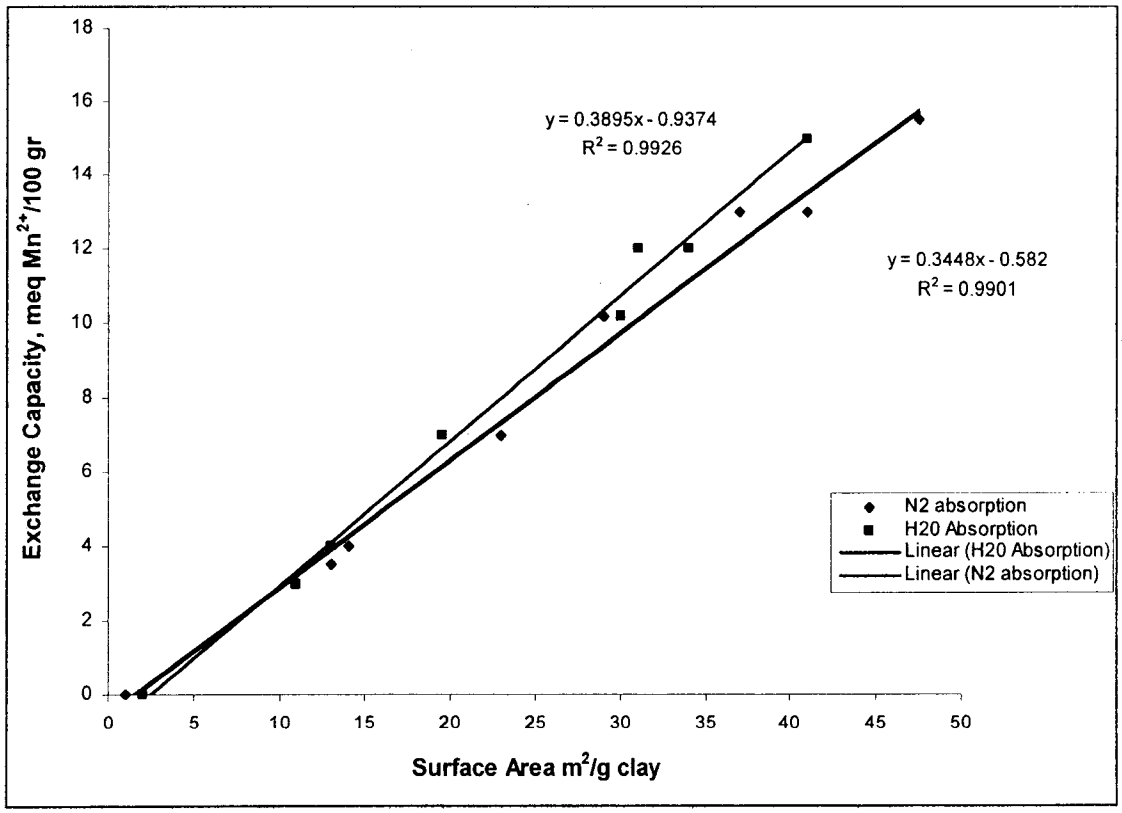

Figure 2.8. Base-Exchange Capacity vs. Surface area for Controlled Particle Size Fractions of Pure Kaolin.

(Perez-Rodriguez et al. , 1988; Sanchez-Soto et al., 1992, 1993, also studied how an increase in mass loss below 200°C occurred by decreasing the particle size of kaolinite. This behaviour is due to particle delamination, agglomeration and degradation (breakdown) and also ascribed to an increase in 'free moisture' of the extremely weakly bound hydroxyl groups.

2.8. Inhibition of Hydrolysis of Salts

Eaton et al. (2005), developed a method for the reduction of hydrochloric acid released when the chloride salt from an alkali or alkaline earth metal in hydrocarbon streams was subjected to hydrolysis at elevated temperatures in the presence of water. The treating agents used by Eaton et al. (2005) are overbase complexes of metal oxides and/or carbonates Mg, Ca, Ba, Sr or Mn, and at least one organic complexing agent from the previous salts. The oxides or carbonates may also be a combination of the metal species, such as a 1:1 by weight mixture. Similarly, the salt may be a combination of metal salts, such as a 1:1 by weight mixture, where the magnesium, calcium or aluminum species are the best choices.

Similarly, Eaton et al.(2005) suggested that non-carboxylic acids such as organic sulfur acids and organic phosphorus acids are the best complexing agents due to their dispersant capabilities, in order to ensure the formation of a finely divided, preferably submicron, particles which form a stable dispersion in oil. As suggested by Eaton et al. (2005), the diameter of the metal oxide or metal carbonate particles should not exceed 0.1 microns. Thus, the authors described the overbases as colloidal dispersions that may be added as "liquids" to the hydrocarbon streams.

Eaton et al.(2005) recommended MgO/Mg carboxylate, $MgCO_3$/Mg sulfonate, $MgCO_3$/Mg carboxylate, MgO/Mg sulfonate+$MgCO_3$ Mg carboxylate MgO/$MgCO_3$ Mg carboxylate MgO/$MgCO_3$/Mg sulfonate as best choices for an treating agent, with a desirable concentration ratio for reducing hydrolysis of at least about 1 ppm by weight of available metal per 1 ppm by weight chloride salt (i.e. a 1:1 ratio of inhibitor to salt). The amount of the additive would vary depending on the chloride salt concentration and type contained in the hydrocarbon stream.

The inhibition takes place when an effective amount of treating agent is added to the stream when its temperature is about 200° C, below the range when hydrolysis of the chloride salt may occur (between 320° to 400° C). As suggested by Eaton et al. (2005), the inhibitor would provide reactive metal bases in the oil to react with the hydrochloric acid, forming a stable salt such as a metal-hydroxychloride rather than hydrochloric acid (Equation 2.15),

$$MgO\ (s) + HCl\ (g) = Mg(OH)Cl\ (s) \qquad (2.15)$$

The role of the inhibitor, therefore, is to complex the chloride in a harmless form to prevent the release of hydrochloric acid into overhead systems.

CHAPTER 3

MATERIALS AND METHODS

3.1. Reagents

The mechanisms of hydrolysis of chlorides in the presence of clays were investigated in a model system consisting of a hydrocracked lube oil base stock with a high boiling range (Paraflex HT-100, Petro-Canada Ltd., Mississauga, ON) used as a stable oil medium, metal salts of NaCl, $MgCl_2.6H_2O$, and $CaCl_2.2H_2O$ (Fisher Scientific, Mississauga, ON) and additives.

Three sets of additives were used for this work: pure clay material, silica and cation-saturated silica.

-One standard kaolinite sample from The Clay Minerals Society repository. KGa-1b is a well crystallized, low defect, kaolinite from Washington County, Georgia. Descriptions as "well" crystallized are discussed by Van Olphen and Fripiat (1979). The clay was received well dispersed, and size distributions as well as XRD and EDX data were verified at laboratory facilities from Canmet, Devon. The composition of this untreated clay is summarized in the table 3.1.

Table 3.1. Kaolinite low defect physical and chemical data. (Olphen and Fripiat, 1979)

ORIGIN	Tuscaloosa formation (Cretaceous) (stratigraphy uncertain) County of Washington, State of Georgia, USA	
LOCATION	32°58' N-82°53' W approximately, topographic map Tabernacle, Georgia 3252.5-W 8252.5/7.5, Collected from face of Coss-Hodges pit, October 3,1972.	
CATION EXCHANGE CAPACITY (CEC)	2.0 meq/100g	
SURFACE AREA: N2 area	10.05 +/- 0.02 m2/g	
THERMAL ANALYSIS: DTA	endotherm at 630oC, exotherm at 1015oC, TG: dehydroxylationweight loss 13.11% (theory 14%) indicating less than 7% impurities	
LOSS ON HEATING	-550°C: 12.6; 550-1000°C: 1.18.	
STRUCTURE	:$(Mg_{.02}\ Ca_{.01}\ Na_{.01}\ K_{.01})[Al_{3.86}\ Fe(III)_{.02}$ Mntr $Ti_{.11}][Si_{3.83}\ Al_{.17}]O_{10}(OH)_8$, Octahedral charge:.11, Tetrahedral charge:-.17,Interlayer charge:-.06, Unbalanced charge:0.00	
CHEMICAL COMPOSITION (wt %):	SiO_2	44.2
	Al_2O_3	39.7
	TiO_2	1.39
	Fe_2O_3	0.13
	FeO	0.08
	MnO	0.002
	MgO	0.03
	CaO	n.d.
	Na_2O	0.013
	K_2O	0.05
	F	0.013
	P_2O_5	0.034

Fine ground commercial silica MIN-U-SIL® 5 from U.S. Silica Company P.O.Box 187, Berkeley Springs, WV 25411-0187 was used in another set of experiments. The silica has mean size comparable with the one of the kaolinite as shown in Table 3.2.

Table 3.2. Silica physical and chemical properties. (US Silica Company, 1998)

HARDNESS (Mohs)	7
HEGMAN	7.8
MEDIAN DIAMETER (μm)	1.6
OIL ABSORPTION (D-1483)	42
pH	6.7
-5 MICRON (%)	96.3
REFLECTANCE (%)	94.5
+325 MESH (%)	0.003
YELLOWNESS INDEX	1.6
SPECIFIC GRAVITY	2.65
TYPICAL CHEMICAL ANALYSIS, wt%	
SiO_2 (Silicon Dioxide)	99.4
Fe_2O_3 (Iron Oxide)	0.031
Al_2O_3 (Aluminum Oxide)	0.26
TiO_2 (Titanium Dioxide)	0.01
CaO (Calcium Oxide)	0.01
MgO (Magnesium Oxide)	0.02
Na_2O (Sodium Oxide)	<0.01
K_2O (Potassium Oxide)	0.03
LOI (Loss on Ignition)	0.3

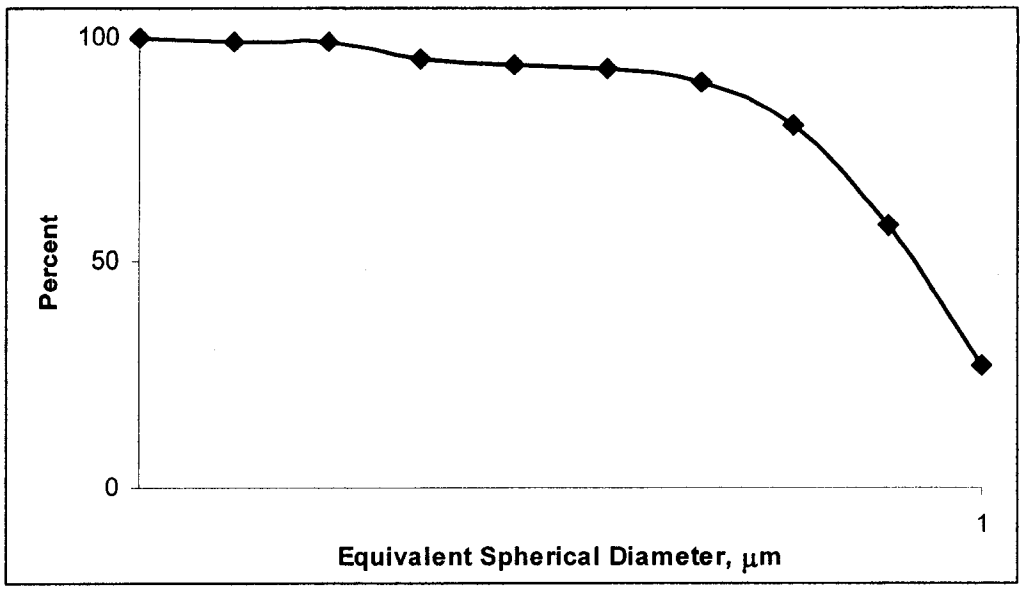

Figure 3.1. Particle size distribution of silica. (US Silica Company, 1998)

Toluene (certified ACS), acetone (FIS.00140), cyclohexane (certified ACS) and nitric acid (reagent ACS) were supplied by Fisher. These reagents were used as received, excepting the nitric acid which is used as a 4N solution for cleaning purposes.

3.2. Sample Preparation and Simulation of Steam Distillation

In selected experiments, a mixture of salts was used to simulate salts in crude oils, with a composition of 70 wt% Sodium Chloride, 20 wt% calcium dichloride dihydrate and 10% magnesium chloride hexahydrate. The metal salts, as well as any of the additives described above (depending on the baseline experimental requirements) were added as a ten to one mass ratio additive to salt solution in ten millilitres of Milli-Q UV deionized water, emulsified into the oil in a high-speed blender, producing a stable suspension.

In the experiments where untreated or saturated Kaolinite was used as an additive. Before being added to the oil, the clay-suspension was sonicated for 10min with a Fisher Sonic Dismembrator (model 300) operated at approximately 18 kcycles/s.

A glass steam distillation apparatus was assembled, according to the design from the early work of Davis et al. (1938). The apparatus shown in Figure 3.2 was made from standard laboratory glassware for conducting steam distillation of a hydrocarbon test fluid in the range 150 °C to 350 °C at atmospheric pressure. The mixture of oil, salts, and other components was added to the reactor. In a typical experiment, 400 ml of oil-salts-additive emulsion were poured into a flask attached to the distillation apparatus as per figure 3.2, and heated by a heating mantle with continuous agitation. Bubbling of nitrogen through the sparger at 2 ml/min ensured agitation and maintained a positive pressure in the apparatus at all times. Steam was generated by pumping water into a heater at a rate of two gram/min and continued until 10 ml of condensate were collected in the first trap at 50 °C intervals between 100 °C and 350 °C. The steam condensate samples were kept in clean vials for subsequent analysis of chloride.

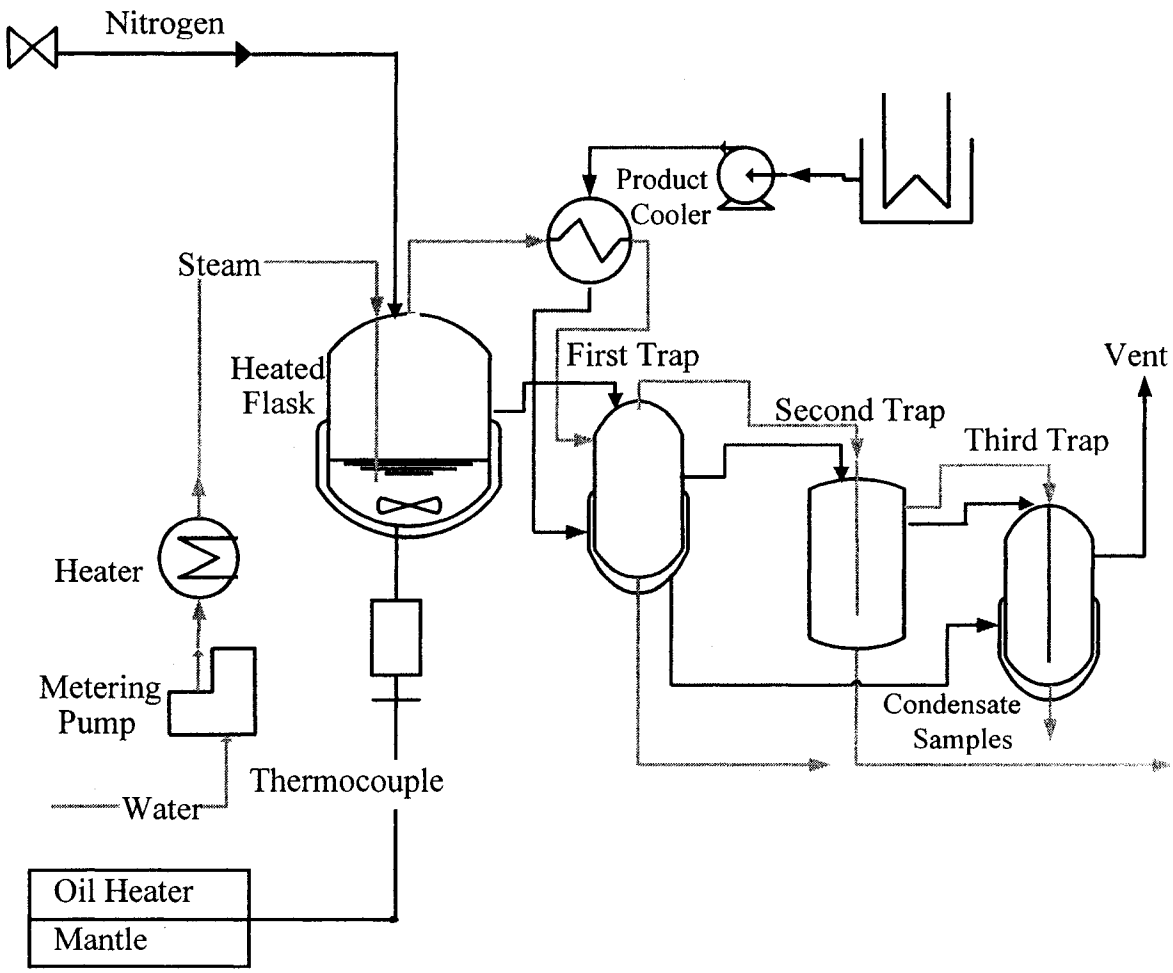

Figure 3.2. Schematic diagram of glass distillation apparatus. (Davis et al. 1938, Eaton, 2000)

3.3. Recovery of solids from the oil

To recover the solids after the hydrolysis reaction, the oil and the solids were rinsed with toluene and vacuum filtered with Millipore ® filter membranes of 0.22 micrometers. The filter cake was the dried under vacuum at 76°C overnight to ensure total evaporation of the solvent.

3.4. Ion Saturation of Clays

The saturated Ca-kaolinite form was obtained following the general procedure of Brindley and Ertem (1971) and Baptista (1989) by treating the KGa-1b kaolinite with a 1M $CaCl_2$ solution. An excess of a 1 M NaCl solution was added to the kaolinite. The suspension was mixed for approximately ten minutes and allowed to stand for two hours, mixed for another ten minutes and allowed to settle overnight. The sample was centrifuged at 15,000 revolutions per minute (equivalent to 28,900 relative centrifugal force (RCF)), the supernatant decanted and the solids were then centrifuged and washed repeatedly in Milli-Q UV water until the chloride concentration of the supernatant decreased to less than 1 ppm.

3.5. Analytical Methods and Instrumentation

3.5.1. Solids Analysis

3.5.1.1. Scanning Electron Microscopy

This analysis involves the evaluation of morphology and chemical composition of the solids. SEM analysis provided black and white digital images at various magnifications using a Hitachi S-2700 Scanning Electron Microscope, as well as the Energy Dispersive X-ray (EDX) chemical data (Princeton Gamma-Tech Imix). This technique allowed us to examine the morphology of the salt crystals and their distribution on the clay particles.

The composition of the solid samples after reaction was determined by a X-ray diffraction apparatus (Rigaku Geigerflex 2173, Tokyo) from the department of earth and sciences at the University of Alberta and used a cobalt X-ray source.

3.5.1.2.Particle Size Distribution

The mean particle diameter was measured by light scattering of a suspension of well-dispersed solids in cyclohexane (wet laser diffraction), using a Mastersizer 2000 instrument (Malvern Instruments, Malvern, UK). The operation of this instrument relies on the fact that particles passing through a laser beam scatter light at an angle that is inversely proportional to their size. It is therefore possible to calculate particle size distributions if the intensity of light scattered from a sample is measured as a function of angle. This angular information needs to be compared with a scattering model (Mie theory) in order to calculate the size distribution. The technique has a very large dynamic range, from 3.5mm to below 100nm, as defined by the range of angles over which the scattering pattern is collected and the instruments optical configuration.

3.5.1.3. X-ray Photoelectron Spectroscopy (XPS)

The XPS technique involves the characterization of a surface by analysis of X-ray induced photoelectrons. XPS is a surface sensitive technique, which has a typical penetration depth range among 10-100 Å. Emitted photoelectrons are identified, in many cases uniquely, by their energy.

From the electron energy of the solids after reaction as will be shown in the results, it is possible to determine the elements from which they are composed, the relative quantity of each element, its chemical state and compositional depth profiling information.

3.5.2. Determination of Chloride Concentrations via Ion Chromatography

Ion chromatography is a useful technique for the measurement of various ionic species in solution. It is based on the principles of chromatographic separation, with detection of the eluted ions by conductivity suppression

The collected liquid sample is delivered to vials and then analyzed for chloride using ion chromatography (Dionex ICS 2000 Ion Chromatograph). This instrument employs conductivity detection as operating principle and has a heated and thermostated high-performance conductivity cell so the measurements are unaffected by temperature variations.

3.5.2.1.Ion Chromatography Principle

Ions in solution of a certain concentration can conduct electrical charges, with a linear correlation between the concentration of the ions and the current conducted. The analyte acts as a resistor to the current and Ohm' Law is observed (Small 1989):

$$R = \frac{E}{i} \qquad (3.1)$$

The conductance (G) of the ionic solution is the inverse of resistance (R), from the equation (Small 1989):

$$G = \frac{1}{R} \qquad (3.2)$$

Conductance is measured in Siemens (S). The conductivity can be measured by multiplying the conductance value G by the conductivity cell constant K. Conductivity (k) is conductance measured in a standard cell with electrodes of 1 cm^2 area held 1 cm apart, and is measured in Siemens per cm (S / cm) (Small 1989):

$$k = K \cdot G \qquad (3.3)$$

Concentration can then be calculated from Kohlrauch's Law, which states that the total conductivity of a solution is the sum of the individual conductivities of its ionic constituents, which is concentration multiplied by each ion's ionic limiting equivalent conductivity constant, $\lambda°$ which has a dependent on temperature (Small 1989):

$$k = \frac{\sum_i \lambda°_i c_i}{1000} \tag{3.4}$$

From equation 3.4, the concentration, c may be determined, using a calibration curve.

3.5.2.2.Ion Chromatography Analysis Method

The apparatus was a Dionex ICS 2000 model, with detailed specifications provided in table 3.3 and analysis process illustrated in figure 3.3. This ion chromatography system detects anions following six steps: eluent delivery, injection, separation, suppression, detection and recording. A sample of anionic salts in aqueous solution is injected into a sample loop automatically. When triggered, the ICS-2000 injects the sample into the eluent stream. The anions to be detected can be separated on the basis of their affinity for the basic functional groups of the resins within the guard and separator column (Dionex 2003). The sample is passed through a guard column, which separates undesired and damaging impurities and is then subjected to the main separator column.

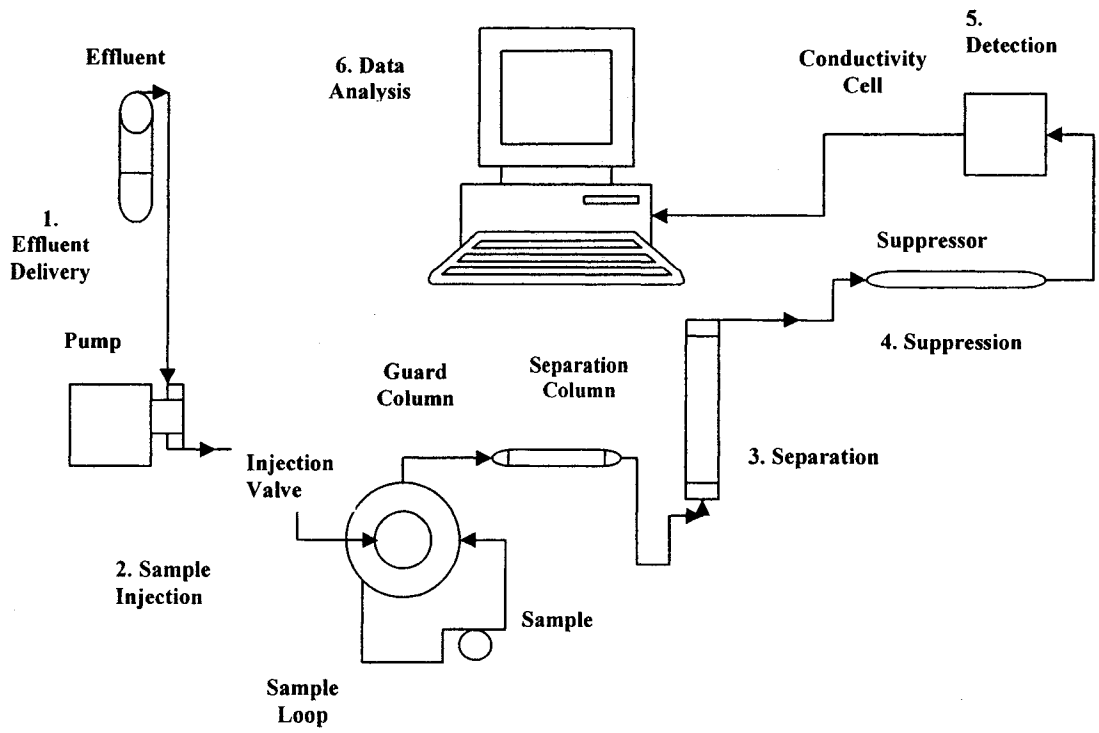

Figure 3.3. Ion analysis process (Dionex 2003)

During the suppression step, a suppressor that selectively enhances detection of the sample ions, while suppressing the conductivity of the eluent. A detector then measures the conductivity of the analyte against that of the eluent, and records in terms of retention time and conductivity, displaying the results as a chromatogram. The area of the peaks may be integrated to give the concentration of analyte within the sample, relative to a standard solution.

3.5.2.3. Analysis of Hydrolysis Condensate Samples

In order to accurately determine the concentration of chloride in solution after hydrolysis, a calibration curve from the concentrations of standard solutions of chloride was produced. Standard eluent chloride anion samples were made using NaCl salt and dissolved and diluted using milliQ filtered deionized water. Within the working range, of two orders of magnitude from 0 ppm to 100 ppm, the curve correlation is linear. The sensitivity of the IC analytical method was calculated from the slope of the linear standard curve attached in the Appendix Section.

Once the ion chromatograph was calibrated, a water blank solution was analyzed to ensure instrumental accuracy and subsequently 1 ml of hydrolysis condensate samples each is injected. The concentration results are subjected to the equation 3.5 below:

$$C = H \times F \times D \qquad (3.5)$$

Where C is concentration, H is peak area (or height) F is the response factor in units of Concentration/Area (height) and D is the dilution factor of the sample from the instrumental method (i.e. sample loop volume, injection volume, etc.).

Table 3.3. ICS-2000 Ion chromatography system specifications. (Dionex Corporation, 2003).

Detector	Electroconductivity Cell
Maximum cell pressure	2 MPa (300 psi)
Maximum operating pressure	35 MPa (5000 psi)
Flow-rate range	0.05–5.0 mL/min in 0.01 increments. Typical operating range is 0.4–2.0 mL/min
Temperature range	Ambient +7 °C to 55 °C
Operating temperature range	Ambient +5 °C to 60 °C
Concentration range	0.1–100 mM (Depending on eluent used)
Maximum operating pressure	21 MPa (3000 psi)
Maximum solvent concentration	Anions: 25% methanol; Cations: no solvents

Inductively Coupled Plasma (ICP) tests from the aqueous sample were performed in order to detect any carryover of salts into the condensate by determining minerals, and elements.

CHAPTER 4

RESULTS AND DISCUSSION

The high surface area and cation exchange capacity of clays may lead to interactions with salts that lead to an increase in the release of hydrochloric acid when the mixture undergoes hydrolysis in the presence of steam. A series of experiments were performed with and without pure clay, in an attempt to address the role of clay surface area in promoting the hydrolysis reaction. Subsequent experiments with ion-saturated clay where performed to determine the role of cation exchange capacity of clays in hydrolysis of salts.

The experimental work of this thesis will provide detailed evidence on the effect of clays on the extent of hydrolysis and on the structure of the salt crystals, through a series of experiments on steam hydrolysis of a test mixture in the range 150 °C to 350 °C. A mixture of salts with a composition of 70 wt% sodium chloride, 20 wt% calcium dichloride dihydrate and 10% magnesium chloride hexahydrate with clay in a ten to one mass ratio clay to salt (selected by comparison to industry) was used for the majority of the experiments, as described in section 3.2. A series of increasing temperatures were used to evaluate the effect of clays in salt hydrolysis by steam over a range of operating conditions.

4.1. Effect of Clays on Hydrolysis of Salts

The data of Figure 4.1 show that hydrolysis was increased at the temperatures of 250 -350 °C by the addition of clay in a 10:1 ratio of clay to salt. The cumulative hydrolysis at 350 °C increased from 1.21 ± 0.17 to 4.5 ± 0.45 % of the total chloride in the oil.

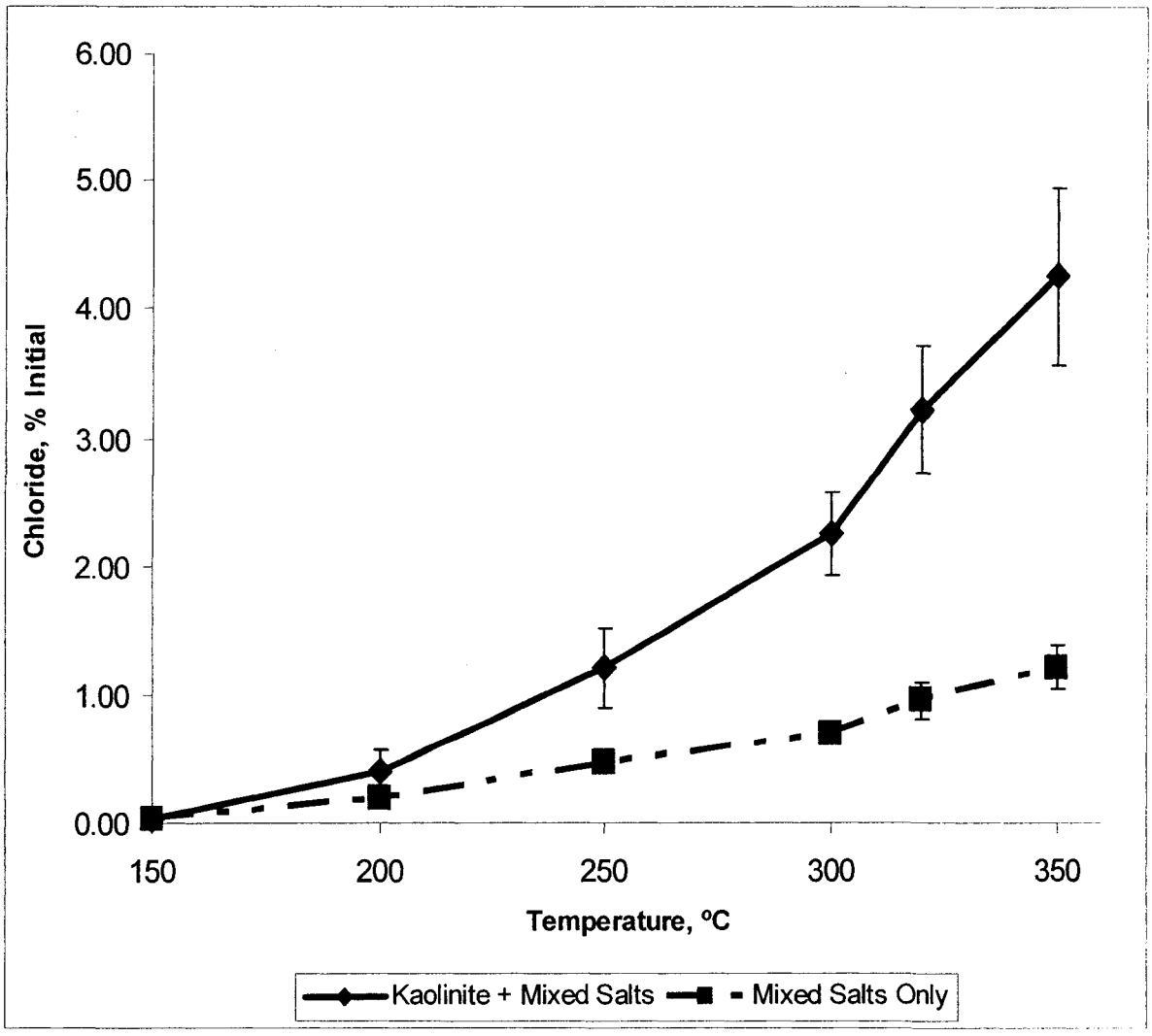

Figure 4.1. Effect of clay on hydrolysis of emulsified chloride salts (70 wt% + 20 wt% $CaCl_2$ 2(H_2O) + 10 wt% $MgCl_2$ 6(H_2O)) on a (10:1 clay to salt weight ratio). The error bars correspond to the standard deviation from 6 replicates

4.1.1. Statistical Significance of the Effect of Clay in Hydrolysis of Salts

A t-test was used to evaluate the statistical difference between the hydrolysis of salts with and without kaolinite. The test was run with 6 replicates for each treatment (in double array). As seen in Table 4.1, the results reached statistical significance ($P < 0.05$), indicating that changes in the underlying variables (presence or absence of kaolinite) correspond to changes in significance levels. Thus, from the data collected it was objectively concluded that the difference between hydrolysis of salts with and without clay is statistically significant above the 95% confidence interval.

Table 4.1. t-test: Two-sample assuming equal variances for the hydrolysis at 150-350 °C of a mixture of salts emulsified in oil as aqueous solution in paraflex and dried at 150 ° C.

	Cumulative Chloride Evolved, %	
	Kaolinite + mixed salts	Mixed salts only
Mean	4.25	1.21
Variance	0.46	0.03
Observations	6	4
Pooled Variance	0.3	
Hypothesized Mean Difference	0	
df	8	
t Statistic	8.56	
P(T<=t) one-tail	1.33E-05	Low probability
t Critical one-tail	1.86	
P(T<=t) two-tail	2.66E-05	Low probability
t Critical two-tail	2.30	

4.1.2. Study of the Correlation between Surface Area, Morphology of Salts and Chloride Evolution

The evolution of the hydrolysis of salts in crude oil may be highly correlated to physical factors that would affect the size and surface area of the salt crystals. The influence of clay on the surface area of salts was investigated by comparing the results obtained from light scattering of the solids after the hydrolysis. This technique provided external surface areas based on measurements of particle size distribution of the solids, using the Malvern Mastersizer 2000 laser diffraction instrument described in Section 3.5. The results are tabulated in Table 4.2. Without the presence of fine solids the release of hydrochloric acid was 1.21% of the initial chloride. The mean diameter of the salt crystals was 107.68 μm. When the same proportion of salts with the addition of clay was hydrolyzed under the same experimental conditions, the solids after reaction gave a much lower mean diameter. These particles could be clay, salt crystals, or clay particles coated with salts. The data of Table 4.2 do suggest that an increase of particle surface area will enhance hydrolysis reactions.

Table 4.2. Extent of cumulative hydrolysis and particle size analysis by light scattering (hydrolysis at 150-350 °C of a mixture of salts of NaCl + $CaCl_2$ $2(H_2O)$+ $MgCl_2$ $6(H_2O)$ emulsified in oil as aqueous solution in Paraflex and dried at 150 °C)

Test Condition	Cumulative Chloride Evolved, %	External Surface Area of Particles in Suspension, m^2/g	Surface Weighted Mean Diameter, μm
Mixed Salts	1.21 ± 0.17	0.0315	107.68
Mixed Salts + Kaolinite (10:1 wt% ratio)	4.25 ± 0.45	0.235	56.75
Mixed Salts + Silica (10:1 wt% ratio)	4.15±0.33	0.108	85.66

Scanning electron microscopy was used to gain a better understanding of the effect of clays on the surface area of the salt crystals by comparing the morphology of the solids after the hydrolysis reaction with and without clay (Figure 4.2). The resulting micrographs of the salts particles after reaction underlined the changes in the morphology of salts due to the presence of clay. The microscopic observations showed large cubic crystals of halite (sodium chloride) when the salts were prepared as an emulsion (Figure 4.2(a)). The kaolin solids were flakes that formed aggregates

with a surface that looked polygonal and plate-like. This clay structure supported much smaller cubical salt crystals (Figure 4.2(b)). This observation was confirmed by EDX analysis (Section 4.1.4), which showed chlorine on the clay surfaces. Consequently, the addition of clay gave supported salt crystals with much smaller diameter and exposed surface area. The micrographs also indicated that the particle size data for the salt + clay mixture was for the aggregated clays, not for the salt crystals. Consequently, the data of Table 4.2 do not give a direct measure of the surface area of the exposed salt crystals.

To gain further information about the mechanism of interaction between the clay and salts crystals during the hydrolysis reaction, the same salt mixture was mixed with fine silica and hydrolyzed following the same experimental procedure. The presence of silica gave almost the same hydrolysis as the kaolinite; 4.15±0.33 % with silica vs. 4.25±0.45 % with kaolinite. These observations were attributed to the fact that silica particles have a high specific surface area that form porous aggregates as the emulsion droplets are dried, providing a high surface area for the formation of small salt crystals. The corresponding SEM micrograph in Figure 4.2(c) showed small crystals on silica surfaces. The particle size distributions of the kaolin-supported salts and the silica-supported salts were similar, as illustrated in Figure 4.3, indicating the aggregation of the two types of particles was similar as the emulsion was dried. Both fine solids gave smaller agglomerates than the salt crystals alone.

The similar increase in hydrolysis for two different metal oxide solids suggests that the dominant mechanism was the distribution of the salts on the surface of the fine solids, giving a much larger surface area for reaction of steam. If chemical

interactions were important, then silicon dioxide should give different results from the alumino-silicate kaolin.

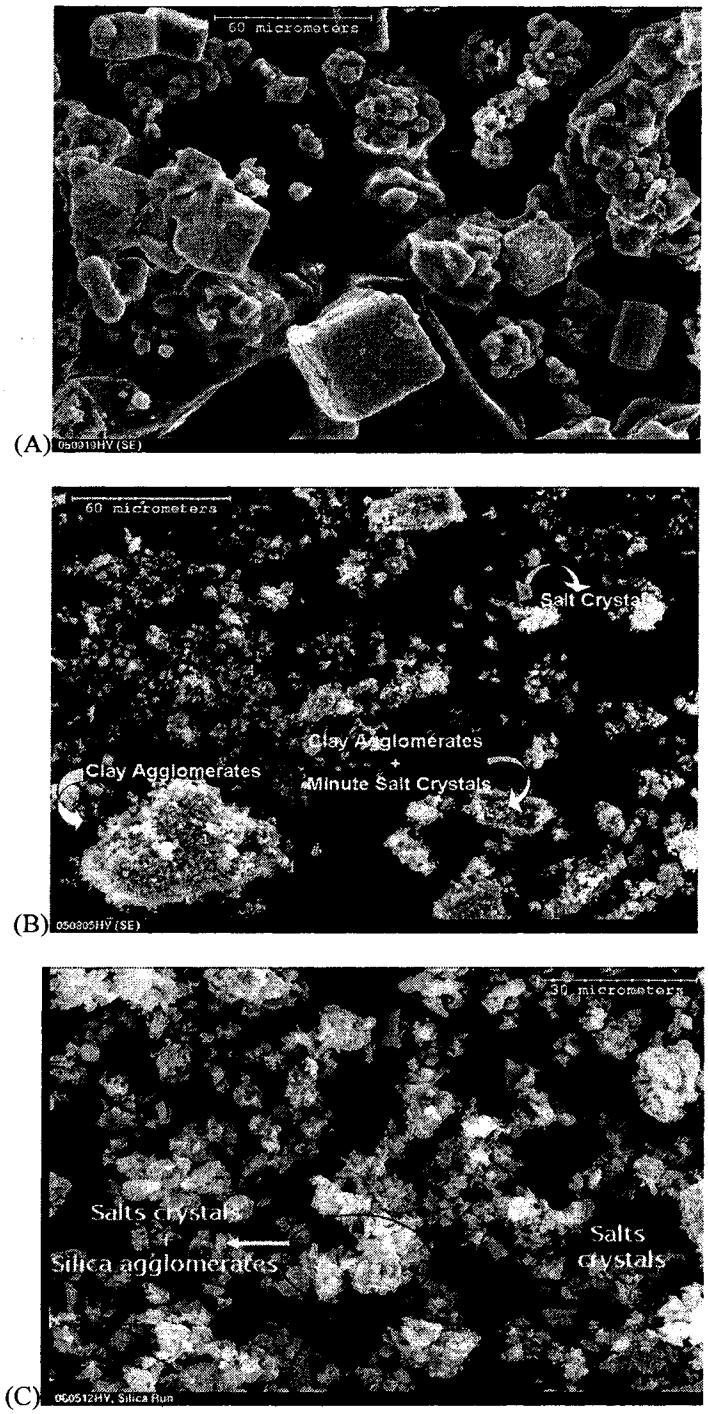

Figure 4.2.SEM micrographs of solids after hydrolysis of an emulsion of salts in oil: a) mixed salts only b) kaolinite + mixed salts c) mixed salts and silica.

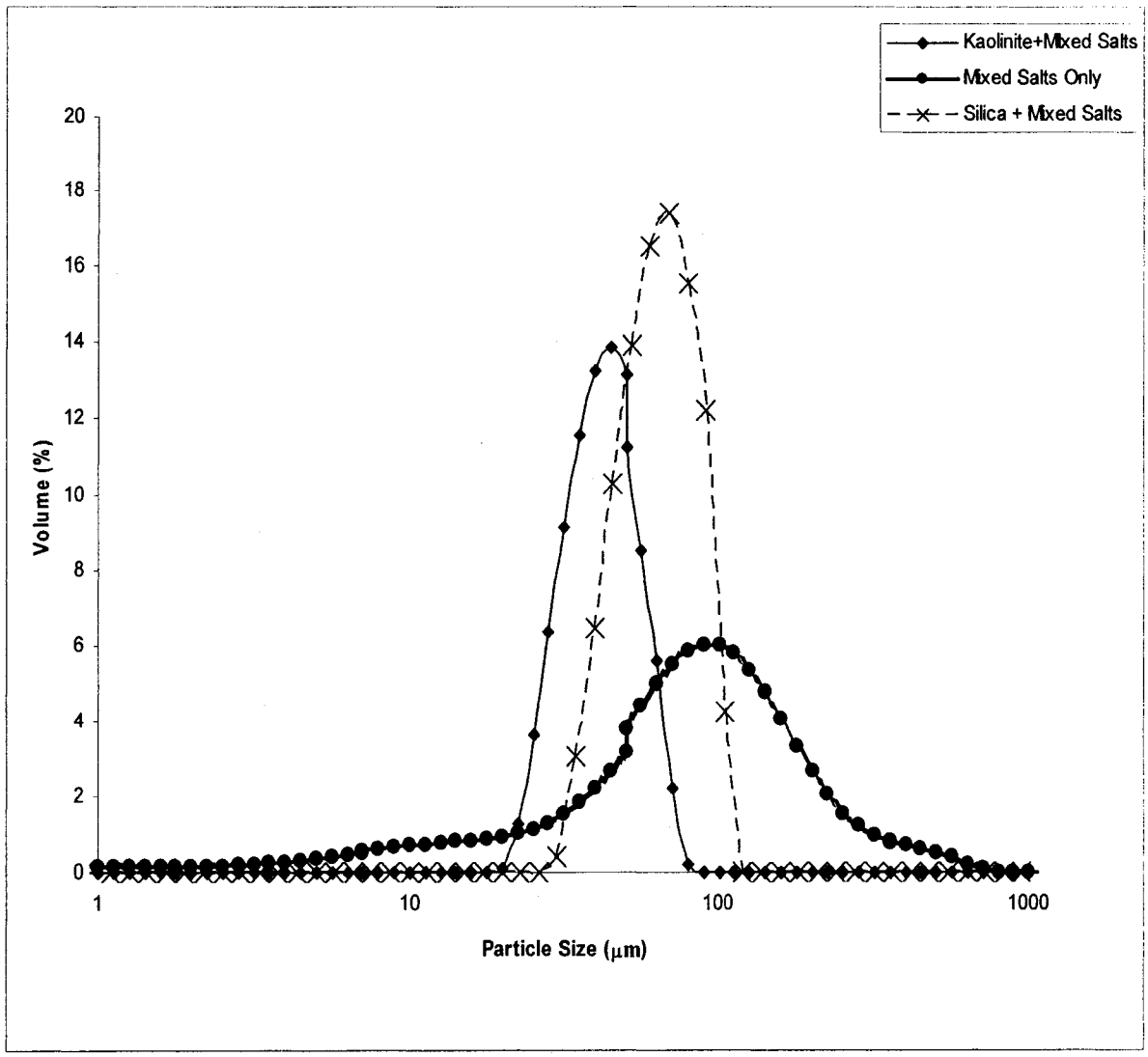

Figure 4.3. Particle size distribution

4.1.3. Cation Content of Condensate Samples

The data of Figure 4.1, combined with the particle-size data, SEM micrographs and the experiment with silica, imply that clays promote the hydrolysis of chlorides in the presence of steam through a surface area mechanism. An alternative explanation would be increased carryover of salts due the added clay. In order to exclude carry over as a potential contributor to the observed results, the condensate samples were analyzed for the divalent and monovalent metal ions by inductively coupled plasma spectrometry (ICP, Seiko Instruments SPS-1500V) to detect any carryover through the hydrolysis (Table 4.3).

The ICP results show that Ca^{2+} and Na^{+} concentrations were less than 10 and 3 ppm respectively in the overhead condensate even at the higher temperatures of hydrolysis (Table 4.3). The chlorine concentration detected by ion chromatography detected under the same conditions was 30 ppm. The cation compositions, therefore, do not support the mechanism of carry-over of salt particles into the condensate. Such a mechanism would give predominantly sodium cations, at a concentration comparable to the chloride.

Table 4.3. Cation concentration in overhead condensate after hydrolysis of an emulsion of mixed salts + kaolinite in pure oil. (Courtesy Randy Mikula CANMET DEVON) .

T(°C)	Ca ppm	K ppm	Mg ppm	Na ppm
150	7	7	2	4
200	11	7	1	1
250	3	7	1	1
300	10	6	1	3
320	7	7	1	3
350	4	8	1	3

4.1.4. Quantitative Analysis of Solids after Reaction

Scanning Electron Microscopy combined with Energy Dispersive X-ray analysis (SEM-EDX) provided a semi-quantitative estimate of the elemental composition of the solids (due to the roughness of the sample surfaces the take-off angle of the x-rays is not a constant) as well as structural changes induced by the temperature of reaction (Table 4.4).

The EDX elemental distributions after reaction revealed bands of aluminum and silicon of constant intensity, but suggested depletion of Cl, Na, Ca as temperature increased. There was no evidence of magnesium as presented in Table 4.4. The Cl/Na

and Cl/Ca ratios in the recovered solids after the hydrolysis reaction were obtained by comparing the peak intensity of each element in the EDX spectrum.

The data show significant redistribution of Na, Ca and Cl, from the outer surface of the clay agglomerates at 150 °C to the interior at 350 °C. The incident electron energy of the EDX analysis used in the solid samples is generated in a region about 2 microns in depth (Walker and Morton), through the agglomerates that exhibited an average diameter of 56.75 μm. These observations suggest that chemical interaction between the clay and the salts could contribute to the observed hydrolysis.

The analysis results illustrated in Figure 4.4 showed that the Cl:Na ratio strongly increases as the result of transformation from cubical bigger to dispersed smaller salt crystals supported by clay agglomerates. Generally, as the particle size decreases, the specific surface area of the salt crystals increases because of the clay effect with the consequent increase in the Cl:Na ratio. On the other hand, intercalation with NaCl between the hydrogen-bonded layers of kaolinite followed by swelling and calcium occupancy between adjacent layers vacant sites of the kaolinite structure (Thompson et al., 1992), might explain why the Cl:Ca ratio indicated by XRD is comparable to Na even though the abundance of Ca is much lower in the salt; therefore suggests a mechanism for loss of salts from the surface of the clays.

Table 4.4. EDX analysis in solids vs. temperature of hydrolysis of an emulsion of mixed salts + kaolinite in pure oil. (Courtesy Randy Mikula, CANMET Devon)

	Temperature, °C					
Element Weight %	**150**	**200**	**250**	**300**	**320**	**350**
O	51.06	53.89	53.17	56.55	58.83	61.97
Na	7.03	6.54	5.11	2.02	0.32	0.4
Mg	0	0	0	0	0	0
Al	13.58	12.71	14.84	17.29	19.03	17.64
Si	14.21	13.14	15.44	18.33	19.99	18.21
Cl	12.75	12.39	9.86	4.23	0.62	0.52
Ca	0.64	0.62	0.72	0.5	0.18	0.1
Ti	0.73	0.62	0.86	0.91	0.9	1.01
Fe	0	0.09	0	0.17	0.13	0.15

Figure 4.4. Energy dispersive x-ray analysis of solids after hydrolysis. Upper panel, salts crystals only. Lower panel, kaolinite aggregates with salt crystals.

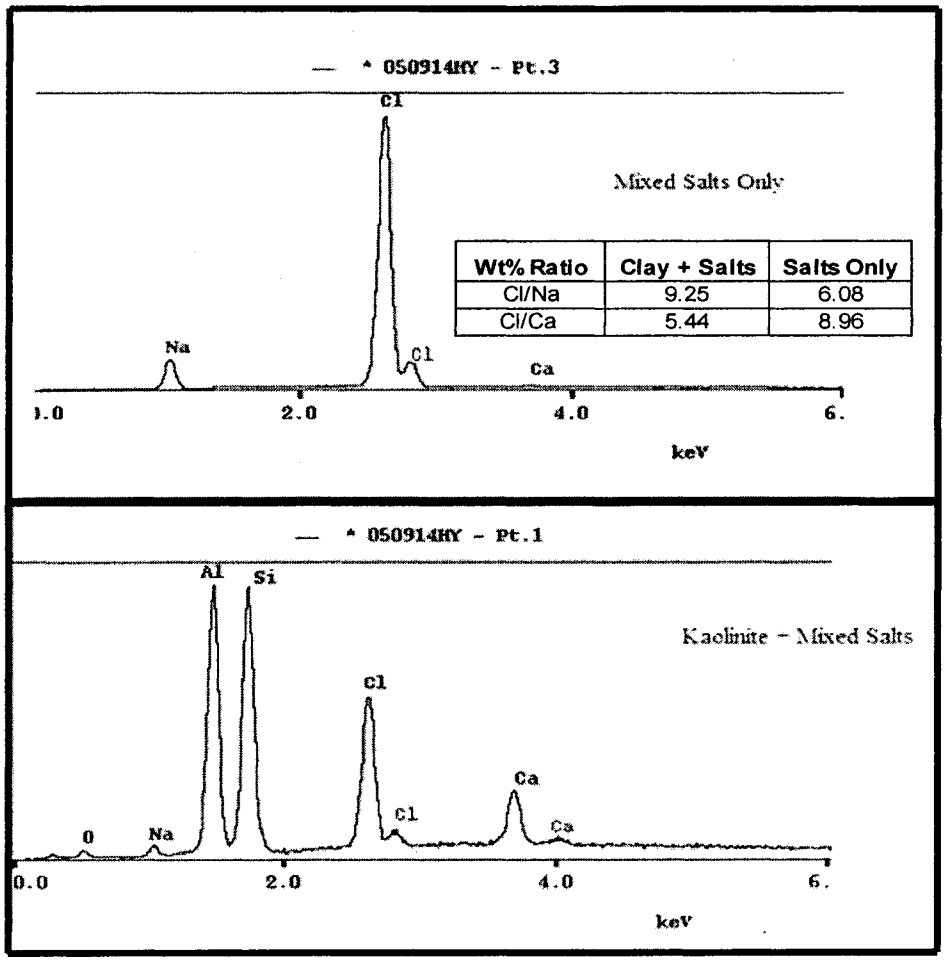

Significant insights on the effect of clays in the hydrolysis of salts were gained by analyzing the evolution of chloride from mixed salts in the presence of fine clays and fine silica particles. The data on particle size and morphology suggested that physical dispersion of the salts was responsible. Although the EDX data also suggested interactions of the cations with the clays, statistical tests on these results would be necessary to confirm this hypothesis. In order to fully investigate the interactions between salts and clays, experiments were conducted with pure salts and with ion-exchanged clays.

4.2 Experiments with Pure Salts

In order to study the effect of cation exchange capacity of clays on the hydrolysis of chloride salts in bitumen, a separate series of experiments with pure sodium chloride, and pure calcium dichloride where performed with and without kaolinite. The amount of salts was calculated by keeping constant the initial chloride input for each test (See Appendix IV). Each salt was diluted in ten milliliters of deionized water, then kaolinite was added in a ten to one mass ratio of additive to salt solution. The resulting mixture was emulsified into the oil in a high-speed blender, producing a stable suspension that went through steam distillation in the range 150°C to 350 °C at atmospheric pressure. The observed results of chloride evolution were compared with those exhibited by a series of blank tests for the pure salts.

When $CaCl_2.2H_20$ was emulsified in oil as an aqueous solution, dried at 150 °C, then hydrolyzed at 150-350 °C a chloride evolution of nearly 3% was observed (Figure 4.5).. For a blank test of NaCl under the same conditions, only a small amount of chloride was evolved (0.6%). When the same pure salts were hydrolyzed with pure kaolinite holding the procedure as well as the chloride input constant for both experiments, the average release of hydrochloric acid for a set of three replicates increased dramatically to 5.87±0.35% and 3.31±0.15% for $CaCl_2.2H_20$ and NaCl respectively (Figure 4.5). These results showed that reactivity of both sodium and calcium chlorides were strongly increased by the addition of clay, and demonstrate that the results observed for mixed salts were not primarily due to interactions between the salts.

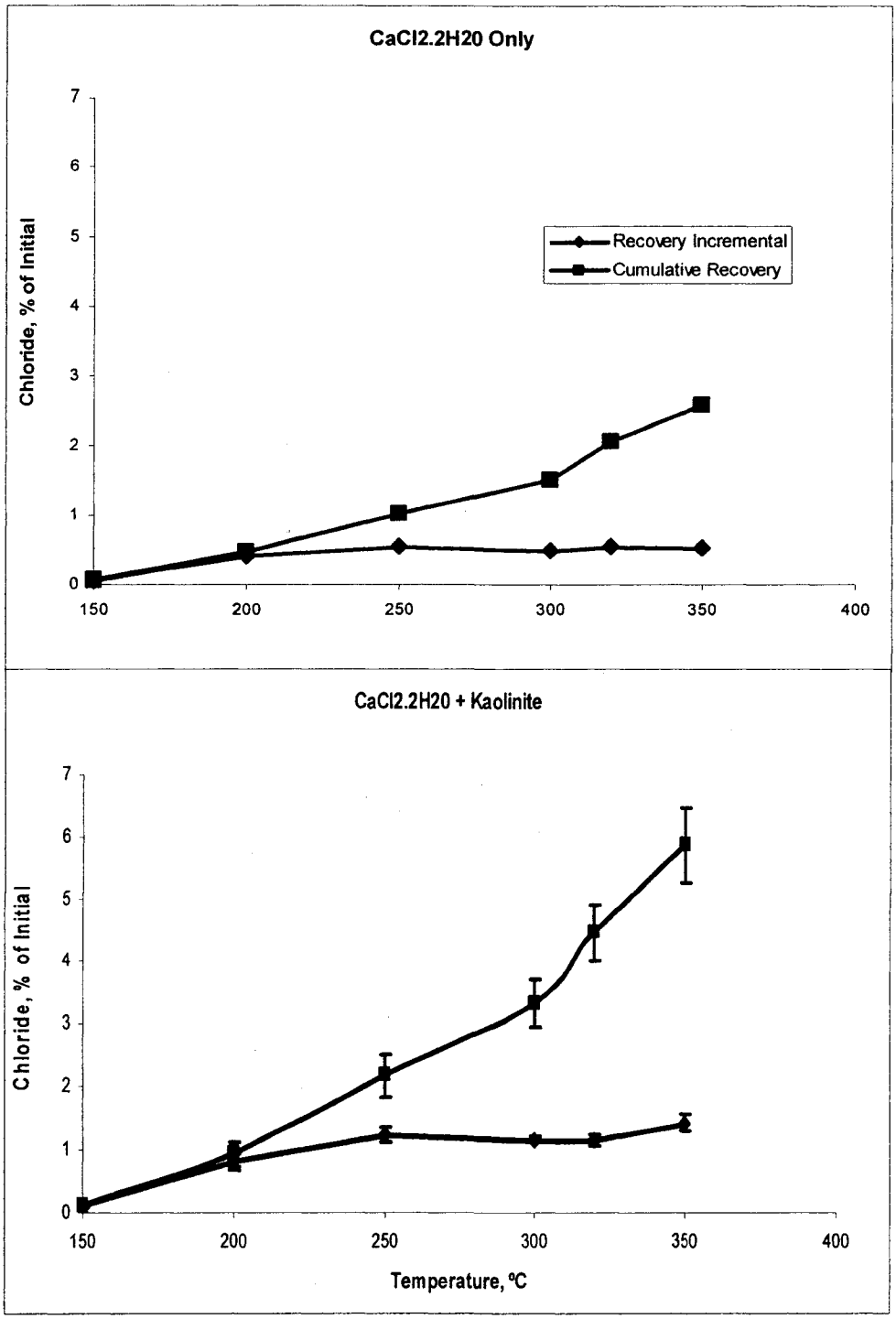

Figure 4.5. Evolution of chloride from $CaCl_2$ 2(H_2O) emulsified with and without clay (10:1 clay to salt weight ratio); the error bars correspond to the standard deviation from 3 replicates. Upper Panel: $CaCl_2$ 2(H_2O) ; Lower Panel: $CaCl_2$ 2(H_2O) with kaolinite

As in the case of mixed salts, the presence of clay dispersed the crystals of NaCl as much smaller domains of the clay matrix (Figure 4.6). The salt crystals are visible as small bright domains on the clay agglomerates. The particle size analysis is less instructive in this case (Figure 4.7), because the clay agglomerates were comparable in size to the salt crystals prepared in the absence of clay. This analysis does not indicate the area of chloride salts exposed to the oil when clay was present.

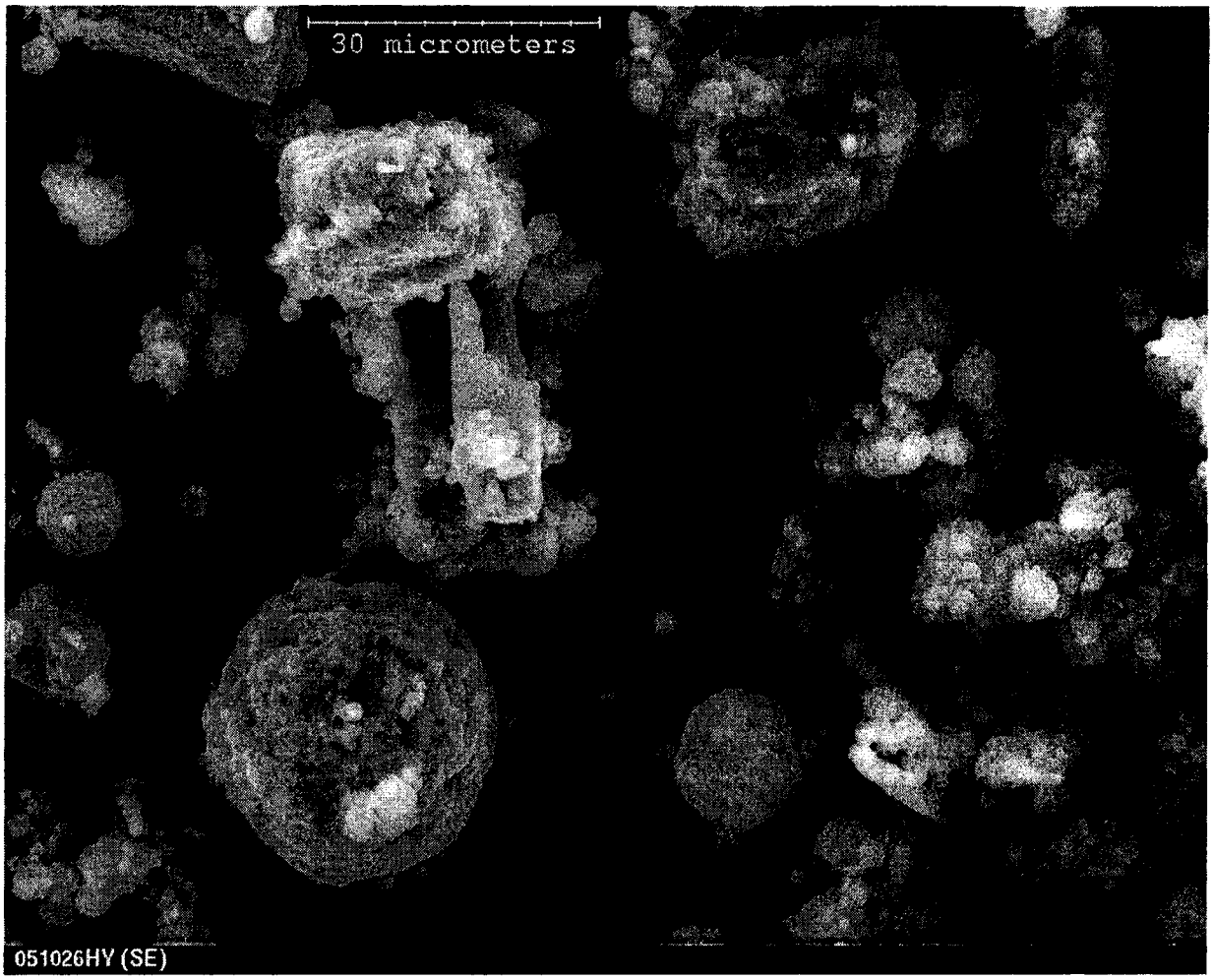

Figure 4.6.SEM micrographs of solids after hydrolysis of kaolinite + NaCl

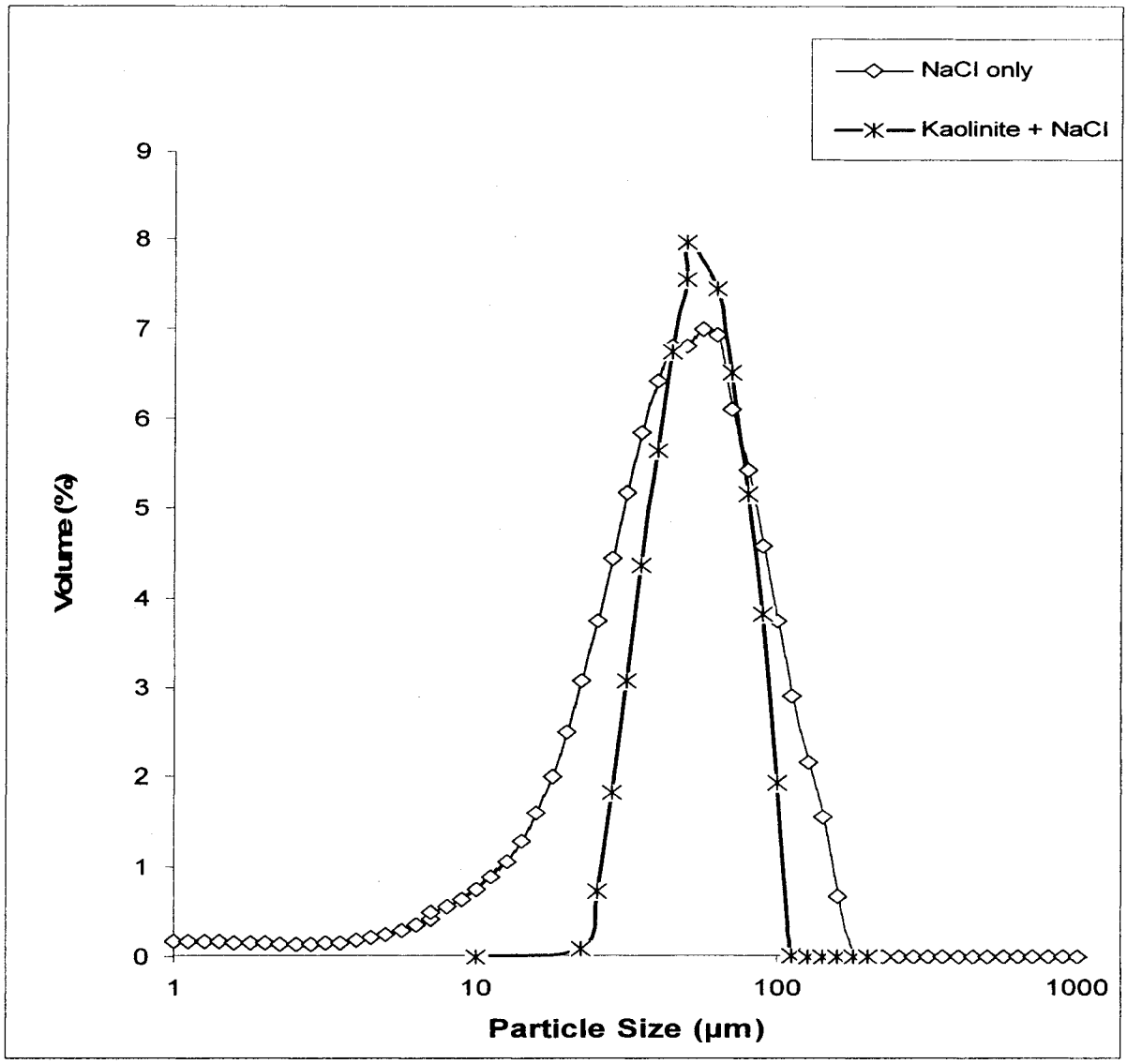

Figure 4.7.Size distribution of solids after hydrolysis NaCl.

4.2.1. Additivity of hydrolysis from pure salts in Kaolinite

A series of tests on the additivity of hydrolysis of Na and Ca on pure kaolinite were performed to validate the hypothesis from the previous results, which suggests cation exchange of clays is a minor contributor as compared to surface area in the promotion of hydrochloric acid evolution.

In order to test for the possible role of ion exchange between the salts and the clay, a 50:50 mixture of NaCl and $CaCl_2.2H_20$ was analyzed in the presence of kaolin. Data are presented in Figure 4.8. The incremental values for the recovery of chloride as a function of temperature in a mixture of pure NaCl + $CaCl_2.2H_20$ were predicted by summing up the individual values of the hydrolysis of pure NaCl + kaolinite and $CaCl_2.2H_20$ + kaolinite at each temperature and dividing by two. Each value was expressed in terms of the percentage of chloride released. Figure 4.8 shows the predicted versus actual values of incremental recovery of chloride as a function of temperature.

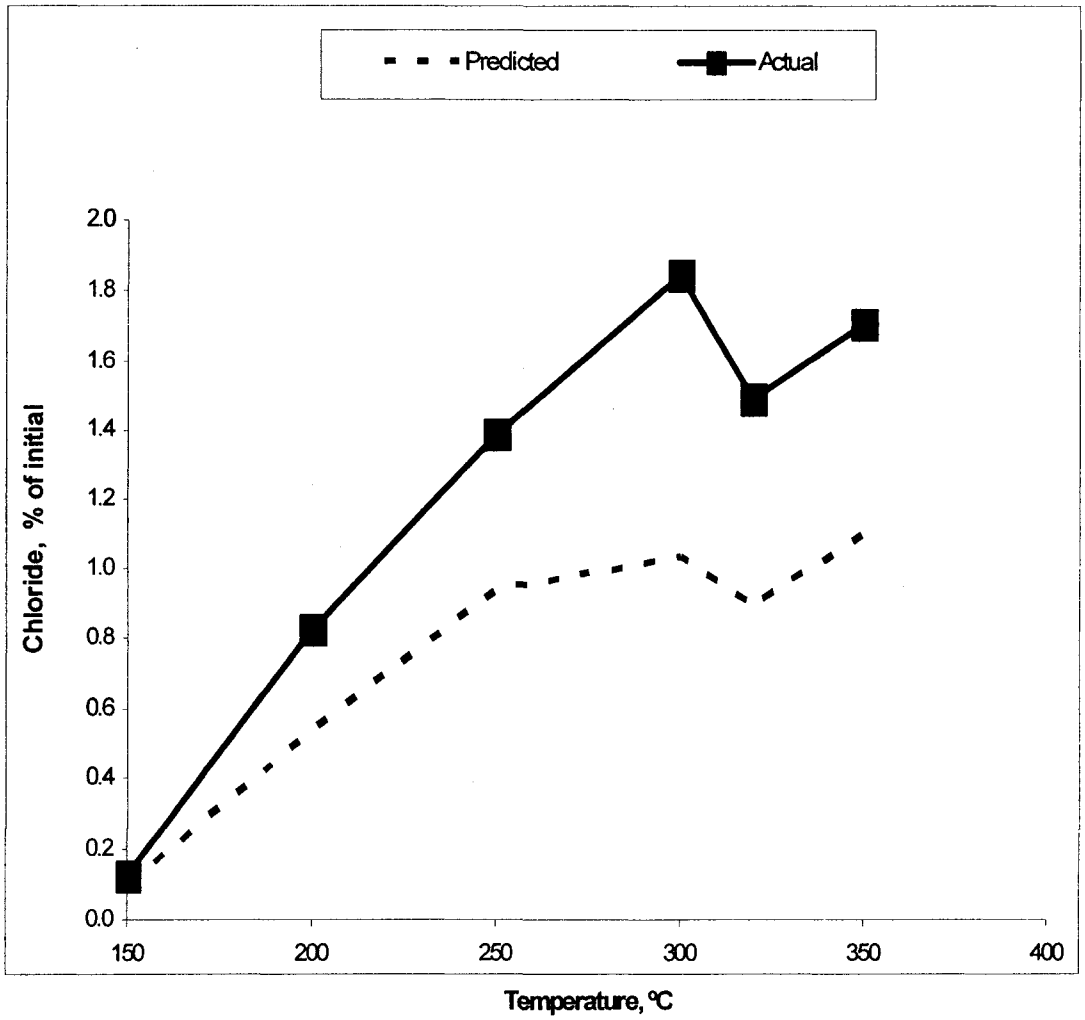

Figure 4.8. Incremental recovery of chloride on the Hydrolysis of Na and Ca mixtures with Kaolinite (on a 50:50 chloride input weight ratio). Predicted results from the means of two experiments with pure salts and kaolinite.

There is a significant gap between the curves, therefore, the predictions based in the sum of the individual incremental chloride yields for the NaCl and $CaCl_2.2H_20$ do not explain the performance of a 50:50 ratio mixture of both salts on pure kaolinite. The predicted cumulative chloride was 4.59% from the single salts/clay mixture, assuming additivity, whereas the actual cumulative chloride was 7.38% (See appendix I for statistical analysis). This significant difference cannot be explained by the physical effect of the surface area of salt crystals with high surface area supported on the clay surface, because the same mechanism would be present for each of the salts alone and in the 50:50 mixture.

The data of Figure 4.8 suggest that simple cation exchange would not predict the interactions between clay and chloride salts during the hydrolysis reactions, otherwise the actual cumulative chloride released from the Na + Ca reaction on kaolinite should be lowered since the Na is less exchangeable than the Ca. Calcium has a much greater affinity for the clay than the sodium (Baptista, 1989). As long as there is enough calcium to occupy all or most of the charge exchanged sites, even when cutting the proportion of calcium and sodium by 50%, the clay exchange sites would still be dominated by Ca. In that situation, the Cl hydrolyzed would be (within some small error) the calcium contribution plus some amount due to the Cl from the sodium salt.

4.2.2. Role of Cation-Saturation of Clay in Hydrolysis of Salts

The kaolin clay was cation-saturated by following the procedure of Brindley and Ertem (1971) and Baptista (1989). The Na and Ca-Kaolinite forms were then emulsified in oil with a mixture of salts and the preparation method as well as the experimental conditions was the same as in the previous hydrolysis tests. Figure 4.9 depicts the incremental as well as the cumulative evolution of chloride as a function of the temperature of the hydrolysis.

Both Ca-kaolinite and Na-kaolinite reactions with mixed salts exhibited a peak of chloride release between 250-300° C. However, the cumulative chloride released from the Na-saturated kaolinite was equivalent to the calcium form, contrary to the expected result based on the mechanism of cation exchange between the clay and the salts in the emulsion. The calcium saturated form of kaolinite could release Ca in presence of concentrated NaCl, which would occur as the emulsion droplets were dried at 150 °C. The resulting dry $CaCl_2$ would be much more reactive than the NaCl, In contrast, the Na-kaolinite could give the opposite trend with the release of sodium and the uptake of the preferred cation, calcium. Ion exchange mechanisms, therefore, would be expected to give a significant difference in hydrolysis of salts between the two types of kaolin. As illustrated in Figure 4.9, the two forms were equivalent.

On the other hand, a relationship between cation exchange and surface area might account for the previous results, as stated by many authors (Worrall et al., 1958; Johnson and Lawrence, 1942; Harman and Fraulini, 1940) who have studied the dependence of the exchange capacity of kaolinite on variations in particle size or

surface area. The formerly authors have demonstrated that there is a practically linear relation between the surface area and the exchange capacity. Thompson et al. (1992), observed a 95% intercalation with NaCl between the hydrogen-bonded layers of kaolinite. This intercalation changes the structure of the kaolinite and swells the mineral, increasing the space between adjacent layers in the surface by as much as 7.8 A° leaving enough room for a divalent cation with higher affinity towards kaolinite, as calcium. In order to define the role of surface area, the surface areas of the ion-exhanged clays were measured by nitrogen adsorption.

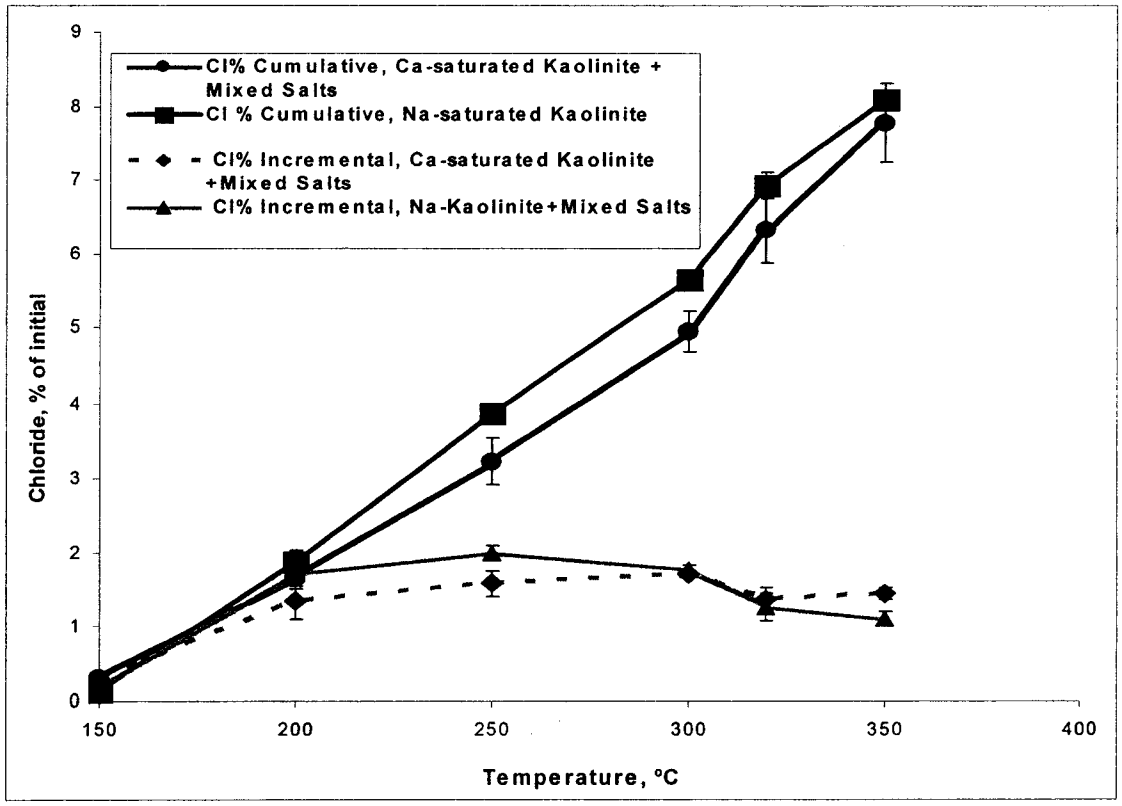

Figure 4.9. Effect of cation-saturation of clay on the hydrolysis of emulsified chloride salts (70 wt% + 20 wt% $CaCl_2$ 2(H_2O) + 10 wt% $MgCl_2$ 6(H_2O)) on a (10:1 clay to salt weight ratio). The error bars correspond to the cumulative chloride standard deviation from 3 replicates.

4.2.3. Characterization of ion exchanged clays

The internal surface area information of each specimen was extracted from the nitrogen adsorption isotherm data according to the Brunauer, Emmett and Teller Method (BET), and is shown in Table 4.5 (measured on an Omnisorp 360, Version 5, 1991). The data of Table 4.5 give the surface areas of the samples and the cumulative hydrolysis results from Figures 4.3 and 4.9. and Table 4.5, it can be observed that the chloride evolution as well as the crystallite surface area is fairly larger for the cation-saturated species.

The experimental work from Ormsby and Shartsis (1960) on the association between surface area and cation exchange of kaolinite seems to agree with the results observed from the surface area measurements on pure and cation-saturated kaolinite + mixed salts. There was not enough sample to calculate the surface area of the salts crystals without clay after reaction. However, the data of Table 4.5 suggest that surface area and extent of hydrolysis are correlated. This relationship shows that the interactions between chloride salts and kaolinite saturated with Ca^{2+} and Na^{+} ions may be due to a larger internal surface area for dispersion of the salts, i.e. area within the clay agglomerates and possibly within the clay particles. The observed increase in surface area of the Calcium-modified samples was consistent with an increase in the average pore diameter between adjacent clay layers (Thompson et al.,1992). However the hydrolysis of the Na-modified form did not correlate well with surface area, suggesting that dispersion might not increase possibly due to the intercalation with Calcium ions that might ocupate the available active sites in the surface of the kaolinite.

Table 4.5. Surface area of solids after reaction calculated by the Brunauer, Emmett and Teller (BET) method from nitrogen adsorption data.

Sample	Measured BET Surface Area, m^2/g	Cumulative Chloride Evolved, %
Kaolinite + Mixed Salts	4.83	4.25 ± 0.45
Ca-Kaolinite + Mixed Salts	8.15	7.72 ± 0.64
Na-Kaolinite + Mixed Salts	12.38	8.10 ± 0.38

The chemical nature of the surface of the mixed salts plus pure Ca-saturated and Na-saturated kaolinite after hydrolysis was determined using X-ray photoelectron spectroscopy (XPS) and is presented in table 4.6 below. Unlike the EDX method which was applied earlier to analyze a volume of the clay agglomerates, the XPS technique is a true surface-sensitive method that reads the composition of the outer 21 nm of a sample (Oswald et al., 2000). Calculation of the salts/clay ratios of the solids based on the peak heights of the spectra revealed that the salts are coated onto an alumino-silicate surface. The sodium was depleted from the surface layer of each of the three observed solid species, whereas the remaining calcium concentration was higher, even though the salt mixture exhibited almost a 4 times higher Na:Si ratio vs. the Ca:Si ratio as observed from the EDX data from table 4.4.

These XPS results, in addition to the previous results for chloride evolution with cation saturated kaolinite and mixed salts agree with the work of Thompson et al. (1992), who after dry grinding of kaolinite with NaCl, followed by the addition of distilled water and subsequent drying by heating, observed a 95% intercalation with NaCl between the hydrogen-bonded layers of kaolinite. This intercalation changes the structure of the kaolinite and swells the mineral, increasing the space between adjacent layers in the surface by as much as 7.8 A° leaving enough room for a divalent cation with higher affinity towards kaolinite, such as calcium. Consequently, the addition of salts results in more complex physical interactions with the clays than the simple deposition of salt crystals on the clay surface.

Table 4.6. XPS Analysis of clay + mixed salts solids after hydrolysis.

Element	Raw Area Relative to Si		
	Pure kaolinite + mixed salts	**Na-saturated kaolinite + mixed salts**	**Ca-saturated kaolinite + mixed salts**
Na	0.11	0.28	0.15
Ca	0.66	0.59	0.32
Cl	0.25	0.26	0.12
Si	1	1	1
Al	0.52	0.54	0.44
Mg	0.02	4.98E-05	0.03

4.3. Inhibition of the Hydrolysis of Salts and Clay

Eaton et al. (2005) developed alkaline-earth oxides as colloidal suspensions stabilized by organic acids to act as inhibitors of the hydrolysis reaction without downstream problems such as fouling, deposition or corrosion. This type of inhibitor was tested with mixed salts, using the same emulsion preparation procedure and hydrolysis conditions as previous experiments. A calcium based inhibitor was added in a 1:1 ratio to the salts, i.e. one gram of inhibitor per gram of salt was added to the model oil suspension after drying at 150 °C.

Results revealed that the inhibition performance varies critically with the nature of the species interacting with the salt crystals. The first experiment was to add the inhibitor to the salt emulsion in the oil, without the presence of clay. By comparing an evolution of 0.76% against 1.21 ± 0.17% of the initial chloride in the oil without inhibitor, the observed inhibition was 37.4%. The second approach added the inhibitor to a mixture of kaolinite and mixed salts; this was the worst scenario, since the reduction of hydrochloric acid release was only 27.6%, from the original 4.25±0.45 % of chloride evolved without inhibitor to 3.08% (Figure 4.10). However, on the basis of the amount of chloride removed, in the case with clay, a lower % of inhibition actually indicates more capture of chloride on a weight ratio basis – without clay, the inhibitor captured 0.45% of the chloride from the sample, compared to 1.17% of the chloride in the presence of clay – more than twice as much capture.

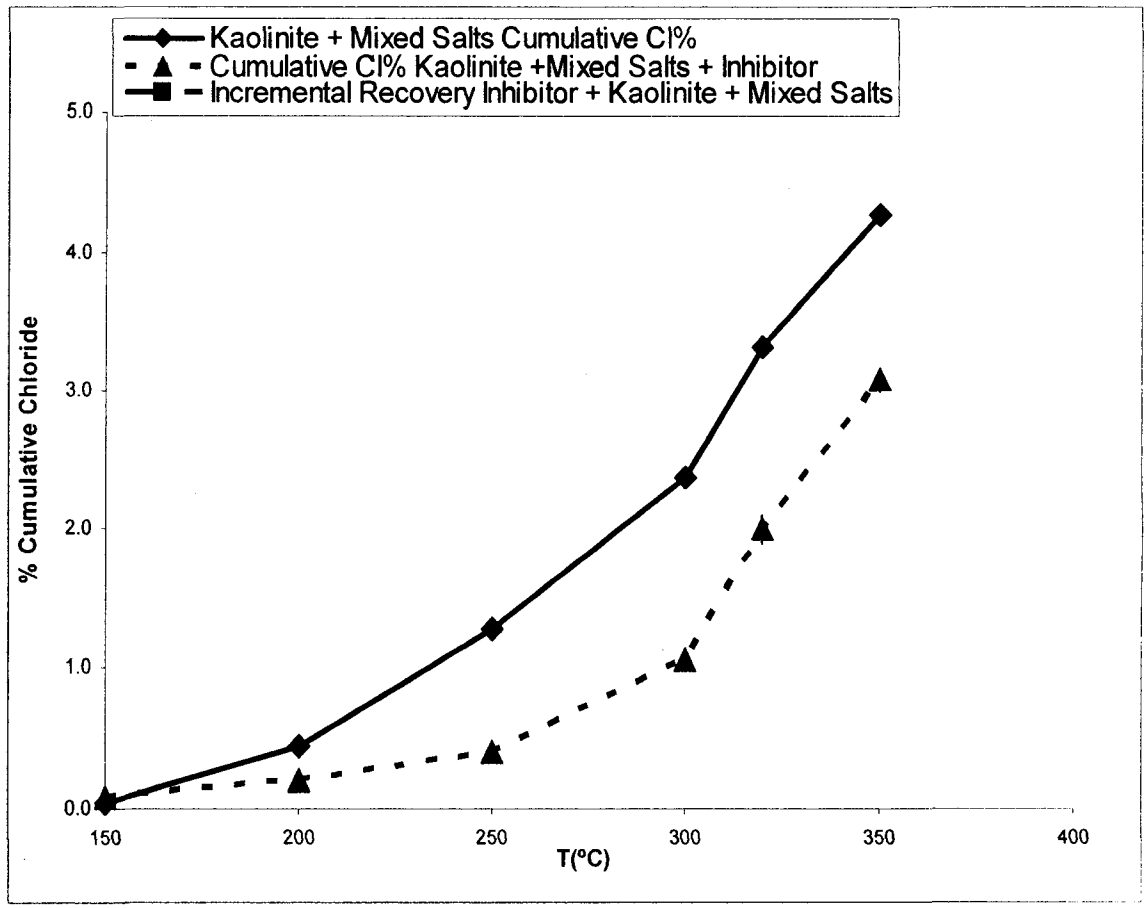

Figure 4.10. Inhibition of chloride evolution at 1:1 weight ratio inhibitor vs. mixed salts

The clay structure might account for the low inhibitor performance. Recent studies from Franco et al (2004) about physically adsorbed water and hydroxyl groups inside the kaolinite skeleton may provide an effective explanation of why clay may reduce the inhibitor action. As Franco et al (2004) showed, a continuous heating rate gave a slight mass loss associated with the dehydration of the loosely bonded adsorbed water on the particle surface of kaolinite between 230 °C and 440 °C. This water release might enhance the hydrolysis of the salts, much the way the hydrated

water in magnesium chloride increases hydrolysis (Gray et al., 2007). This mechanism was tested comparing the incremental chloride release as a function of temperature after the hydrolysis for the emulsion of salts and clay with and without inhibitor in oil (Figure 4.11). The associated percentages of inhibition are presented in table 4.7 where the tabulated data indicate that between 320 °C and 350 °C the clay + salts the inhibitor is less effective. This observation is consistent with the release of water from the clay to enhance the hydrolysis of the salts. This mechanism of water release could contribute to the hydrolysis by both clay and silica.

Table 4.7 Percentage of inhibition as a function of temperature of hydrolysis for an emulsion of kaolinite + mixed salts

T (^{0}C)	% Inhibition
150	46.97
200	80.26
250	77.08
300	36.95
320	14.55
350	19.38

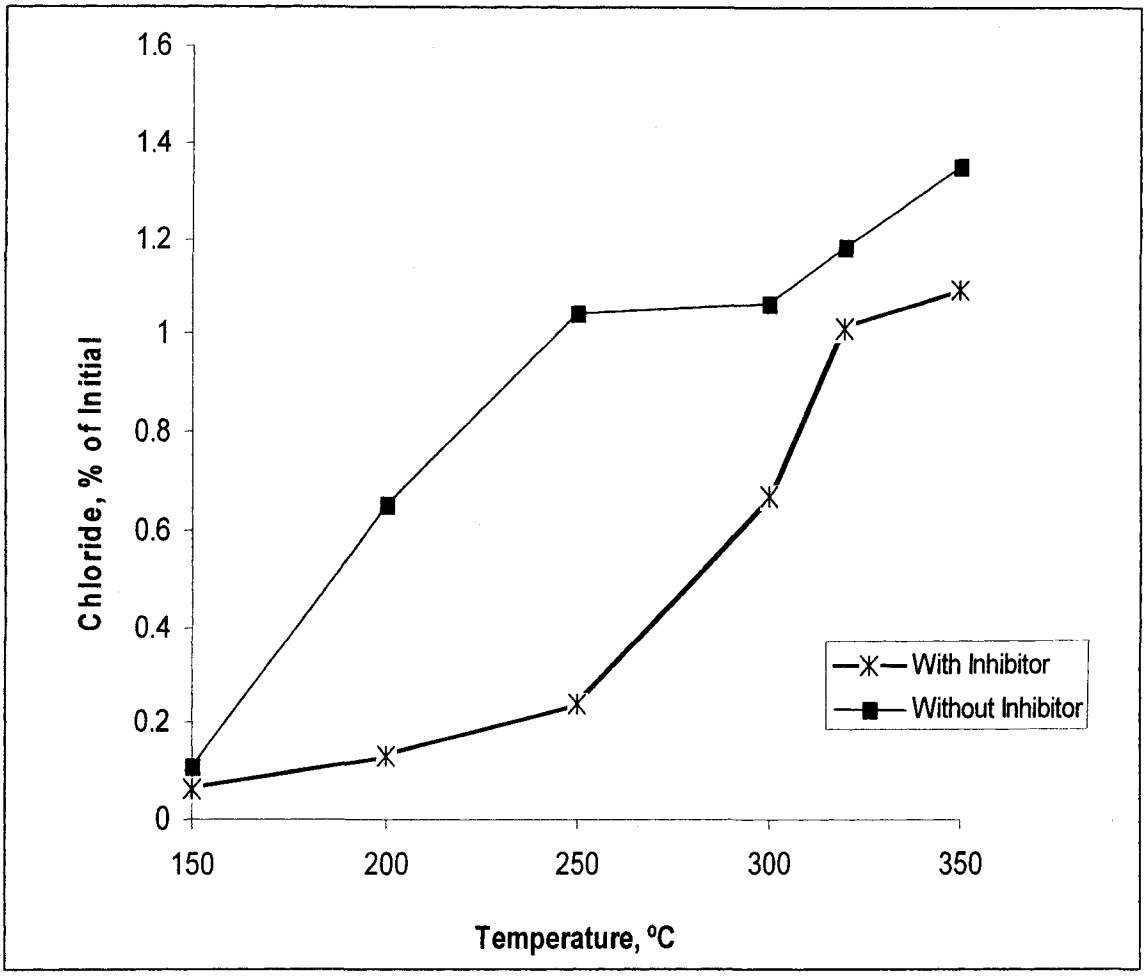

Figure 4.11. Incremental release of chloride for the hydrolysis of kaolinite + mixed salts + inhibitor emulsified in oil.

The average diameter of the solids after the inhibited hydrolysis was 127 μm vs 57 μm without inhibition (Figure 4.12). The observed values for specific surface area were 0.0471 m^2/g and 0.235 m^2/g respectively, i.e. 5 times smaller for the inhibited reaction. Consequently, the inhibitor could react with Cl to form hydroxychlorides as proposed by Eaton et al., (2005), but it could also reduce hydrolysis by reducing the available surface area for reaction.

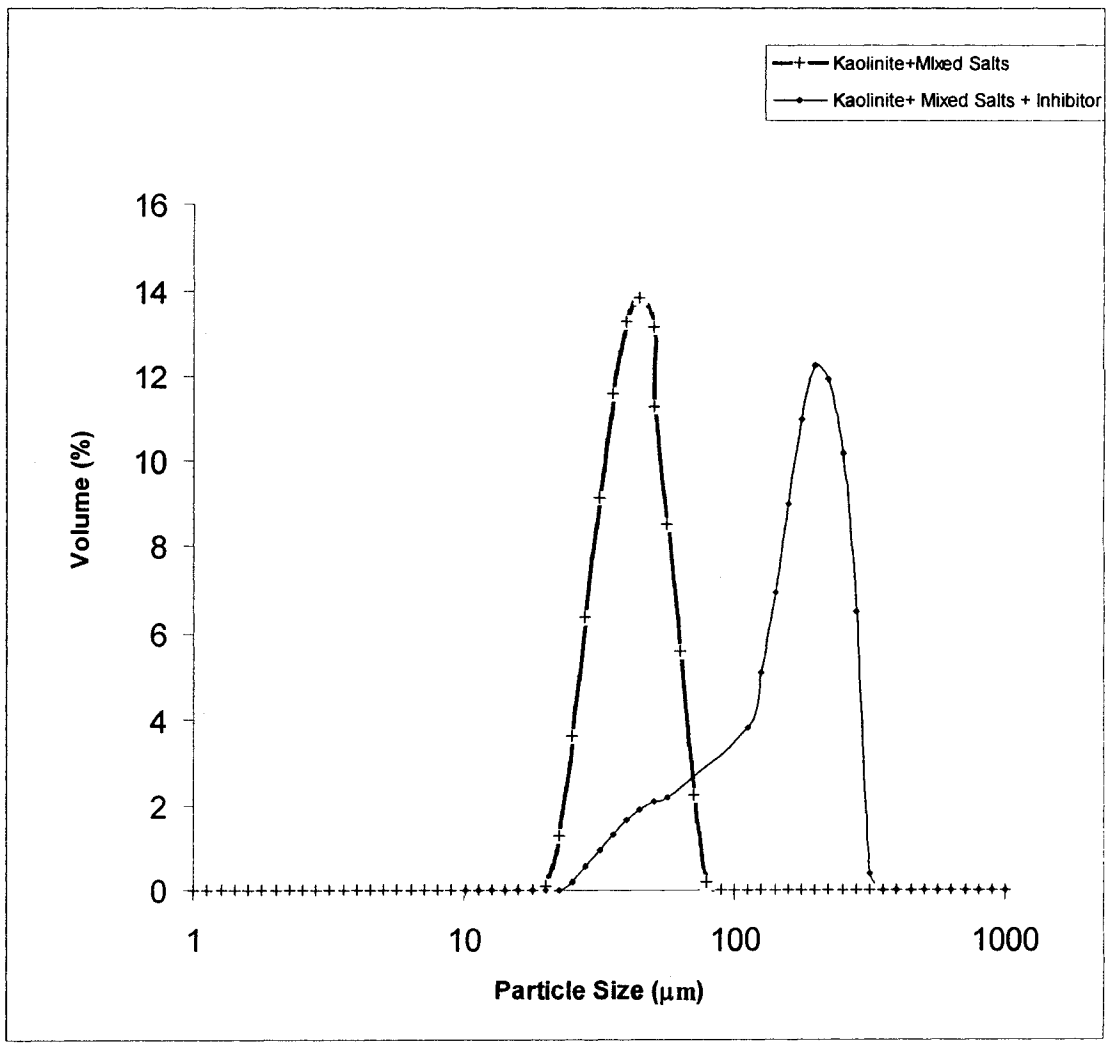

Figure 4.12.Particle size distribution mixed salts + clay with and without inhibitor

CHAPTER 5

CONCLUSIONS AND RECOMMENDATIONS

5.1. Conclusions

The results of the experimental studies, together with the data reviewed from literature, permitted to study the mechanisms of interaction between clays and chlorides in bitumen during hydrolysis reactions in the presence of steam. On that basis, the following conclusions can be drawn:

1. Clays accelerate the reaction of NaCl, $CaCl_2$ $2(H_2O)$ and $MgCl_2$ $6(H_2O)$ in the presence of steam.
2. Surface area is of critical importance when studying the interactions between clays and chlorides in bitumen. Clays are likely to promote the release of hydrochloric acid during the hydrolysis reaction by dispersing the salt crystals as much smaller domains of the clay matrix, giving more active sites available for the hydrolysis reaction to occur. This conclusion was supported by the experiment with silica, which gave similar results to kaolinite.
3. The experiments on pure salts suggested that simple cation exchange would not dominate the interactions between clay and chloride salts during the hydrolysis reactions, otherwise the actual cumulative chloride released from the Na + Ca reaction on kaolinite should be lowered since the Na is less exchangeable than the Ca. Moreover, there was no difference in chloride evolution for the hydrolysis of pure salts of sodium and calcium with pure

kaolinite vs pure salts on ion saturated kaolinite. The hydrolysis reaction seems to be more sensitive to the surface area of the salts.

4. The results of chloride evolution observed in metal ion-modified samples of clay + mixed salts show that the interactions between chloride salts and kaolinite saturated with Ca^{2+} and Na^{+} ions are accompanied by an increase of surface area. The higher surface area was attributed to an increase in the average pore diameter between adjacent layers due to the intercalation of ions in the surface of the kaolinite.
5. The changes in the salts/clay ratios with temperature, from XPS and EDX analysis, revealed that the addition of salts results in more complex physical interactions with the clays than the simple deposition of salt crystals on the clay surface.
6. Results revealed that the performance of a dispersed calcium inhibitor varied critically with the nature of the species interacting with the salt crystals. Clay structure and dehydroxylation at process temperatures might be accountable for retarding the inhibitor action to prevent the increase in chloride evolution performance. If the water from the clay enhanced the hydrolysis at these temperatures, then the inhibitor could be less effective.
7. The smaller values for average agglomerate diameter and specific surface area exhibited by the clays and salts after the inhibited reaction imply that the inhibitor could also reduce hydrolysis by reducing the available surface area for reaction.

5.2.Recommendations

The following suggestions for further development of this research program are proposed:

1. Further studies on the additivity of hydrolysis from pure salts in Kaolinite are suggested to test the relationship between surface area and cation exchange capacity of the clays during the hydrolysis reactions.
2. Study the interactions between clays and chlorides in actual crude oils. Components of crude oils, such as naphthenic acids and asphaltenes, could further modify the interactions defined in this thesis.
3. Experiments in with mixtures of kaolinite, illite and montmorillonite with mixed salts may be more representative of interactions of salts and clays in an authentic oilfield. Actual clay mixtures should be evaluated for comparison.
4. A better understanding of how much of a role is surface area and how much is water when studying the interactions between clays and chloride in bitumen still needs to be gained.
5. Further experimentation need to be done to test the role of Ph in the mechanisms of interaction between clay and salts during the hydrolysis reactions

REFERENCES

Amonette, J. E., and Zelazny, L. W. (1994). "Quantitative methods in soil mineralogy." *Soil Science Society of America*, Miscellaneous Publication, Madison Wisconsin.

Anonymous. (1997). "Optimizing desalter operations can help refiners cope with heavy crudes." *Oil & Gas Journal.*, 95(43), 71.

Balan, E., Allard, T., Boizot, B., Morin, G., and Muller, J. P. (1999). "Structural Fe^{3+} in natural kaolinites: new insights from electronparamagnetic resonance spectra fitting at X and Q-band frequencies." *Clays and Clay Minerals*, 47(5), 605-616.

Baptista, M. V. (1989). "Role of exchangeable cations of oil sand clays in oli sand processing." *AOSTRA Journal of Research*, 5(3), 237.

Barker, T. (2007). Personal communication.

Bartley, D. (1982). "Heavy crude stocks pose desalting problems." *Oil & Gas Journal*, 80(5), 117-124.

Bayliss, P., and Levinson, A. A. (1976). "Mineralogical review of the Athabasca oil sands deposits." *Bull Can Pet Geol*, I(24), 211-214.

Beardow, A. (2000) "Problem Ores." *First Extraction Fundamentals Seminar*, Interpretive Centre, Fort McMurray.

Bergaya, F., Dion, J., and Alcover, F. (1996). "TEM study of kaolinite thermal decomposition by controlled-rate thermal analysis." *Journal of Material Science*, 31, 5069-5075.

Briner, E., and Roth, P. (1948). "Recherches sur l'hydrolyse par le vapeur d'eau et chlorures alcalins seuls ou additiones de divers adjuvants." *Helvetica Chimica Acta*, 31(V), 1352-1360.

Chen, J., Anandarajah, A., and Inyang, H. (2000). " Pore fluid properties and compressibility of kaolinite." *Journal of Geotechnical and Geoenvironmental Engineering*, 126, 798–807.

Choi, D. W. (2005). "How to buy and operate desalters." *Hydrocarbon Processing*, Vol.84(3), 75-79.

Chung, K. H., Janke, L. C. G., Dureau, R., and Furimsky, E. (1996). "Leachability of coke from Syncrude stockpiles. ." *Journal of Environmental Science*, 9(2), 50-53.

Cookson, D. J. (2000). Personal communication to Dr. M. R. Gray, Edmonton.

Davis, L. L., Jones, J. M., and Neilson, C. A. (1938). "Laboratory control of corrosion of distillation equipment and desalting processes." *Oil & Gas Journal*, 38(2), 62-73.

Devidal, J., Dandurand, J., and Gout, R. (1996). " Gibbs free energy of formation of kaolinite from solubility measurement in basicsolution between 60 and 170 °C." *Geochimica et Cosmochimica Acta*, 4(553-564).

Eaton, P. (2000). "Hydrolysis of metal salts in synthetic crude oil." *AIChE National Conference*, Atlanta, Georgia.

Eaton, P. E., Venter, P. J., and Jones, G. B. (2005). "Method of reducing hydrolysis in hydrocarbon streams." US6902662.

Eaton, P. E., Gray, M. R., Le, T., and Londono, Y. "The Impact of Naphthenic Acid on Salt Hydrolysis." *Proceedings of Eurocorr 2005, European Corrosion Congress*, Lisbon, Portugal.

Fialips, c., Petit, S., Decarreau, A., and Beaufort, D. (2000). "Influence of synthesis ph on kaolinite "crystallinity" and surface properties." *Clays and Clay Minerals*, 48(2), 173-184.

Fong, N., Ng, S., Chung, K. H., Tu, Y., Li, Z., Sparks, B. D., and Kotlyar, L. S. (2004). "Bitumen recovery from model systems using a warm slurry extraction process: effects of oilsands components and process water chemistry." *Fuel*, 83, 1865–1880.

Fong, N., Ng, S., Chung, K. H., Tun, Y., Li, Z., Sparks, B. D., and Kotlyar, L. S. (2004). "Bitumen recovery from model systems using a warm slurry extraction process: effects of oilsands components and process water chemistry." *Fuel*, 83(2004), 1865–1880.

Franco, F., Pérez-Maqueda, L. A., and Pérez-Rodríguez, J. L. (2004). "Influence of the particle-size reduction by ultrasound treatment on the dehydroxylation process of kaolinites." *Journal of Thermal Analysis and Calorimetry*, 78, 1043–1055.

Gray, M.R., Eaton, P., and Le, T. (2006). "Kinetics of hydrolysis of chloride salts in model crude oil." *Petroleum Science and Technology*, submitted for publication.

Gray, M. R., Eaton, P., and Le, T. (2007). "Inhibition and promotion of hydrolysis of chloride salts in model crude oil and heavy oil." *Petroleum Science and Technology*, in press, January 2007..

Gray, M. R., and Masliyah, J. H. (1998). *Extraction and upgrading of oilsands bitumen. Intensive short course*, Department of Chemical and Material Engineering. University of Alberta, Edmonton.

Grim, R. E. (1953). *Clay Minerology*, McGraw-Hill Book Company, Inc, New York

Hall, S. E., and Tollefson, E. L. (1982). "Stabilization and destabilization of mineral fines-bitumen-water dispersions tailings from oil sand extraction plants that use the hot water process." *Canadian Journal of Chemical Engineering*, 60, 813-821.

Harman, C. G., and Fraulini, F. (1940). "Properties of kaolinite as function of its particle size." *Journal of the American Ceramic Society*, 23(9), 252.

Jackson, M. L. S. C. (1979). *Soil Chemical Analysis—Advanced Course*, University of Wisconsin, Madison.

Kelley, J. (1939). "Specific Heats at Low Temperatures of Crystalline Ortho, Meta and Disilicates of Sodium." *Journal of American Chemical Society*, 61, 471-473.

Klever, and Kordes. (1930). *Silikatforsch*, 3(17). Veroffentlich. Kaiser Wilhelm-Institute. Berlin-Dahlem.

Laird, D. A., Scott, A. D., and Fenton, T. E. (1989). " Evaluation of the alkylammonium method of determining layer charge."*Clays and Clay Minerals*, 37, 41–46.

Lawrence, W. G., and Johhson, A. L. (1942). "fundamental study of clay: IV, surface area and its effect on exchange capacity of kaolinite." *Journal of the American Ceramic Society*, 25(12), 344.

Levine, S., and Sanford, E. "Clay-bitumen interactions and their relevance to tar sand processing." *30th Canadian Chemical Engineering Conference: Oil Sands, Coal and Energy Modelling*, 112-124.

Levine, S., and Sanford, E. (1985). "Stabilization of emulsion droplets by fine powders." *Canadian Journal of Chemical Engineering*, 258-66.

Lim, C. H., and Jackson, M. L. (1982). "Dissolution for total elemental analysis." *Agronomy*, 9, 1-12.

Ma, C., and Egglenton, R. A. (1999). "Cation exchange capacity of kaolinite." *Clays and Clay Minerals*, 47(2), 174-180.

Meunier, A. (2005). *Clays*, Springer, Berlin.

Mineralogy Database. http//webmineral.com. (Accessed September 2006)

Mitchell, J. K. (1993). *Fundamentals of Soil Behavior*, Wiley, New York.

Nelson, W. L. (1958). *Petroleum Refinery Engineering*, McGraw-Hill, New York.

Oelkers, E. H., Schott, J., and Devidal, J.-L. (1994) T. (1994). "The effect of aluminum, pH, and chemical affinity on the rates of aluminosilicate dissolution reactions." *Geochimica et Cosmochimica Acta*, 58(9), 2011-2024.

Olphen, V. H., and Fripiat, J. J. (1979). *Handbook for Clay Minerals and Other Non-metallic Minerals*, Pergamon Press,New York.

Oscarson, D. W., and Dixon, D. A. (1988). "The effect of steam on montmorillonite." *Applied Clay Science*, 4, 279-292.

Oswald, S., Hassler, W., Reiche, R., Lindner, J., and F., W. "XPS depth profile analysis." *Solid state analysis: proceedings of the 10th symposium*, Vienna, Austria, 303-306.

Popp, V. V., and Dinolescu, V. D. (1997). "Dehydration and Desalting of Heavy and Viscous Crude Oil Produced by In-Situ Combustion." *Society of Petroleum Engineers Journal*, 12(2), 95-99.

Pruneda, E., Escobedo Borrell Rivero, E., and Vasquez Garfias, J. (2005). "Optimum temperature in the electrostatic desalting of maya crude oil." *Journal of the Mexican Chemical Society*, 49(1), 14-19.

Roberts, C. H. M., Stenzel, R. W., and Ebert, W. F. (1939). "Determination of salts in crude oil." *Petroleum Engineer*, 10(7), 144-146.

Romanova, U. G., Valinasab, M., Stasiuk, E. N., Yarranton, H. W., Schramm, L. L., and Shelfantook, W. E.(2004) "The effect of bitumen extraction shear conditions on froth treatment performance." *Canadian International Petroleum Conference*, Calgary.

Sagues, A. A., Davis, B. H., and Johnson, T. (1982). "Coal liquids distillation tower corrosion. Synergistic effects of chlorides, phenols and basic nitrogen compounds." *Ind. Eng. Chem. Process Des. Dev*, 22, 15-22.

Sainz-Diaz, C. I., Hernandez-Laguna, A., and Dove, M. T. (2001). "Modelling of dioctahedral 2:1 phyllosilicatesby means of transferable empirical potentials." *Physics and Chemistry of Minerals*, 28, 130-141.

Schofield, R. K., and Samson, H. R. (1954). "Flocculation of kaolinite due to the attraction of oppositely charged crystal faces." *Discussions of the Faraday Society,*, 18, 659–673.

Spark, K. M., Wells, J. D., and Johnson, B. B. (1995). "Characterizing trace metal adsorption on kaolinite." *European Journal of Soil Science*, 46, 633-640.

Sparks, B. D., Kotlyar, L. S., O'Carroll, J. B., and Chung, K. H. (2003). "Athabasca oil sands: effect of organic coated solids on bitumen recovery and quality." *Journal of Petroleum Science and Engineering*, 39, 417– 430.

Spei, S. (1949). "Effect of Adsorbed Electrolytes on Properties of monodisperse clay-water systems." *Journal of the American Ceramic Society*, 23(2), 33-38.

Suraj, G., Iyer, C. S. P., Rugmini, S., and Lalithambika, M. (1998). "Adsorption of cadmium and copper by modified kaolinites." *Applied Clay Science*, 13(4), 293–306.

Surinder, P. (2003). "Crude Desalting." Refining Processes Handbook, Elsevier.

Tipman, R., Power, W., Long, Y., and Dabros, T. (2001). "solvent process for bitumen separation from oilsands froth." US 5876592.

Tu, Y., J.B., O. C., Kotlyar, L. S., Sparks, B. D., Ng, S., Chung, K. H., and Cuddy, G. (2004). "Recovery of bitumen from oilsands: gelation of ultra-fine clay in the primary separation vessel." *Fuel 84*, 84, 653-660.

Verwey, E. J. W., and Overbeek, J. T. G. (1948). *Theory of the Stability of Lyophobic Colloids* .,, Elsevier Publishing Company, Inc, Amsterdam.

Walker, C., and Morton, S.(1995) "EDX - Energy Dispersive X-ray Analysis or EPMA - Electron Probe Micro Analysis." Lawrence Berkeley National Laboratory http///www.uksaf.org/tech/edx.html. (Accessed January 2007)

Wallwork, V. (2004) "Water reuse and treatment issues in the oil sands industry." *CONRAD Oil Sands Water Usage Workshop*, Fort Mc Murray.

Warren, K., W. "New tools for heavy oil dehydration." *SPE International Thermal Operations and Heavy Oil Symposium and International Horizontal Well Technology Conference*, Calgary, Alberta.

Warren, K., W., and Armstrong, J. (2001). "Desalting heavy crude oils - the Venezuelan experience." NATCO Group, Inc., Houston, TX 77092. http/// http://www.natcogroup.com/PDFContent/ConsultingResearch/TechnicalPapers/Desalting%20Heavy%20Crude%20Oils%20-%20The%20Venezuelan%20Experience.pdf . (Accessed November 2005)

White, S., and Barletta, T. (2002). "Refiners processing heavy crudes can experience crude distillation problems." *Oil & Gas Journal*, 100(47), 46.

Ye, X. (2000). "Gas oil desalting reduces chlorides in crude." *Oil & Gas Journal.*, 98(42), 76.

APPENDICES

APPENDIX I: Dixon's Test for Outliers Detection

A test for detection of outliers was performed to validate the statistical significance for the predicted cumulative chloride values in experiments made with pure salts, since only a single data set was available. This test was based on the statistical distribution of "sub range ratios" of ordered data for the predicted and actual cumulative chlorides in order to find the statistic experimental Q-value calculated as the difference of the highest chloride value from its nearest one divided by the range of the values.

The obtained Q value of 2.45 was greater than the critical value of 0.76 corresponding to a 95% confidence. Consequently, the null hypothesis confirmed that there is a significant difference between the actual (7.38 % ± 0.15) and the predicted (4.59 ± 0.51) cumulative chlorides released from the hydrolysis reaction of Na + Ca in kaolinite and can be concluded that that the actual value for the cumulative chloride is statistically different and an outlier from the predicted set observations of cumulative chloride for the additivity of pure salts in kaolinite.

APPENDIX II: Additivity of Clay, Acid and Inhibitor

Baseline Conditions: dry ground salt (0.05g), 0.08 g naphthenic acid, 0.5 g Kaolinite + inhibitor in toluene (10% weight in toluene solution), no clay, no water (Salts to inhibitor ratio 1:1)

II. a. Differential Recovery of Chloride

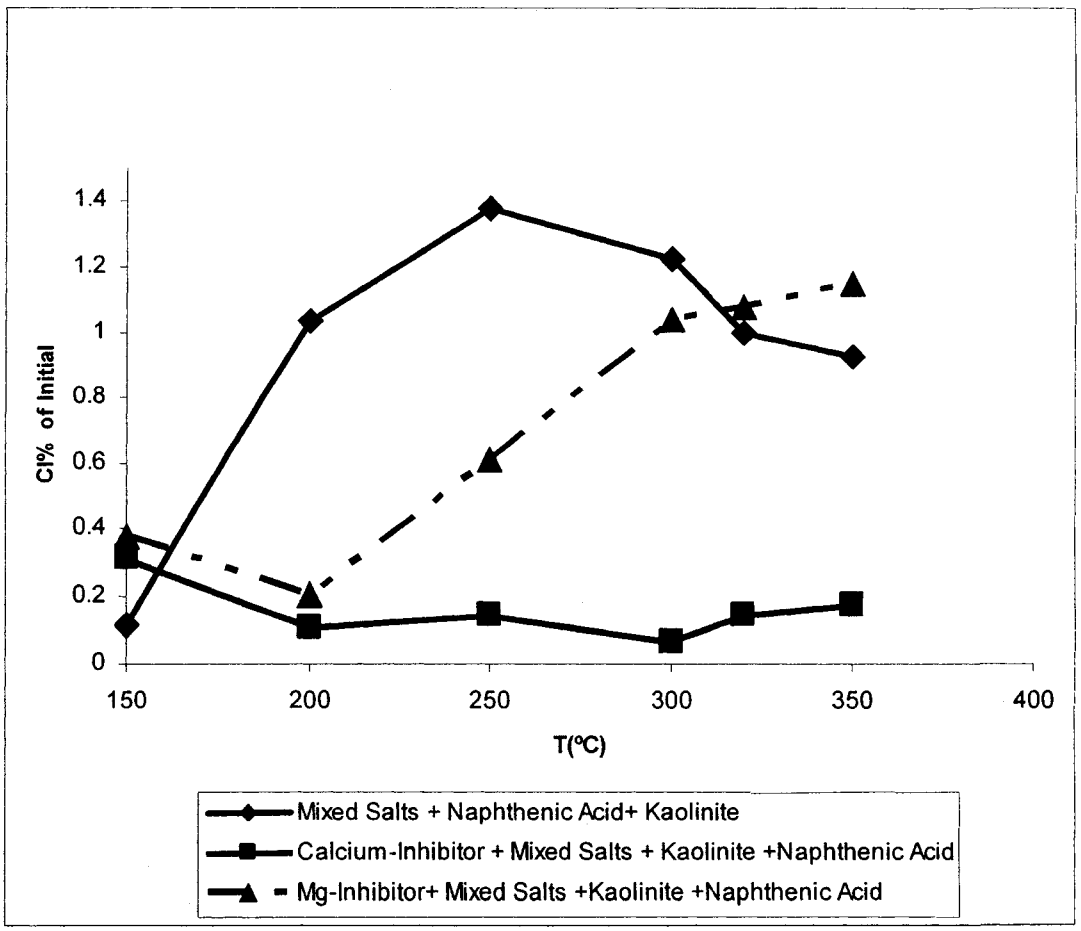

II. b. Cumulative Chloride Evolution

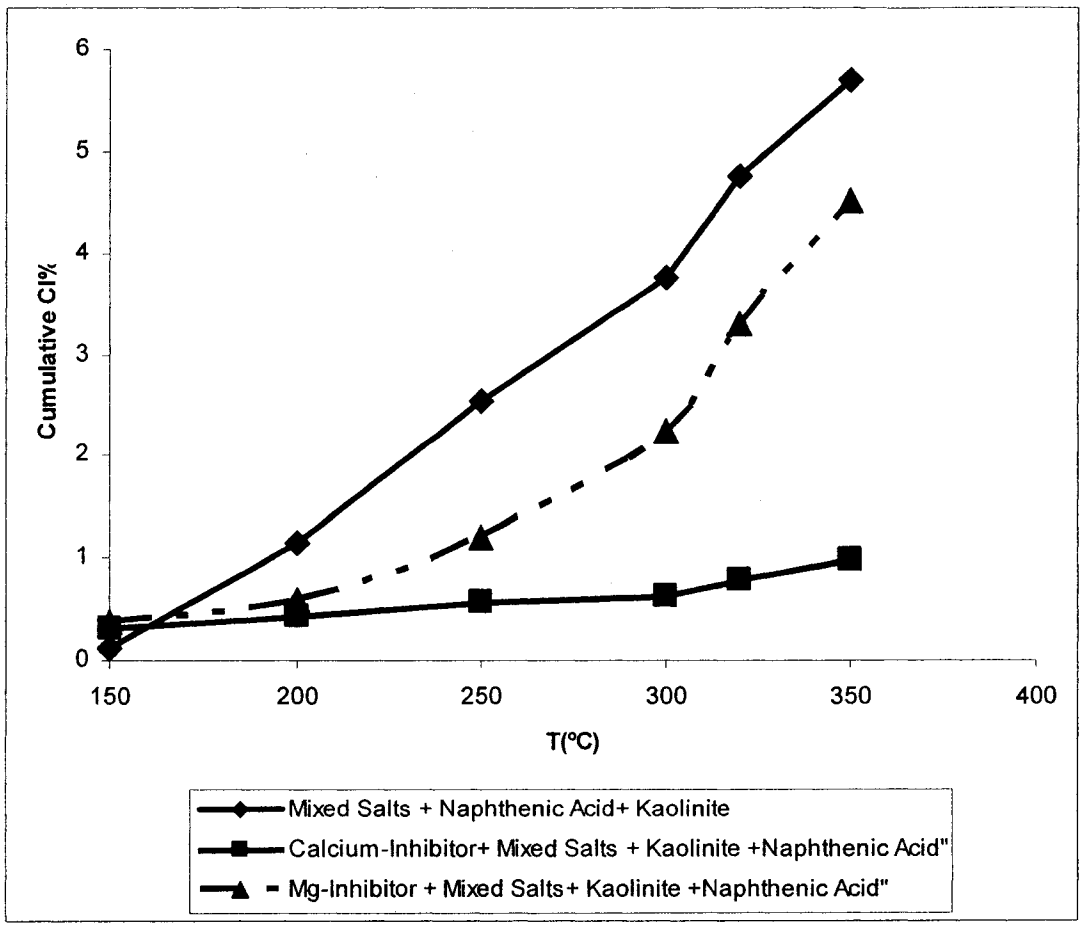

II. c. Comparison of Inhibitors

Inhibitor	Chloride evolved, %	Inhibition%
none	5.7	Baseline
Mg	4.53	20.6
Ca	0.92	83.9

APPENDIX III: Data for Different salt/clay ratios

Baseline Conditions: Series of experiments with different ratios of clay to mixed salts. These experiments will hold the procedure constant except clay content.

III. a. Differential Recovery of Chloride

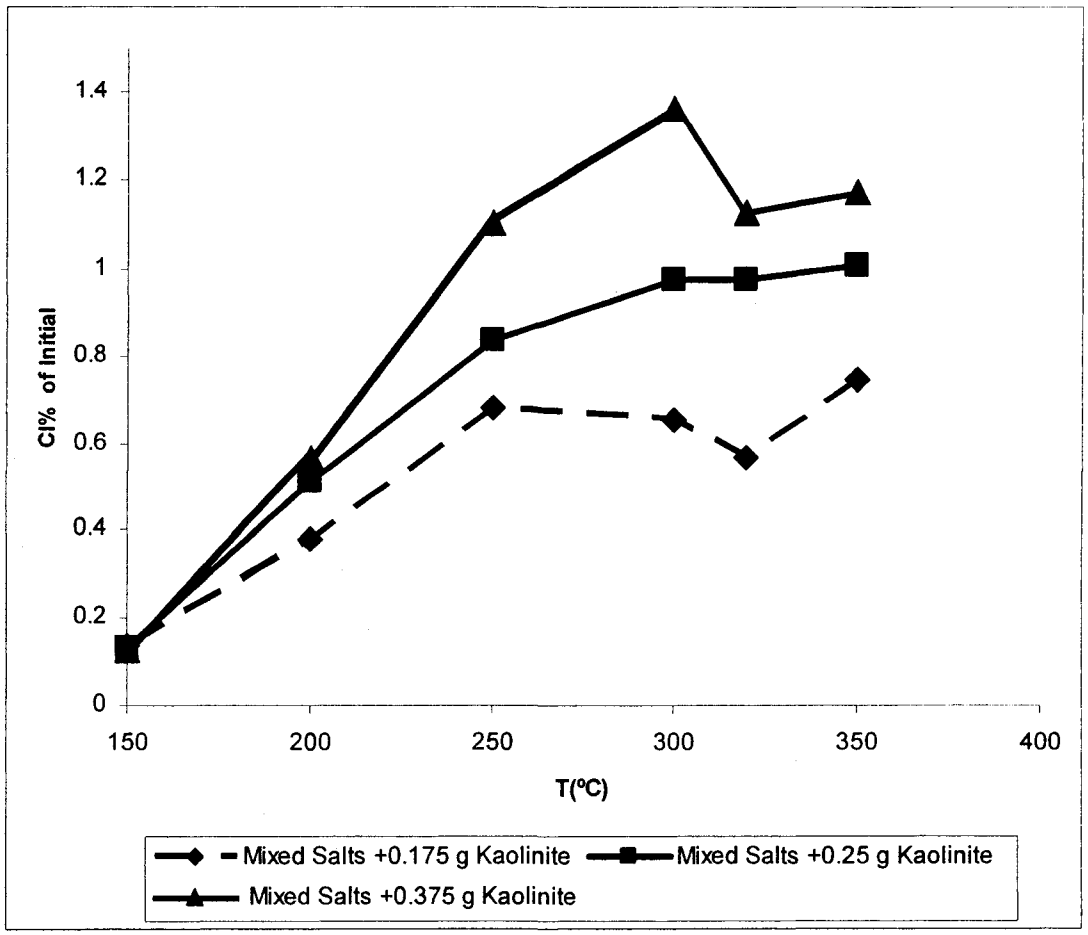

III. b. Cumulative Chloride Evolution

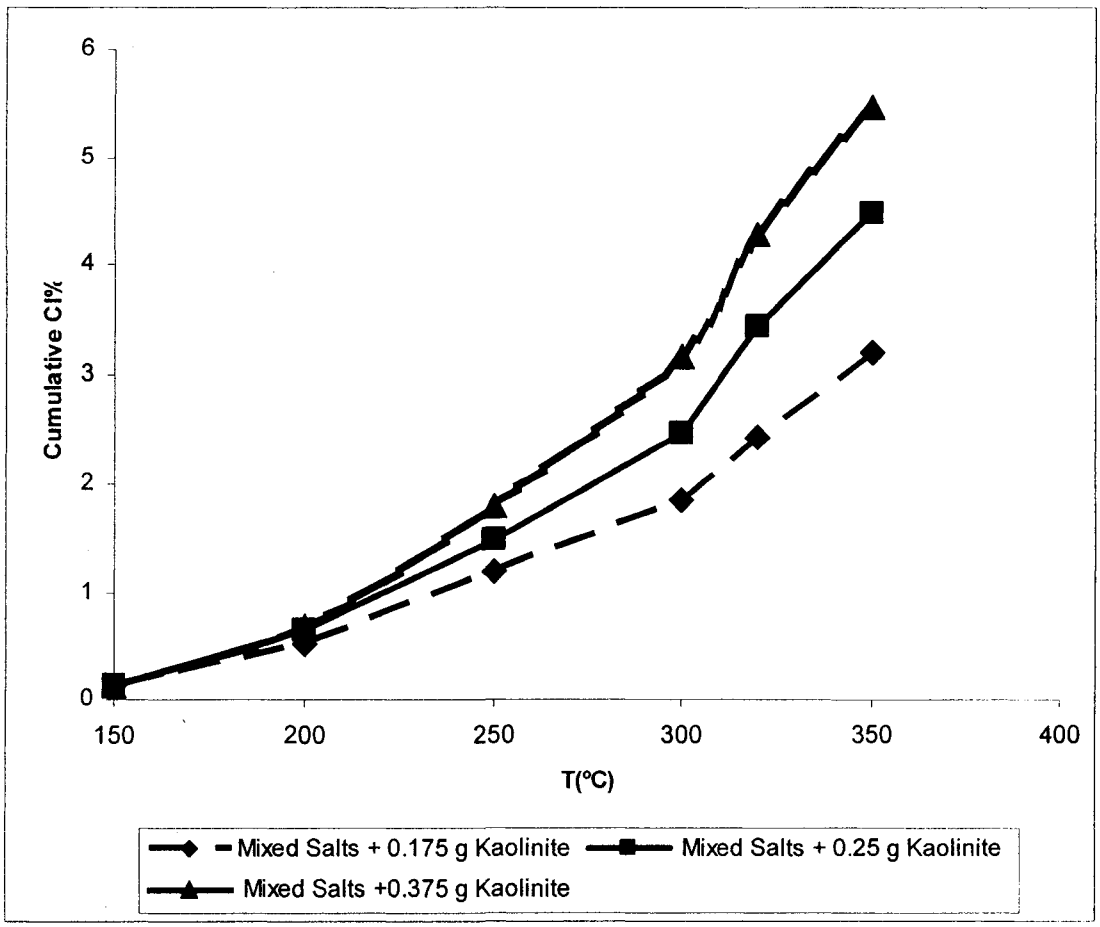

APPENDIX IV: Chloride Input

IV. a. Baseline Conditions: mixed salts 0.05 grs (70%NaCl + 20 % $CaCl_2$ $2(H_2O)$+ 10% $MgCl_2$ $6(H_2O)$)

Cl Input Sodium (g)	0.606182
Cl Input Calcium (g)	0.482317
Cl Input Magnesium (g)	0.348772
Total Cl Input (g):	0.027783
Total Cl Input (mg):	**27.78342**

IV. b. Baseline Conditions: Pure salts 0.0628 grs (100% NaCl)

Cl Input Sodium (g)	0.030309
Cl Input Calcium (g)	0
Cl Input Magnesium (g)	0
Total Cl Input (g):	0.030309
Total Cl Input (mg):	**30.30912**

IV. c. Baseline Conditions: Pure salts 0.05 grs (100% $CaCl_2$ $2(H_2O)$

Cl Input Sodium (g)	0
Cl Input Calcium (g)	0.062841
Cl Input Magnesium (g)	0
Total Cl Input (g):	0.030309
Total Cl Input (mg):	**30.30912**